gear
TECHNOLOGY®

METALS &
METALLURGY
HEAT TREATING, FORGING AND MORE

gear TECHNOLOGY®

MAR/APR 2021

A Publication of
**The American Gear
Manufacturers Association**

32

features

technical

[www.geartechnology.com]

contents

gear TECHNOLOGY®

Vol. 38, No. 2

departments

gear TECHNOLOGY®

MAR/APR 21

METALS & METALLURGY
HEAT TREATING, FORGING AND MORE

CASE STUDY ON MICROPITTING CALCULATION
P.48

Cover Photo by Seco/Warwick

Liebherr Performance.

Maximum flexibility:
Gear Grinding Machines LGG 180/280 and 400 M

- Generating grinding, profile grinding, and internal grinding in one machine
- Changeover from external to internal grinding in less than 30 minutes
- Flexible grinding technologies: Topological profile and generating grinding, polishing, generating grinding with small tools and asymmetric gear teeth
- Digital recording of measured values via LHOpenConnect (Gear Data Exchange)
- Extensive possibilities for machine automation

Liebherr-Gear Technology, Inc.
1465 Woodland Drive
Saline, MI 48176–1259, USA
Phone: +1 (734) 429-7225
info.lgt@liebherr.com
www.liebherr.com

LIEBHERR

THE GEAR INDUSTRY'S INFORMATION SOURCE

www.geartechnology.com

Liquidtool Manager

With the Liquidtool Manager, Liquidtool Systems introduces the first intelligent, IoT-based solution for monitoring coolants. It is the first product ever to combine a plug & play solution and a cloud-based platform with intelligent, automated and reliable measurement into an innovation that takes metalworking companies a step closer to Industry 4.0. Learn more here:

www.geartechnology.com/ videos/Liquidtool-Manager-/

3D Metrology Center

This unique, 5-Axis 3D Metrology Center based on a machine tool motion system with fully integrated high-resolution 3D metrology sensors offers the reliability and long-life performance. Learn more here:

www.geartechnology.com/ videos/3D-Metrology-Center-from-EDM-Intelligent-Solutions/
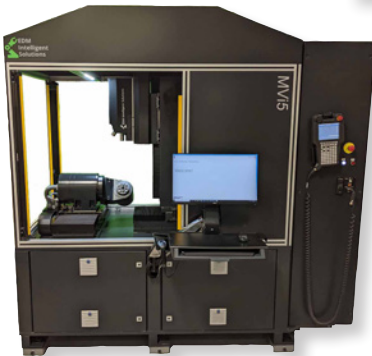
GT Revolutions
A Lesson in Workholding Fundamentals

This informative article by Michael Weas at Helios Gear Products examines the fixturing design required to cut a quality part at an aggressive speed. Learn more here:

www.geartechnology.com/ blog/lessons-learned-3/
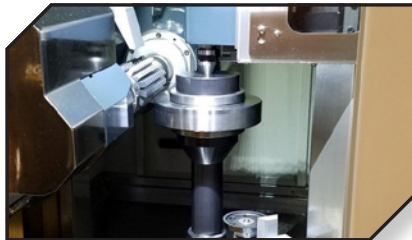
Stay Connected

Join the Gear Technology Facebook group at
www.facebook.com/groups/210890932629794/

Follow us on Twitter
twitter.com/#!/Gear_Technology

Connect with us on LinkedIn
www.linkedin.com/groups/3893880/

Subscribe Online
www.geartechnology.com/subscribe.htm

---

gear
TECHNOLOGY®

ZE26C

GearGrindingMachine

MITSUBISHI
HEAVY INDUSTRIES AMERICA, INC.

MOVE THE WORLD FORW▶RD

The Mitsubishi ZE26C
Gear Grinding Machine:
Precision Gears for Precision Systems

Optimized for Electric Vehicles & Robotics

Greater Structural Rigidity

Shorter Non-cutting Time

Lower Running Costs

Smarter Industrial IoT remote monitoring - DIASCOPE

Born from the widely acclaimed ZE-B series, the all new ZE26C has been specifically designed to meet the exacting demands of the electric vehicle and robotics industries.

Featuring increased rigidity of the column, table and grinding wheel head—coupled with revamping of the spindle structure—the ZE26C produces finished gears with enhanced grinding precision and stability. By increasing cutting speed and reducing non-cutting time by roughly 50%, the ZE26C maximizes high-volume production capability and promotes lower running costs. The expanded wheel width provides longer wheel life and supports the use of combination grinding/polishing wheels for improved gear surface finish, making the ZE26C a compact and operationally efficient machine that's responsive to in-factory needs. To learn more about how the ZE26C has been optimized for the evolving needs of the industry, visit **www.mitsubishigearcenter.com** or contact sales at **248-669-6136**.
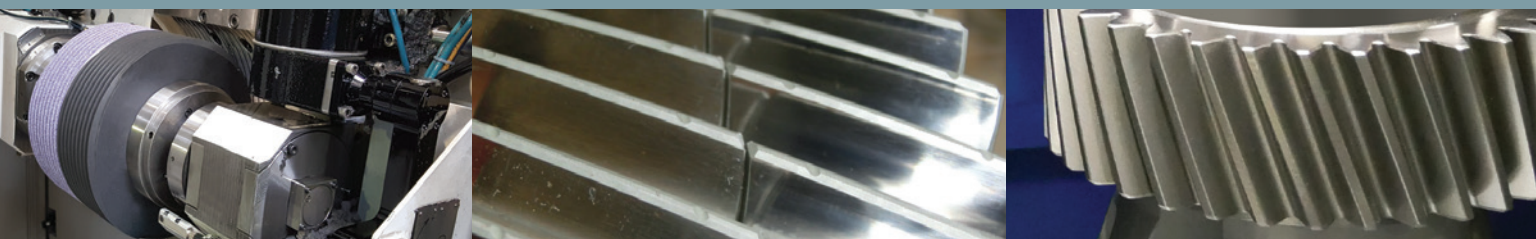
It's Gonna Be Alright

Publisher & Editor-in-Chief
Randy Stott

"February was the fourth-straight month of year-over-year gains in manufacturing technology orders, signaling the recent strength is likely the beginning of a sustained recovery following the 2020 recession."

— *Douglas K. Woods, president of AMT.*

"The March Manufacturing PMI® registered 64.7 percent, an increase of 3.9 percentage points from the February reading of 60.8 percent. This figure indicates expansion in the overall economy for the 10th month in a row after contraction in April."

— *Timothy R. Fiore, CPSM, C.P.M., Chair of the Institute for Supply Management® (ISM®) Manufacturing Business Survey Committee.*

"Don't worry about a thing,
'Cause every little thing gonna be all right."

—*Bob Marley (Lyrics from "Three Little Birds").*

OK. Maybe Bob Marley's take is a little too optimistic to be applied to today's circumstances. After all, COVID-19 has taken a huge toll on the world. It has affected — and continues to affect — virtually every aspect of life. But at least as far as the economy goes, the more people we talk to, and the more statistics we hear from reliable sources, the more we think maybe Bob Marley was onto something.

Last issue we presented our annual "State of the Gear Industry" report, and we were generally pleased and even a little bit surprised by the overall positive attitude we saw among our gear industry audience. Since that time, we've had a number of conversations with gear manufacturers, participated in some virtual meetings and seen presentations by industry and economic experts — all of which confirm what we saw in our annual survey: that the gear industry and manufacturing in general appear to be on a solid path to recovery.

Owners of gear manufacturing job shops tell us they are busy. Maybe not as busy as they want to be, but certainly busy enough that they're not worried about survival. Instead, they're worried about very normal business-related things — like managing their supply chains, staying on top of technological innovations, and hiring, training and keeping their skilled workforce.

Likewise, those who work in captive shops at OEMs are also busy, and they're probably going to keep getting busier. The government keeps putting money back into the economy, and people appear to be spending it. According to the *GDPNow* statistical tool produced by the Federal Reserve Bank of Atlanta, real GDP growth is estimated at 6% (as of the time of this writing) for the first quarter of 2021.

You may be sitting there thinking you've survived the crisis. The economy is humming along. Pretty soon we'll be back to normal.

But "normal" is a fallacy created by our memory of how things were. But things never stay the same, especially in a business that's driven by technology. There is no such thing as normal. In fact, the only thing normal is that things will continue to change.

Only those who think ahead and plan for that change will survive and prosper. So now that you're through the crisis, my advice is to be ready, because things are going to change again.

How will gears be made 10 years from now? How will the industries you support change over the next decades? What's the impact of the new government administration on corporate taxes, import/export, infrastructure and so forth? Are you prepared for what's coming?

If you're not thinking about those things, you should be. And if you don't know where to turn for information, I have a few ideas. Number one: engage with your industry's association. Whether you are a member or not, the American Gear Manufacturers Association can help you navigate these questions.

And when it comes to technology, there's no substitute for seeing it in person. AGMA's MPT Expo is coming to St. Louis in September, and although it will likely be a different show than what we're used to, it will still be the first real opportunity many of us have to gather with peers, gage the pulse of the industry and figure out what's next. Visit motionpowerexpo.com for more information.

No matter how you plan to navigate the "new normal," having a positive attitude is key. Put on some reggae if it helps. But just remember that it will only be alright if you work today to make it so.

Randy Stott

Klingelnberg
EXAMINES FATIGUE STRENGTH AND SERVICE CALCULATION OF GEARS

Bevel gear design is well-established. Flank geometry optimization is used worldwide to ensure satisfactory low-noise emissions and specific values for surface and bending stress.

But what about calculating the service life of gears? To its familiar KIMoS (Klingelnberg Integrated Manufacturing of Spiral Bevel Gears) software package, Klingelnberg has added a module for calculating the service life of a bevel or hypoid gear set that is based on the latest R&D work in service life calculation.

Designing bevel gears is a rather complex task. Unlike cylindrical gears, bevel gears are always designed in pairs. The design engineer must take numerous conflicting objectives into account, including minimum dimensions, maximum load capacity, noise reduction, and ease of manufacture on shop floor machines.

But one aspect is often left out: What about the gear's fatigue strength?

If the maximum load on a tooth does not exceed the load limits of the material, the tooth returns to its initial state after the load is removed. This assumption is valid for several hundred load applications. But when we are talking about several million load applications, damage will occur at much lower loads than the load limits of the material. This phenomenon is
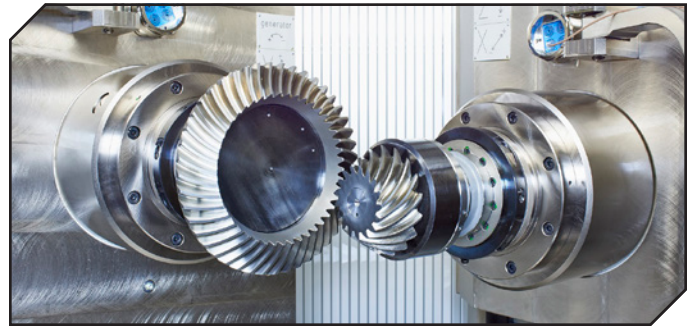
Fig. 1: Automated bevel gear test stand.

known as fatigue.

Fatigue strength testing—a core competence of OEMs and Tier 1 gear suppliers—is accomplished through time-consuming testing of transmissions. These tests are performed with an empirically defined load spectrum that inflicts the same damage that would occur under practical service conditions. One of the machines used for these endurance tests on bevel gears is the Oerlikon TS 30 bevel gear test stand.

What if we could calculate the service life of a bevel gear instead of having to subject each design to costly,
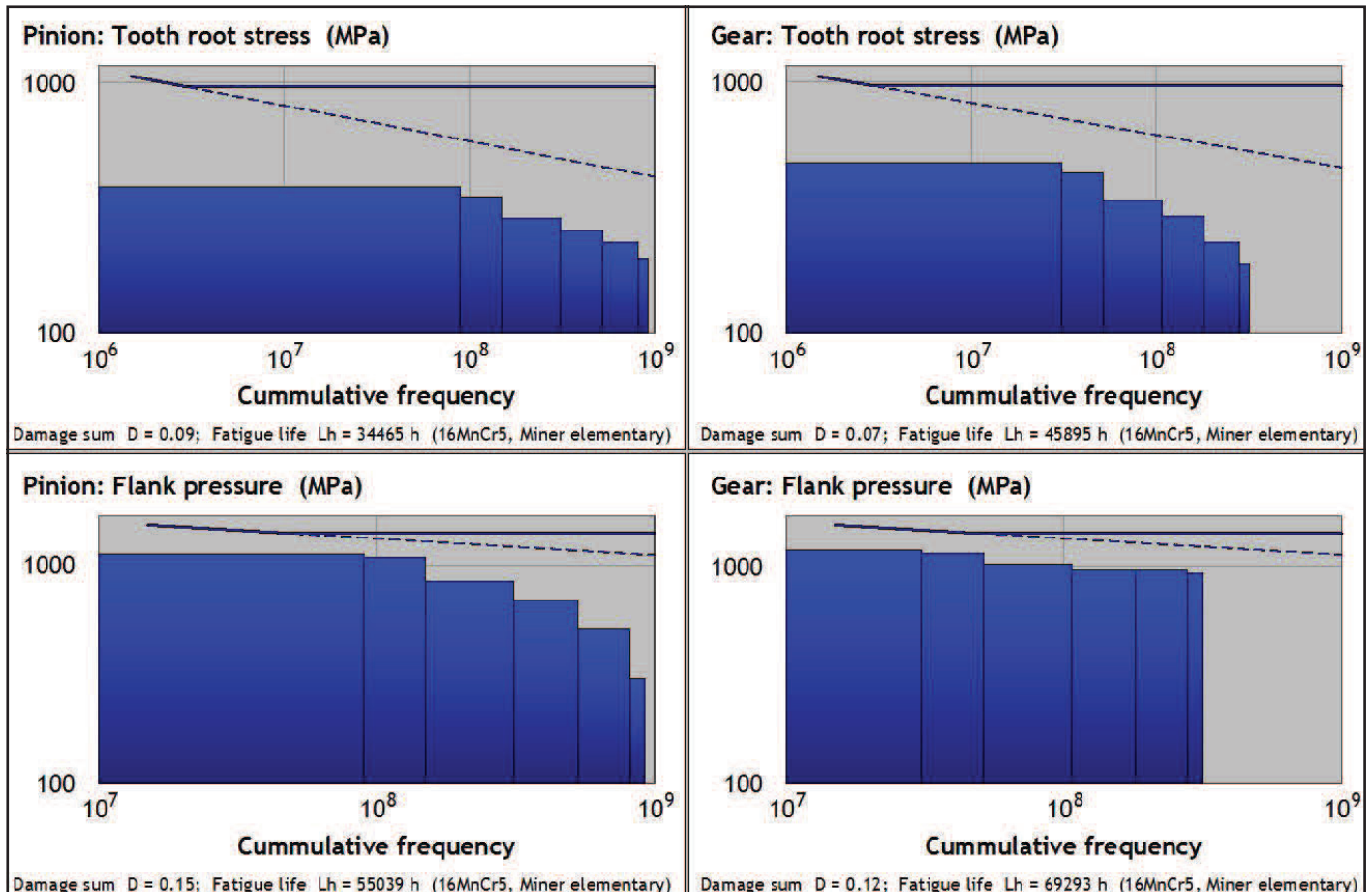
Fig 4: Load spectrum and Wohler curves of the gear without tooth flank modification.
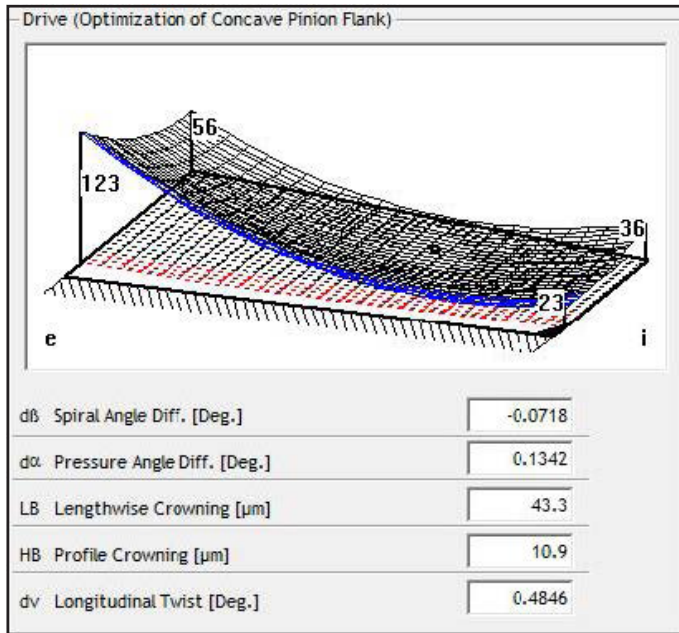
Fig 2: Ease-off without tooth flank modification.
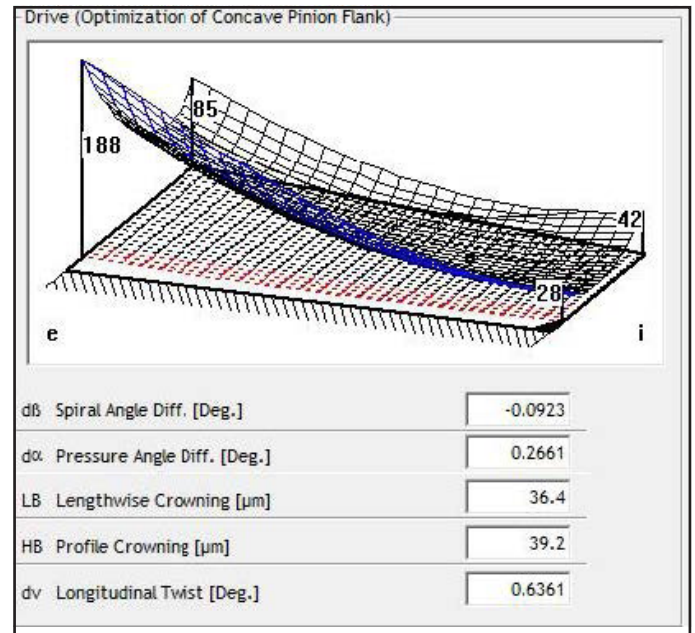
Fig 3: Ease-off with tooth flank modification.

time-consuming tests?

In the latest version of KIMoS, Klingelnberg makes it possible to calculate a bevel gear's service life for specific operational loads, as well as for face hobbing design and face milling.

To calculate the fatigue strength of a bevel gear, three basic elements must be known: the precise shape of the gear, the properties of the material, and the running conditions of the gear set. All of these elements are taken into account in KIMoS. Fatigue strength is calculated using Miner's rule based on the linear cumulative damage hypothesis.

The cumulative damage to a gear pair can be predicted by combining the load spectrum, the load concentration on the
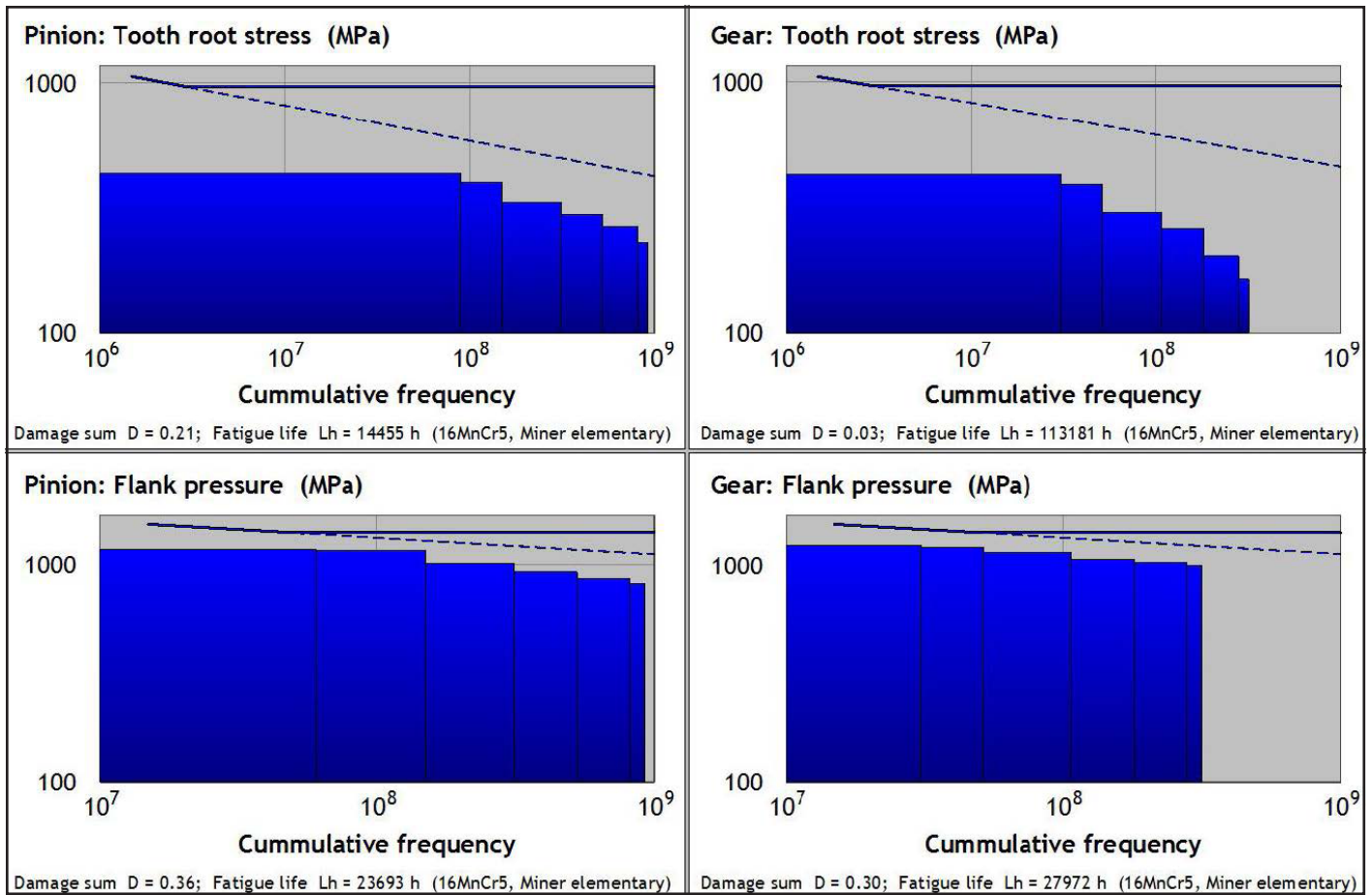
Fig 5: Load spectrum and Wohler curves of the gear with tooth flank modification.

tooth surface, as well as the bending stress in the tooth root and the cyclic stress-strain properties of the material. If the total cumulative damage for pitting and breakage is available, KIMoS can calculate the service life of the bevel gear set.

To generate a load spectrum with an extremely limited number of load cases, one of the counting methods must be used for the load cycles. If real load conditions comprising many different load cycles (for example with the rain flow method) are used to start with, these cyclic events can be counted, making it possible to convert real operational load cycles with an extremely reduced number of load cases into a load spectrum.

Will service life calculation of toothed gears replace endurance testing in the future?

The answer is a clear no. But calculating the fatigue strength enables an extremely effective comparison of different designs. The expected service life of a gewar pair can be estimated quite accurately when endurance test data exist for one of the designs.

That is why KIMoS gives the design engineer the ability to create a design that not only meets the geometry and noise emission requirements, but also takes fatigue life into account.

The following example shows two designs with the same dimensional data, but different with and without flank form modifications shown in Figure 2 and 3. The toothed gear data are z=13/38 teeth, the outside pitch diameter of the ring gear is 250 mm, and the hypoid offset is 20 mm.

This example shows the potential of tooth flank modifications. The design on the left has a service life of approx. 14 000 h, which is limited by the tooth root stress on the pinion. The design on the right has a service life of approx. 34 000 h, but here, too, the calculated cause of failure will be tooth breakage on the pinion.

Not only does KIMoS empower the design engineer to optimize noise behavior and load capacity, but it also enables service life optimization of a gear set for specific load cases. This paves the way for new potential in lightweight design and enables more efficient and robust gear designs.

www.klingelnberg.com

MANDO G211

Segmented mandrel for gear cutting

- Segmented mandrel with slim interference contour
- Rigid radial clamping with pull-back effect
- Large clamping range and vibration dampening due to vulcanized clamping bushings
- In-stock standard segmented clamping bushings
- Three end-stop levels
- Integrated flushing channels

1.800.281.5734
Germantown, WI USA
www.hainbuchamerica.com

America
HAINBUCH
WORKHOLDING TECHNOLOGY

Forest City Gear
ADDS ZEISS CMM TO QUALITY ASSURANCE DEPARTMENT

Forest City Gear has expanded the capabilities of its Quality Assurance Department with the addition of a Zeiss ACCURA Coordinate Measuring Machine.

The next-generation bridge-type Zeiss is Forest City Gear's fourth CNC inspection system, and is particularly well suited for very fast, complete analytical inspection of all types of high precision fine- and medium-pitch cylindrical gears. A variety of interchangeable Zeiss sensors provide a high degree of flexibility and faster calibration, approach and scanning for lead, involute, pitch, surface finish and other critical features across a wide size range.

The system also features a particularly compact and ergonomic design, making it ideal for Forest City Gear's fast-expanding, busy Quality Assurance room. The Zeiss ACCURA's bridge, for example, is made of steel and aluminum, making it extremely rigid, yet slim and compact. The reduced weight of the moving parts improves the dynamic rigidity and speed of the machine.

"The added capacity of the Zeiss ACCURA has now enabled Forest City Gear to move its existing Zeiss CONTURA CMM to meet the quality requirements of its new, stand-alone gear blanking facility," according to Forest City Gear Quality Assurance Lead, Amy Sovina. "The ACCURA couldn't have arrived at a better time, freeing up the CONTURA so we could put it in close proximity to the blanking operation and thus
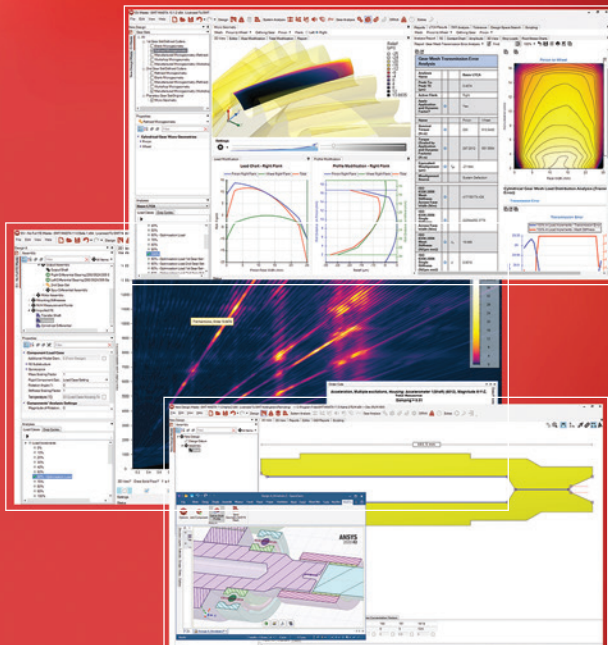
eliminate the travel time for inspection of blanks," says Sovina. "The Zeiss ACCURA checks all the metrology boxes. With quality and throughput requirements never higher in all the industries we serve, this system is the perfect addition."

Liebherr

EXPANDS GENERATING AND PROFILE GRINDING TECHNOLOGY

Liebherr recently introduced a new series of generating and profile grinding machines for hard machining of external and internal gears on workpieces with diameters of up to 500 millimeters. The LGG series follows the successful Liebherr LCS 300-500 series. With an impressive range of added features, they offer more flexibility and grinding performance with a significantly reduced footprint.

The LGG 500 and its sister models the LGG 300, LGG 380 and the manual solution LGG 700 M are Liebherr's new series to succeed the LCS 300-500 generating and profile grinding machines that have been popular all over the world. The machines are suitable for generating grinding, profile grinding and both processes combined. The new series also retains essential features such as maximum precision, robust machine design and high flexibility. Corundum and CBN tools are available, the latter from Liebherr's own production. The high level of performance and versatility now also extends to hard machining of internal gears: changing from external to internal profile grinding is possible in less than 30 minutes. There are also newly developed grinding heads and even more machine options.

On the outside, the first thing that catches the eye is the machine's new, compact monolith design. With the footprint reduced by a third, the work area is just as big as the one of the previous model, ensuring maximum ease of use even with manual loading. With an axial travel range of up to 1,000 millimeters, the machine column allows the machining of long shafts, for example for commercial vehicles.

Three different directly driven grinding heads with optimized rigidity are available for the new series, and can be configured precisely as the customer requires. The grinding heads have a large effective speed range, which allows the use of large and small grinding worms at optimal cutting speed. Liebherr is a pioneer when it comes to machining collision gears with dressable and dressing-free grinding worms: the compact counter bearing ensures the highest grinding and polishing quality for critical components. Optionally, the grinding heads can be equipped or retrofitted with an auxiliary spindle or an internal grinding arm.

The most powerful grinding head, the GH 320 CB, can easily handle generating grinding jobs up to module 14 mm. Grinding worms with a volume of up to 320 millimeters in diameter and 250 millimeters in length are used. Cutting speeds of up to 80 m/s achieve high grinding performance for dimensionally critical components at much shorter grinding times, especially for

workpieces with long face widths.

The selection of direct drive tables is tailored to the specific component range with regard to the component weight (up to 100 kilograms), required machining speed and optimum pitch quality. The robustly built table allows speeds of up to 2,000 rpm for generating grinding and highly accurate positioning for profile grinding.

The new LGG machine generation offers the best possible compatibility with the available clamping fixtures, so that the existing equipment can be used or inexpensively modified. The Liebherr OpenConnect concept allows GDE data to be imported and exported which, together with the gear check integrated in the machine, ensures short setup times for heavy components.

"With the new generation of machines, the customer is not buying a specialist machine, but an all-rounder that embodies maximum flexibility combined with optimum grinding performance and quality," explains Martin Schwarzmann, product manager for gear cutting machines at Liebherr. "A fully equipped grinding machine for external and internal gears with immense grinding performance as well as an automation system — that's a very versatile combination and pretty unique in the market."

The machine offers flexibility for small and medium batch sizes. With its integrated ringloader automation system and configurable Liebherr storage systems, it creates a unique basis for highly efficient large-scale production, for example of complete planetary gears, including ring gears. The huge scope of possibilities allows companies, and in particular small businesses, to carry out a wider range of processing so that they can respond much more flexibly to future market requirements.
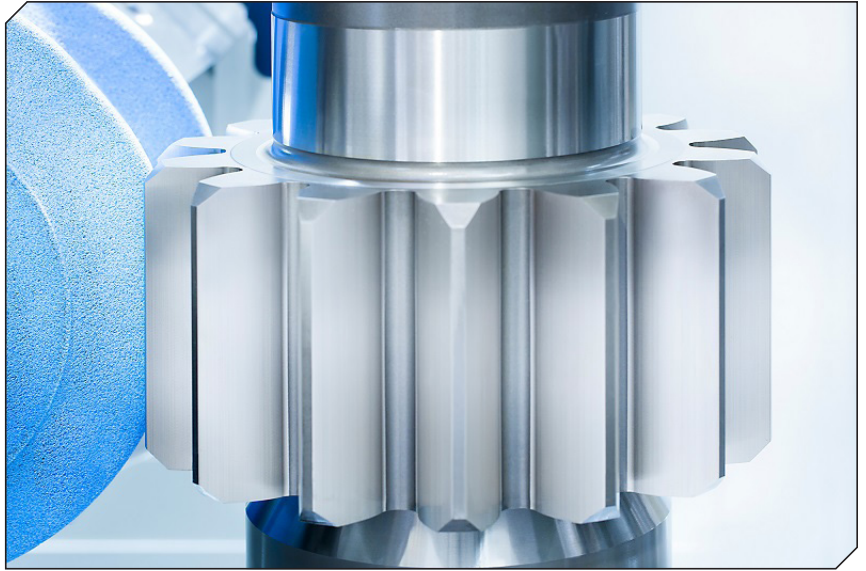
www.liebherr.com
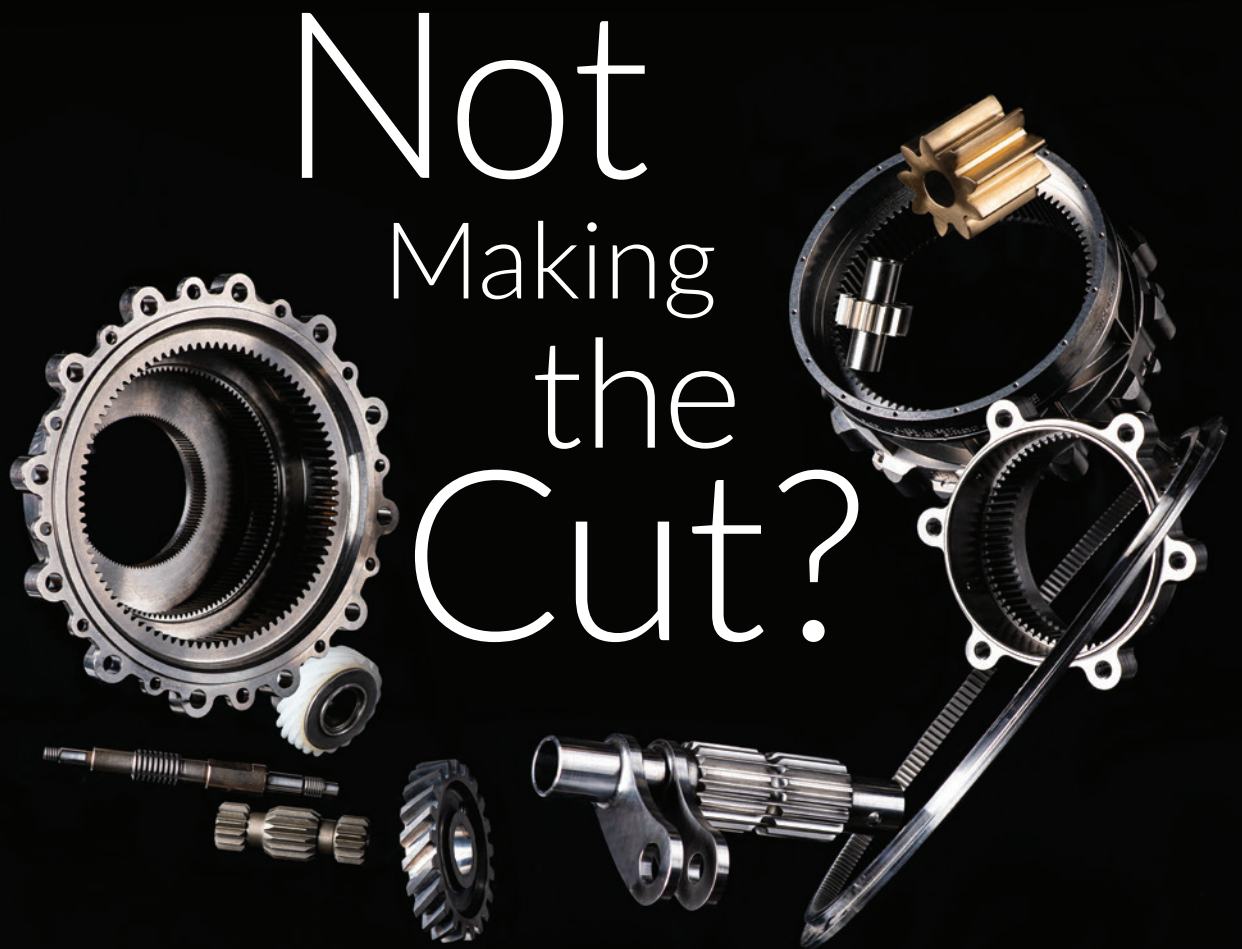
Motus Labs
OFFERS M-DRIVE SERIES

Motus Labs, a designer and manufacturer of mechanical motion control solutions for the industrial, service, and collaborative robot and automation markets, has announced commercial availability of the Motus Labs ML1000 series of M-Drives. The disruptive drive architecture uses mating blocks or surfaces instead of traditional gear teeth resulting in a more rigid drive at a lower weight with up to twice the torque density and 15% greater efficiencies compared to competitive strain wave drives. These performance benefits provide a lower overall solution cost, increased precision, reach, speed, and longer life — significantly improving the ROI for robot end-users.

"We are excited to bring to market a revolutionary new drive that enables robot manufacturers the ability to differentiate their robots and create more value for their end-users," said Joe Pollard, chief executive officer and co-founder at Motus Labs. "Robot end-users gain superior price to performance, often saving up to $100,000 over the life of the robot and the ability to extend into markets previously unattainable, basically enabling companies to build what they can imagine," added Pollard.

The M-Drive architecture was awarded its first patent in 2016 after five years of research and development by Carlos Hoefken, inventor, and automation engineer. Hoefken identified an opportunity to design a significantly new robotic gear drive that would increase performance and add value. The drive is the most critical, differentiating, and expensive component of the robot, that determines positioning accuracy and speed of operation. The patented design utilizes a series of cam-driven blocks that engage over 80% of the output ring surface area versus 10 -15% with traditional drives. Motus Labs currently has seven U.S. patents granted and eight additional patents pending.

"Industry 4.0 is on the horizon, and AI-driven robots require smart actuators that require smart gear drives — and that is where we started with the M-Drive," said Carlos Hoefken, inventor, and founder at Motus Labs. "The M-Drive architecture aims to address three objectives. First, increase precision and drive performance and lower overall robot

Ipsen
PDMETRICS OFFERS ADDITIONAL DIAGNOSTICS

solution costs. Second, be an enabling technology for new applications in adaptive robotics. Finally, continue our innovative approach and bring to market smart robot components as the industry shifts from traditional automation to smart manufacturing," added Hoefken.

The M-DRIVE ML1000 Series of hollow shaft drives includes standard gear drive sizes ranging from 17–40. The family of drives accommodates the requirements of a fully articulated robot which has up to seven actuators or joints from the 'shoulder' or largest drive to the 'wrist' or smallest drive. The M-Drive series has up to twice the torque-to-weight ratio of the strain wave counterpart in the same size, resulting in reduced gear drive size and weight at each joint, lower overall arm mass, and moment of inertia, and smaller motor size and weight.

www.motus-labs.com

A new feature on the PdMetrics dashboard monitors incoming three-phase utilities, voltage and frequency on Ipsen's Titan 2.0 vacuum furnaces. This addition offers further diagnostics for the diffusion pump heater assembly.

By adding these parameters, PdMetrics adjusts the expected kilowatt usage based on incoming line voltage, reporting precise diagnostic data, avoiding the potential for false alarms. Ipsen has nearly 100 Titan 2.0 furnace installations with the software.

Ipsen's predictive maintenance software for vacuum furnaces was developed in 2016 and helps customers minimize high-cost events and maximize up time. The software is available on any model of Ipsen furnace new or old.

Ipsen's product development team is continuously working to improve the capabilities of PdMetrics to provide faster and smarter diagnostics. The latest features also include a snooze button to silence alarms while they are being addressed and an automated health report.

www.ipsenusa.com

Mazak

EZ SERIES OFFERS STREAMLINED STRUCTURE AND ADVANCED MACHINING TECHNOLOGY

The Mazak Ez Series includes QT-Ez CNC Turning Centers, VC-Ez Vertical Machining Centers and MAZATROL SmoothEz CNCs.

With their space-saving footprints, the Mazak Ez Series fits in any shop without sacrificing rigidity or performance. The redesigned sheet-metal enclosures and structures aren't just more compact, they also pair easily with automation solutions such as Mazak's CC-10 cobot system. To achieve the best-possible price-to-performance ratio for your shop's application requirements, the series also includes a range of standard or optional integrated chip management and coolant systems.

Optimizing per-part costs requires much more than smart product design — every part of the Mazak iSMART Factory production system was rigorously reexamined to make the Ez Series as affordable as possible. The result is a simplified, accelerated machine assembly process that places high-quality machines in customers' shops ASAP.

A key benefit of the Ez Series is its new 200V electrical system, which makes bulky transformers unnecessary for many shops and helps reduce overall power consumption. A single, common electrical cabinet can support the entire machine series, providing efficient production and additional cost savings.

Prudent lightweighting and advanced machine bed design render these machines stiff enough to handle tough applications and materials, yet light enough to transport with a forklift. These machines aren't just "Ez" in terms of usability — the transportation, rigging, installation and serviceability have all been built to be Ez as well, saving everyone time that's better spent cutting parts.
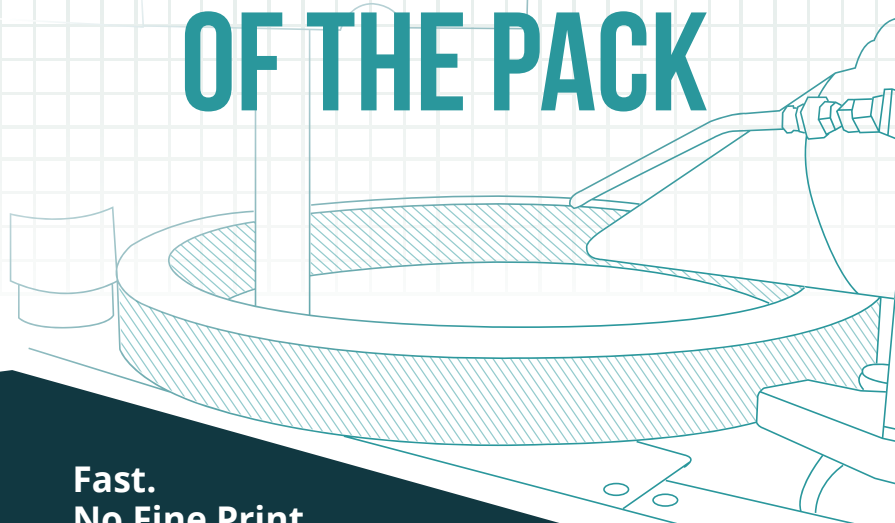
www.mazakusa.com

MHI

INTRODUCES GEAR SHAPING MACHINE FOR SMALL-MODULE GEARS USED IN ROBOTS

Mitsubishi Heavy Industries Machine Tool Co., Ltd., a Shiga-based part of Mitsubishi Heavy Industries, Ltd. (MHI) Group, has newly developed the "SE25FR Plus," a gear shaping machine dedicated to making high-precision small-module gears used in robots. The company has simultaneously developed a small-module cutting tool specifically for the new gear shaping machine. Full-fledged marketing of both new items will commence in March. By providing this dual support in high-precision gear cutting machines and cutting tools from a single source, MHI Machine Tool looks to respond to the need for reduction gears of increasingly higher precision in the expanding global robot market.

MHI Machine Tool launched its "FR Series" of high-precision gear cutting machines in August 2020. The new SE25FR Plus is a high-end model developed especially for shaping strain wave gears which require high precision. Outstanding rotation precision has been achieved through the adoption of ultra-high-precision bearings and direct-drive motors in the two core components: the worktable and the cutter head. This provides gear cutting precision of ISO class 3, enabling cutting precision higher than the model SE25FR, which is of ISO class 6.

The small-module cutting tool to be launched together with the SE25FR Plus features a newly developed dedicated tool material and a special coating, "MightyShield μ" for micromachining. The tool material incorporates carbide particles offering improved toughness and wear resistance, while the new coating produces a uniform thin film below 2 micrometers (μm) thick that has no impact on tool shape error. The result is outstanding shaping even with difficult-to-cut materials, and the ability to achieve gear shapes down to the submicron level. Furthermore, MHI Machine Tool provides one-stop support in gear cutting machines and cutting tools, from the prototype development stage through mass production.

www.mitsubishigearcenter.com

Siemens Digital
ENHANCES SIMCENTER TESTLAB

Siemens Digital Industries Software has announced the availability of the latest release of *Simcenter Testlab* software. It is part of the *Simcenter* portfolio of simulation and test solutions within the *Siemens Xcelerator* portfolio of integrated software and services. The latest release includes updates to *Simcenter Testlab Neo*, enhanced model-based systems testing, introduces a new technology for accelerating structural dynamics called *Digital Image Correlation*, and frontloads analysis of full vehicle noise, vibration and harshness (NVH) during the design process. Test and simulation engineers as well as test campaign managers can benefit from this latest release for multi-disciplinary test-based performance engineering, specifically designed to offer test and simulation teams new capabilities to innovate smart products more productively.
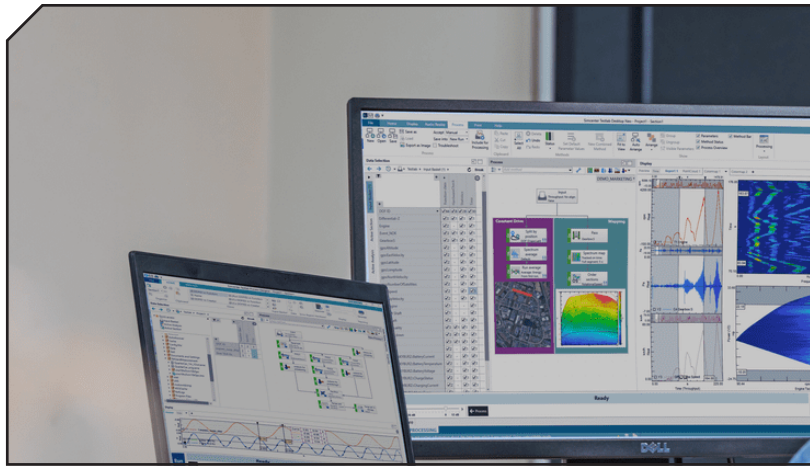
The latest developments within industry can bring innovation, but also bring new demands and requirements, including the need to achieve realistic and predictive results more efficiently than ever before. Test teams are now working closely together with simulation teams, as the ever-declining number of prototypes available calls for the use of digital twins in the early stages of development. At the same time, there is an ever present need to obtain the most information possible from massive amounts of data, collected by testing and generated by simulation.

In *Simcenter Testlab*, test engineers have access to new technologies that can increase productivity when collecting and processing data. The effort to compare and correlate test and simulation results is minimized, and validated simulation models - digital twins - can be used during the physical testing activities to generate valuable extra data. At the same time, *Simcenter Testlab* provides direct data access to many simulation results formats, enabling simulation engineers to benefit from the data processing capabilities within the software as well as the consistency of selected processing functions and parameters between the physical and virtual tests.

Schunk
IMPROVES ACCESSIBILITY WITH 5-AXIS VISE
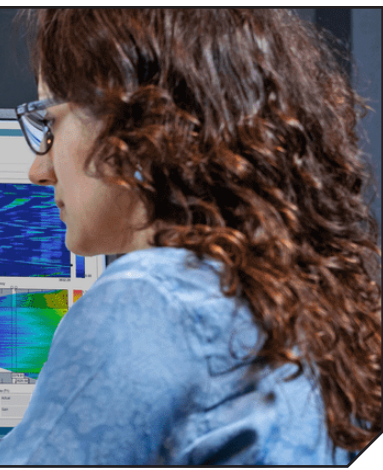
Characterizing the structural behavior of materials and structures under load is a key enabler to improving designs and developing high performance products. New developments in digital camera technology in combination with high-performant *Digital Image Correlation* (DIC) techniques allow users to extract full-field 3D geometry, displacement and strain information, under any load and for almost any type of material, with limited instrumentation. DIC can then be used to identify material properties, validating numerical models and assessing the strength of materials and components, and analyze structural vibrations and dynamic responses to enable faster and more responsive development cycles.

The component-based transfer path analysis solution with *Simcenter Testlab* also enables the evaluation of vehicle performance in early design stages. It maximizes the usage of all available information on sub-systems and components, whether that be measurement data or simulation results. This unique and comprehensive solution can measure, post-process and publish accurate and consistent component NVH models, offering users improved component characterization methods and predictive NVH synthesis supporting performance evaluation of virtual prototype assemblies.

The new *Simcenter Testlab 2021.1* software release brings these and many other enhancements to offer test and simulation teams a solution to integrate physical testing and virtual simulation throughout the development cycle, bringing new capabilities to innovate smart products more efficiently.

www.sw.siemens.com

The KONTEC KSX-C2, a 5-axis vise from Schunk, provides new opportunities for high-precision 6-sided machining. With a striking, upwardly tapered outside contour, the KONTEC KSX-C2 improves accessibility with standard tools. With its active jaw pull-down the KONTEC KSX-C2 achieves excellent results in terms of plane-parallelism and perpendicularity, and therefore creates ideal preconditions for challenging 6-sided machining.

The vise is also setting benchmarks with its adjustable center, even when it comes to set-up times: due to a tool-free jaw quick-change system, reversible jaws for enlarging the clamping area as well as a unique basic jaw stroke of 130 mm which is second to none on the market, the vise can be quickly and precisely converted for a new range of parts. A broad range of quick-change jaws is available for this purpose. Moreover, the clamping range can be enlarged with a standardized piston rod extension.

Integrated elastomer damping

A torque wrench is used for continuously adjusting the clamping forces of the KONTEC KSX-C2, and a maximum of 40 kN at a torque of 120 Nm can be achieved. Therefore, this expert vise in 6-sided machining has a lot of power for safe holding — even in the case of minimum clamping surfaces. The forces for clamping sensitive parts can be finely adjusted. The long guiding system and the arrangement of the clamping mechanism ensure a rigid, dimensionally stable set-up. The integrated elastomer damping absorbs occurring oscillations during machining, resulting in excellent workpiece surface quality and tool service life. The drive and adjustment mechanisms of the 5-axis vise are fully encapsulated, making it perfectly equipped against chips, dirt, and coolant.

Comprehensive standard program

The Schunk KONTEC KSX-C2 is maintenance-free and is offered in four base body lengths (330 mm, 430 mm, 500 mm, 630 mm, 800 mm) and in two different heights (175 mm, 214 mm). It seamlessly fits into the modular system for high-efficient workpiece clamping from Schunk and can be quickly combined with the VERO-S quick-change pallet system or exchanged at a maximum repeat accuracy on the machine table. The necessary clamping pins can be directly integrated in the base body of the 5-axis vise without requiring adapter plates. As clamping is done by tension, no bending load occurs on the base body if a quick-change pallet system is used.

Schunk.com

WE'RE ALL IN »»

MOVING THE FUTURE.

3M Science. Applied to Life.™

Advanced Heat Treat Corp.

ASH GEAR AND SUPPLY — WORLD'S LARGEST GEAR TOOL INVENTORY

Bevel Gears (India) Pvt. Ltd.

Blaser. SWISSLUBE

BK BOURN & KOCH

BUNTING Bunting-DuBois

CAPSTAN ATLANTIC

CGI

Circle Gear

Columbia Gear Corporation — A SUBSIDIARY OF INDUSTRIAL MANUFACTURING COMPANY

Dontyne Systems

DOPPLER GEAR COMPANY

DTR PERFECTION MOVES US

DVS TECHNOLOGY AMERICA

EMAG

ENGINEERED ABRASIVES®

euro·tech

FOREST CITY GEAR

FOERSTER

Gear Motions Precision in Motion

GEARSolutions

Gleason

GREAT TAIWAN GEAR

GWJ TECHNOLOGY

America HAINBUCH WORKHOLDING TECHNOLOGY

HAYES MANUFACTURING

HELIOS gear products

HOFFMANN — Hoffmann Filter Corporation • Your Partner in Filtration

ph HORN ph

IMT FORGE GROUP

Member IMC Group Ingersoll Cutting Tools

INNOVATIVE RACK & GEAR We Help You Move the World

CELEBRATING 25 YEARS

IPM Precision Machining & Gear Cutting

KAPP NILES

KLINGELNBERG

LIEBHERR

LOUIS BELET Swiss cutting tools

MTB Machine Tool Builders — REBUILDING • RECONTROLLING • SERVICE

MIL MAGNETIC INSPECTION LABORATORY, INC.

MB METAL TECHNOLOGIES

MOTION + POWER
TECHNOLOGY EXPO

CFC Fixtures Increase Productivity in Carburizing, Nitriding and FNC

Mark Hemsath, Seco/Vacuum Technologies

Furnaces for heat treating require capital expenditures, they take up valuable plant floor space and they can be a bottleneck to productivity in a manufacturing cell. For smaller and critical component part sizes, like gears, properly fixturing the parts is a necessity. Fixturing needs to be designed for best heat transfer, for proper surface engineering and for maintaining critical dimensions. Cast and wrought alloys are most widely used as furnace fixtures, but they consume a large amount of the available load weight, which limits furnace throughput. As well, they lose shape over time and with rapid cooling can lose shape quickly.

Recently, CFC tooling (commonly called Carbon Fiber Composite) has been employed allowing significant benefits in heat treating, of which weight reduction is a major benefit. However— depending upon the heat treatment or surface engineering process—there are additional benefits to CFC tooling, as well.

In recent years CFC material has become more affordable and designs have become much better proven. Manufacturing methods for CFC have matured to the point where we now can expect long fixture tooling life, which decreases ownership costs, even compared to alloys.

However, component manufacturers and furnace manufacturers have been slow to specify these fixtures, mainly due to high initial tooling costs and perceived lack of robustness of the tooling during material handling. Applications for CFC in heat treatment are not just for vacuum furnaces for aerospace applications anymore. Applications today range from ferritic nitrocarburizing and nitriding to gas carburizing, oil quenching and even air tempering. Figure 1 shows tooling for a gear application for nitriding and atmosphere stress relieving. CFC tooling is emerging as an alternative and as a workhorse in standard, high volume manufacturing plants. As more CFC tooling has been hitting the market, papers and testimonials are proliferating.

Why CFC Furnace Tooling?

In recent months there has been quite a bit of information published by manufacturers of CFC fixtures used in heat treating (Refs. 1–3). Referenced here are some of these articles and they are excellent resources. To recap, the most important features of CFC versus alloy are:
• CFC fixtures are much stronger at high temperature (Ref. 2).
• CFC fixtures retain their precision shape during heating,
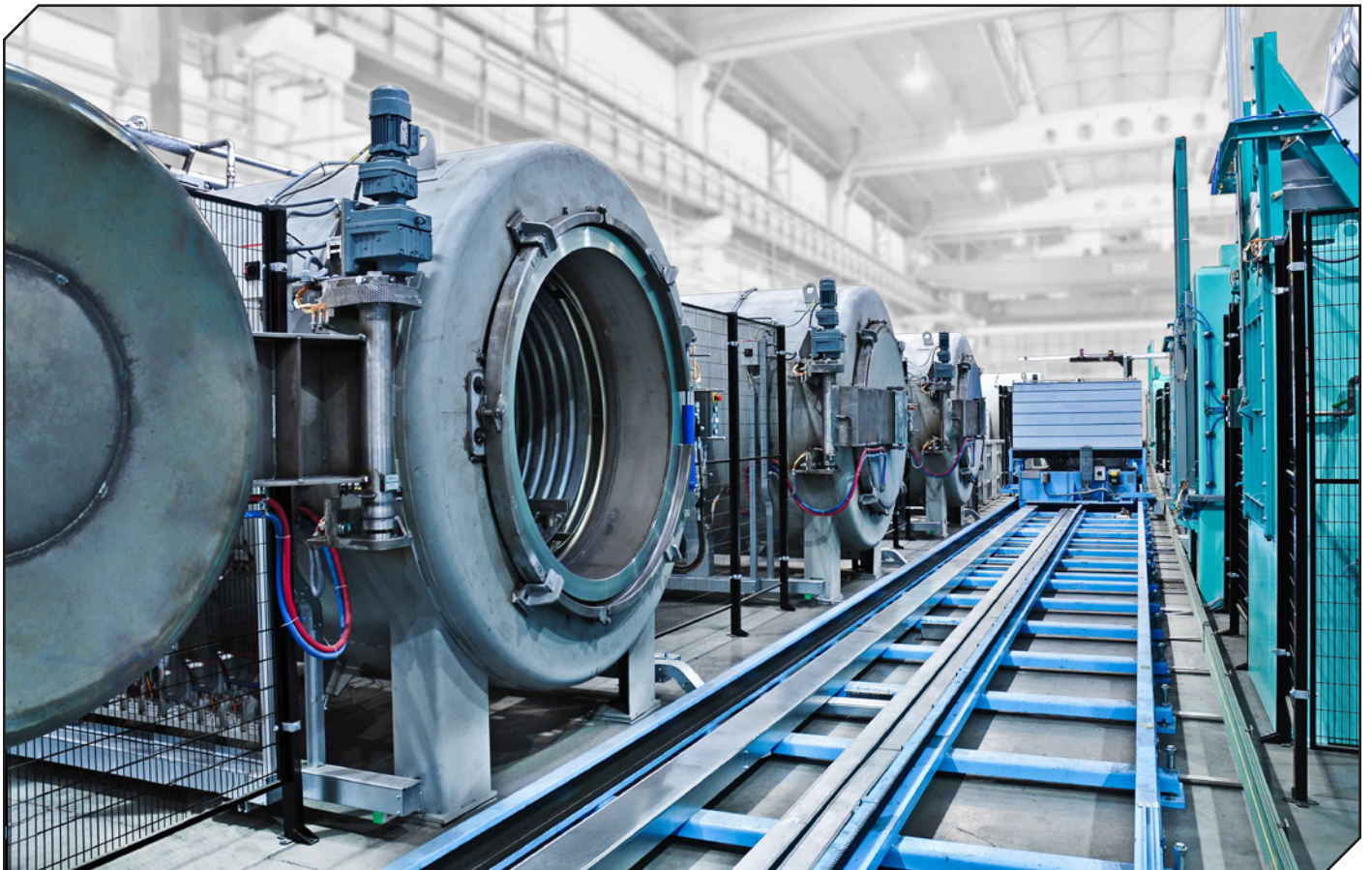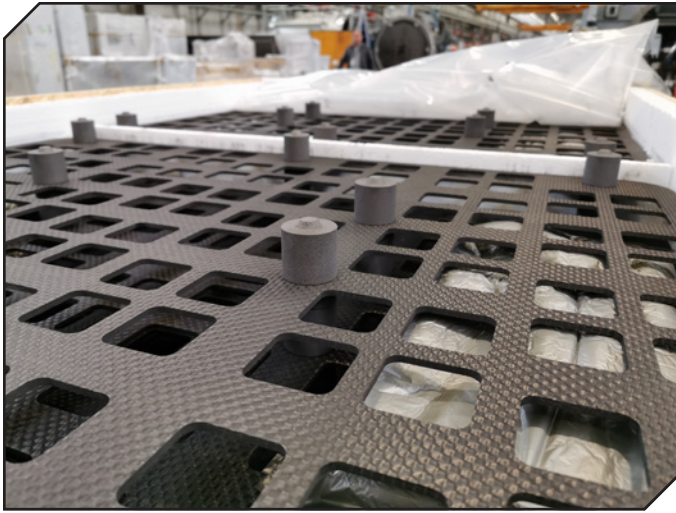
Figure 1 CFC fixture designed for holding gears, for maximum gases flow, and for supporting the layer above (courtesy of Nippon Kornmeyer).

Figure 2 Furnace for nitriding and ferritic nitrocarburizing (photo courtesy of Seco/Vacuum Technologies).

Figure 3 Precision internal furnace fork loading for oil quenching compatible with CFC trays.

Figure 4 Clean integral quench carburizing furnace with no toxic gases and precision, high-volume carburizing for gears, shafts, and various other components.

quenching, and over time (no alloy creep).
- CFC fixtures can be coated to prevent oxidation and oil degradation.
- CFC fixtures are around 10–20% of the weight of alloy (Refs. 1,2).

Concerns with CFC fixtures include:
- CFC fixtures, at elevated temperatures (typically over 2,000F), may need to employ special holders for contact points with metal parts due to eutectic welding and some further reaction issues with the carbon (Ref. 3).
- CFC Fixtures are not very impact resistant and must be handled differently than alloys.

In standard integral oil quench carburizing furnaces, for example, it may be more advantageous to use alloy base plates (Ref. 3). However, this again adds weight and potential for base plate distortions. New furnace designs exist in the integral quench market which can easily use CFC base plates (Ref. 4). In this newer and modern furnace design, loading and internal movement from heating chamber to oil quench is more advantageous to CFC fixtures where a fork-style loader is used internally (Figures 3 and 4) to carry the load, rather than pushing or pulling the load. As a further example of productivity gains, in carburizing, with a load capacity of 1500 kg, an all-alloy fixture can be around 300–700 kg just for the fixtures. This can mean up to 50% of the load is fixture weight when using alloy fixtures. Even at 20% of the alloy weight, CFC fixtures would only consume 140kg, or less than 10% of the load weight. This translates into much more net production and fewer furnaces needed when using CFC for the same annual production.

As well, CFC fixtures can be coated to prevent oil and oxygen degradation. In the application shown in Figure 1, using a nitriding furnace like is shown in Figure 2 can require a pre-oxidation step during ferritic nitrocarburizing (FNC) at around 350ºC. This step helps activate the surface of the metal part and CFC fixtures are not affected. In harden and quench applications, if quenched parts would be air tempered (following any carburizing/hardening), then a coating—known as chemical vapor infiltration (CVI)—would be recommended which allows air tempering with oxidation resistance up to 820ºC

(1500°F) for the carbon fixtures.

As well, with oil quenching applications, the load and fixtures must be washed of oils. The coating helps to stop oil infiltration into the carbon fiber voids by instead adding carbon infiltration via the CVI process. CVI is a type of CVD (chemical vapor deposition) in which the gases infiltrate the pores and cause a densification of the structure of the material (*source: Nippon Kornmeyer data sheet [NK-PyC]*). This resists absorption of oils (and water) into the fiber matrix pores and allows washing of the fixtures. Any remaining oils and moisture after washing would come out during the tempering process.

CFC Fixtures are Becoming Common

The loading density possible by using CFC fixtures allows for much more compact and precision loading of parts, which can translate into fewer furnaces. Figure 5 shows how tightly packed parts can be positioned and still allow for adequate gases flows and precise part support. In one heat treating department, we found that CFC fixtures allowed for very dense loading of light gears and allowed the reduction of required furnaces from close to 4 units to only two units. This saved significant floor space in the cell (floor space is extremely tight in any manufacturing plant). CFC fixtures allow for more compact and precision loading of the parts, which translates into more parts per load and the costs of the fixtures was more than offset by fewer furnaces.

As an example in Figure 5, with a large enough batch furnace, 1,000 gears are possible per load. The weight of the tooling on a large size load would be only about 10% of the load. The layering of parts on a very flat surface is also critical for minimizing distortion. This type of load creation is just not possible with alloy mesh separation sheets, cast alloy or fabricated alloy. The upfront cost differential of CFC tooling is totally offset by longer tooling life and by higher furnace productivity. It should be noted that the installation shown in Figure 2 processes over 1 million gears per year for FNC.
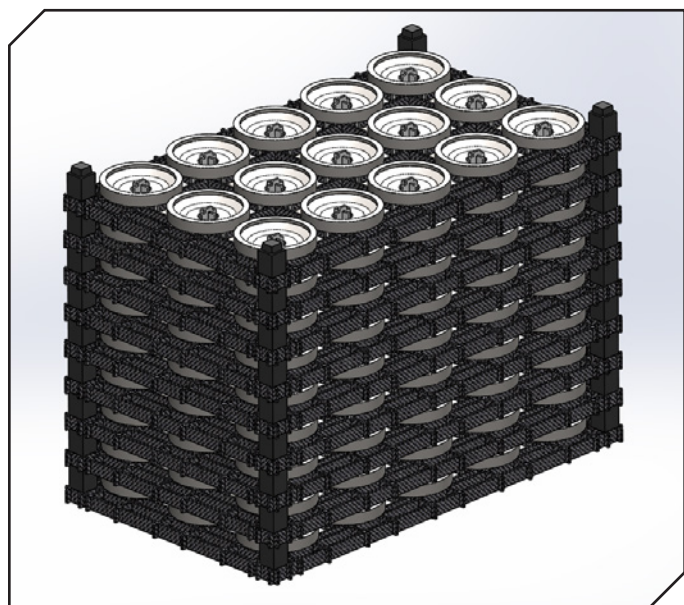
Advanced Fixtures, Advanced Clean Furnaces

Figure 2 shows gas nitriding furnaces with vacuum purging, and also, the option for ferritic nitrocarburizing with pre and post oxidation. CFC fixtures work with all these options. In addition to advanced fixturing, furnaces today need to run cool, run quiet and run without excessive toxic gases. Often, they are located near CNC machining centers and in climate-controlled buildings. This means vacuum tight construction allows these advanced furnace designs to co-exist in a cleaner room environment. Both the gas nitriding furnaces shown and the gas carburizing furnace shown in Figure 4 can operate and co-exist with CNC type equipment. The furnaces operate cool and without ammonia odors or toxic carbon monoxide. They run with minimal noises, no hot walls or doors, no billowing smoke, or flames. It is now much easier to "in-source" heat treating, as these machines can be turned on and off with no issues and no idling required between shifts or on weekends. The days of hot, smokey, smelly and dingey heat treating are gone. As well, being co-located with manufacturing, this all saves work-in-process time compared to outsourcing heat treating. Freight costs and handling damages are virtually eliminated.

Long Parts and CFC Tooling

In heat treating vertical parts, keeping very hot parts straight when they are dunked into oil and rapidly quenched is very difficult. By the nature of lowering a load into oil, or even gas quenching with variable gas flows, non-uniform cooling is guaranteed in all instances. Controlling these massive thermal forces and distortions is critical and any changing uniformity leads to excessive part distortions. For lowering long parts into oils, straightness of entry as the part enters the oil is mandatory. However, it is difficult to assure straight entry in a high production environment. CFC tooling allows for precision fixturing designs. When one combines this with precision internal movement, repeatable results are assured. Alloy fixtures distort and creep over time, so precision fixturing is never guaranteed.

Figure 6 For vertical applications and oil quenching, precision positioning of parts like shafts is critical.

Figure 5 Typical CFC tooling with gears closely spaced to maximize volume (courtesy of Nippon Kornmeyer).

CFC stays straight and precise, even after being subjected to quench oils over and over. Alloy fixtures distort much like the parts they are holding. Figure 6 shows how a precision fixture, made of CFC, looks for long parts.

Conclusion

Heat treating is changing, and it is changing rapidly. Advances in furnace designs and fixturing are opening up new ways of thinking. Precision fixtures like CFC allow weight reduction, long life, and precision load building. Furnaces take up valuable plant floor space, so methods need employed that maximize their use. Critical parts, like gears, demand precision tooling which only CFC can offer. CFC is lighter, stronger at temperature and keeps its shape even after the abuses it sees with years of use in a furnace environment. Combining all these benefits of CFC tooling, the savings may far exceed the initial capital cost premium and should be considered, especially with today's modern furnaces. ⚙

References

1. Kornmeyer, Torsten "Graphite, CFC and Insulation Materials in Furnace Construction" paper presented at AWT Heat Treaters' Circles (*awt-online.org*), February 2017.
2. Demmel, Joerg "Why CFC Fixtures are a Must for Modern Heat Treaters," Furnaces North America presentation, October 2020.
3. Cronite Group, "CFC/Alloy Hybrid — The Next Generation Solution" *The Monty* website (*www.themonty.com*) August 2020.
4. Hemsath, Mark "Intelligent Gas Carburizing with Super IQ" *Thermal Processing*, September 2019.
5. Hemsath, Mark, et al "Nitrocarburizing of Gears using the ZeroFlow Method in Large Volume Production" *Thermal Processing*, September 2015.

Mark Hemsath is vice president, Super IQ and Nitriding at Seco/Vacuum Technologies, LLC, a Seco/Warwick Group Company. With 30 years of experience in heat treating and the industrial furnace equipment market, he is in charge of all North American furnace sales for gas nitriding and gas carburizing.

For Related Articles Search

heat treating

at www.geartechnology.com

Challenges and New Market Opportunities in Heat Treating

Gear Technology recently caught up with Mark Hemsath, Seco/Warwick, for a brief discussion on the heat treat industry in 2021:

GT: What's the current state of the heat treat market in 2021?

MH: Had I answered this a year ago, it would have been "It's great!" So now, there are definite challenges, thanks to a year of COVID. However, all things considered, there is strength in a lot of areas with really aerospace being the main problem area. MTI, which supports commercial heat treaters, is showing growth in most months since last summer, but we are far away from maximum capacity. Recent data shows that the U.S. economy had the best showing last year of all the major developed countries, except for China. So, we are coming out of COVID damaged, but not destroyed and heat treating is the same. There have been major structural changes everywhere, but in general, it could have been a lot worse.

GT: What market trends will be noteworthy in the coming years for heat treating gears and other power transmission components?

MH: I have heard a lot of chatter about electric vehicles due to the differences in power transmission and how that affects the heat treat market. Will the next few years bring a bigger push in EV? I think that is probably a given. EV means different heat treat needs and different materials. Autos, in general, are still going to have to get better mileage if they use gasoline and that means lighter transmissions and more speeds and probably some more hybrid options. As far as auto demand, we had a huge trend to Uber before COVID and now with the emptying of big cities, will more people want or need cars? We have emptied retail stores, and everyone is used to fast home delivery. How does that effect demand for heat treated parts?

GT: How is the demand for heat treating changing in areas like automotive, aerospace, and the steel and metal processing industries?

MH: I read an article that said manufacturing in the United States is looking up for a number of structural reasons. The manufacturing Purchase Managers' Index is strong, as well. Both sources suggest we will see strength this year in manufacturing. At the same time, I do not think we have ever seen such major structural changes in such a short time. COVID stunned commercial aerospace. We are still 18 months away from it getting back to some normalcy. Throw in the Boeing issues before COVID (737 MAX and 777x) and it may be longer. Military and Space are, however, strong. Leisure and sporting are at a frenetic pace. Guns, Marine, RV's, ATV's are all selling like crazy. Automotive will continue to move away from heavier steels, but demand seems to be holding for cars, trucks, etc. Steel prices are very high right now due to demand being higher than supply.

GT: What new and improved technologies are playing a key role in the heat treatment of gears today?

MH: Is it finally time to really go to low pressure carburizing as a substitute for standard atmosphere carburizing? We, as a company, think so, so we have invested big in the most revolutionary heat treating product in decades, our Super IQ furnace. Super IQ offers LPC qualities with capital investment and operating costs comparable to standard atmosphere carburizing. We think Super IQ is revolutionary and will allow heat treating to move away from a dark and dirty plant environment to an Industry 4.0 environment that any manufacturer can be proud of.

GT: What are the greatest challenges for your heat treat customers in gear manufacturing in 2021?
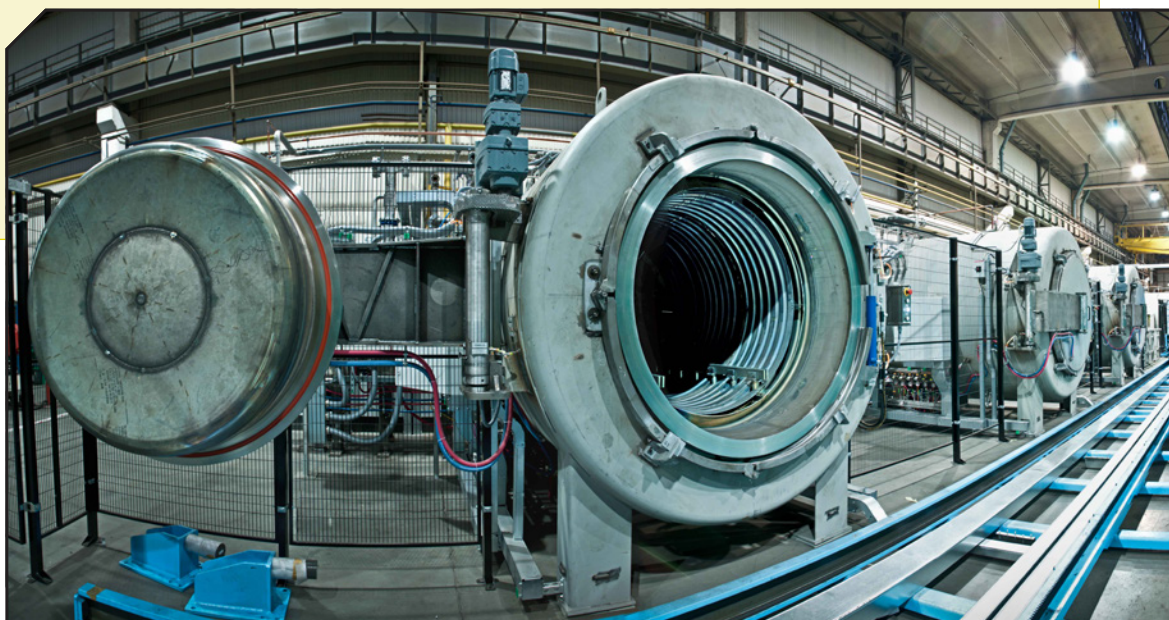
MH: Can gear manufacturers take the time, with confidence, to step back and look at their business, the changes that are occurring and invest in new equipment and advance their art? Or…, is it survival and business as usual?

GT: How important is it for your gear customers to have a working knowledge of part materials and the chemistries involved in manufacturing?

MH: This is a major challenge. How do we get materials engineers, heat treat engineers and power transmission engineers to really look at how steel grades, heat treating (carburizing, ferritic nitrocarburizing, or nitriding) and market demands and trends work hand in hand? I think many more advances are possible, but getting these experts to work together to make changes is always challenging.

GT: Do you offer training or educational opportunities to keep customers up to date on new heat treat technologies and processes?

MH: I try to present one or two webinars a year. I try to write a few articles each year. I will happily visit anyone and discuss all these issues. It is my passion. Before COVID we were planning a "Road Show" to go to larger companies and have many of these discussions. I am still ready to help and to travel.

GT: How will the heat treat market evolve in the coming years? How can gear manufacturers better prepare for this evolution?

MH: Gears cover a broad range of power transmission needs from autos to aerospace to heavy industrial. Heavy industrial seems to be an area of largest growth possibility as we move to more infrastructure work and more manufacturing. Combined with recreational needs, this means more gears in smaller volume runs, for demanding applications that need high quality. ⚙

Heat Treat and Metal Education Opportunities

AGMA and ASM International offer a diverse range of steel, metallurgy and heat treat courses both in-person and virtually in 2021. Education and training in these areas are still one of the greatest challenges in manufacturing. Please note that both AGMA and ASM International will have a variety of educational programs in St. Louis during Motion + Power Technology Expo and the co-located Heat Treat from September 14–16 (*motionpowerexpo.com*, Home - Heat Treat (*asminternational.org*))

AGMA Steels for Gear Application

This virtual course takes place June 15–16.

Attendees will gain a basic understanding of steel and its properties. Learn to make use of steel properties in an application and understand the potential that different steel and heat treatment options can offer. Explore how performance of the material depends on how the steel is produced. The course is intended to support gear engineers, gear designers, material specialists or metallurgists at OEMs, Tier 1s, Tier 2s, etc., production engineers, technicians and managers. A webcam on your computer equipped with a microphone and speakers/headset are required for participation in this virtual course. Space is limited to 20 participants per course. Course materials will be mailed in hard copy.

Objectives include:

- Describe how material properties are affected by steel quality and heat treatment.
- Describe how stresses are introduced by heat treatment process and surface modification treatments.
- Explain how to select a steel and heat treatment combination to meet the demands of the application.
- Review influence of material selection on the manufacturing of components.
- Discuss how to verify and specify required steel properties.

www.agma.org/education/ advanced-courses/2021-steels-for-gear-application/

AGMA Operator Precision Gear Grinding

This course takes place September 28–29, 2021 at Daley College in Chicago.

Attendees will explore gear grinding processes, machine kinematics and setup, pitfalls, failures and expectations related to finish ground gearing. Learn definitions of gearing component features, process steps from blanking, through heat treatment to finished part ready to ship. Study aspects of Quality Assurance, Inspection Documentation and corrective actions for measured non-conformances. Understand pre-heat treat, heat treatment and post heat treatment operations including the how's and why's to produce finished gears that conform and perform to end user expectations. This course is taught at Daley College. A shuttle bus is available each day to transport students to and from the hotel. Class will take place 8:00am–5:00pm each day.

Objectives include:

- Review and challenge control of part datums for pre-heat treatment operations, use datum's consistently through

finishing operations given part prints.
- Anticipate and correct for part distortion during heat treatment knowing the actual heat treatment process used.
- Understand gear grinding kinematics for both form and generating machines along with allowable metal removal rates and wheel dressing intervals based on type of grinding wheels being used.
- Ask questions of gear designers and manufacturing engineers to acquire all information required to produce conforming finished gears.
- Accurately apply and inspect pre-calculated micro-geometry modifications derived from complex contact analysis software.
- Perform component finishing machine setup, alignments, component inspection and calibrations to established ISO standards with hands on lab if available, or, run calculations on grinding cycle times based on various target accuracies and grinding techniques.
- Select the optimum grinding wheel specification given part print and heat treatment used.
- Achieve compliance with finished

parts to meet print requirements and customer performance expectations.
- Accurately measure pre and post finish gear tooth thickness given finished tooth thickness specifications.
- Avoid and detect the presence of Twist Error.
- Avoid and detect presence of grind burn temper.
- Avoid typical gear fatigue failure modes resulting from improper finishing.
- Identify common non-conformances, apply problem solving techniques and corrective actions.

www.agma.org/education/advanced-courses/2021-operator-precision-gear-grinding/

AGMA Gear Heat Treatment Operator/Operations

This course takes place November 9–10, 2021 at Daley College in Chicago.

This course provides the heat treat operator and operations team, the means to perform the heat treatment of steel gears in a manner that meets the AGMA and customer requirements in a safe and efficient manner. The course identifies the key requirements for proper

processing. Sufficient metallurgical background is provided to allow the student to identify how this information relates to the required processing and properties of the gear. This course is taught at Daley College. A shuttle bus is available each day to transport students to and from the hotel. Class will take place 8:00am–5:00pm each day.

Objectives include:
- Identify and locate the required information for material, process, and equipment for gear heat treatment.
- Recognize how the various heat treatment processes apply to the relevant AGMA documents.
- Perform preparation to product and equipment for heat treatment in an efficient and safe manner.
- Operate and monitor heat treat equipment and perform quality control processes.
- Perform post-heat treatment processes, Go/No-Go material inspections and cycle documentation reviews.

www.agma.org/education/advanced-courses/2021-heat-treatment-equipment-operator/

ASM International
Basics of Heat Treating

This virtual course takes place July 26–28, 2021.

Heat treating is considered the least understood, but most integral part of the manufacturing processes. An efficient heat treating process reduces the overall manufacturing costs associated with energy use, scrap, re-work, and quality issues. Heat treating is critical for your business and industry.

The Basics of Heat Treating course provides an interactive approach to learning the basic elements associated with the heat treating of metals. The course includes a variety of real-life manufacturing situations for discussion. There is also an interactive question and answer sessions integrated throughout the course.

Objectives include:

- Explain the importance and application of the Iron cementite diagram (iron carbon equilibrium Diagram) and its application.
- Describe the Time Temperature Transformation diagram and it influence on phase transformations and microstructure.
- Predict the mechanical properties and microstructures resulting from heat treatment initiated by thermal transformation.
- Identify and solve heat treat problems using the material, atmosphere, time, and temperature (M.A.T.T.) procedure demonstrated in class.

www.asminternational.org/
learning/courses/online/-/journal_
content/56/10192/27395478/CLASS

ASM Component Failure Analysis Online Course

This online course focuses on the practical materials and processing knowledge necessary to perform failure analysis on these widely used component groups. The course materials and instruction will provide insight into the manufacturing of components, circumstances resulting in degradation, and diagnostic features for failure analysis and prevention. Half day component sections include shafts and bearings; mechanical fasteners; cast and wrought materials; welded, brazed and soldered joints; gears; boilers and heat exchangers; and pressure vessels. Engineers and

technicians involved in the maintenance, failure analysis and failure prevention of components will benefit from the course. General knowledge of materials and some background in failure analysis principles would be helpful but not mandatory. ASM courses in principles of failure analysis would be good preparation for the detailed treatment of each of the component types covered, but are not mandatory.

Objectives include:

- Understand normal failure modes for the different types of components.
- Identify the fabrication factors and service characteristics that can lead to those failure modes.
- Participate in or help plan failure analysis investigations of these components.
- Interpret failure analysis conclusions in order to help identify preventative action.

www.asminternational.org/
learning/courses/online/-/journal_
content/56/10192/40217544/CLASS

ASM Case Hardening of Steel — Digital Course

This digital course examines case hardening as an important part of heat treating. It is particularly useful for the manufacture of machine parts, carbon steel forgings and carbon steel pinions.

In many metallurgical applications, strength is of minor importance and wear resistance is the major consideration. In other applications where wear

resistance is still the prime consideration, a high level of strength and considerable toughness are also required. To produce these conditions, it is necessary to employ specialized techniques that result in a relatively thin surface layer of the steel being space hardened. This thin layer is termed the case and the technique to produce the layer is termed case hardening. In this self-guided digital course, students will learn — with the help of rich visuals, narrated animations, and interactive quizzes — the different case hardening processes including carburizing, carbonitriding, and nitriding; quenching of case hardened parts; induction hardening; and the various types of furnaces used in commercial heat treating processes.

Objectives include:

- List the reasons for case hardening.
- Outline the advantages of carburizing, carbonitriding, nitriding, and induction surface hardening.
- Describe in general the operation of batch-type and continuous furnaces.
- Compare surface hardening by induction to other processes.
- Give the reasons for quenching of case-hardened parts.
- Differentiate between effective case depth and total case depth.

www.asminternational.org/
learning/courses/online/-/journal_
content/56/10192/37494537/CLASS

REGISTRATION OPENS MAY 1

Now accepting hotel reservations.

MOTION+POWER
TECHNOLOGY EXPO

GEAR
ELECTRIC
FLUID POWER
>>>>>>>> MOVING THE FUTURE.

At MPT Expo, you'll see the full range of power transmission solutions, including hybrid solutions, utilizing mechanical power transmission, pneumatics, hydraulics, electric motors, and drives.

SEPTEMBER 14–16, 2021
AMERICA'S CENTER CONVENTION COMPLEX
ST. LOUIS, MO

Your safety is our priority. Regular updates posted at MotionPowerExpo.com.

Formerly Gear Expo   Owned by   **American Gear Manufacturers Association**

Introduction to Pericyclic Transmissions

Dr. Hermann J. Stadtfeld

Pericyclic transmissions consist of 4 to 8 bevel gears. Each pair of bevel gears has a shaft angle which is close to 180°. The number of teeth of each pair of meshing bevel gears differs by one or two. Figure 1 shows a gear pair with nearly the same number of teeth and a shaft angle 14 (Σ) close to 180° in a conventional arrangement (not pericyclic). Pericyclic transmissions use between two and four bevel gear pairs like the one shown in Figure 1 as base elements and introduce a pericyclic nutating motion to two or four of the bevel gears in order to achieve high reduction ratios.

The lowest possible shaft angle difference to 180° of the mating bevel gears as shown in Figure 1 is defined by the whole depth of the teeth. In order for the teeth to mesh only in one zone 15 at the circumference and be disengaged at the opposite side, zone 16, the shaft angle needs to be at least:

$\Sigma = 180° - \arctan\{[(\text{hole depth})*2 + \text{clearance}]/(\text{outer cone distance})\}$
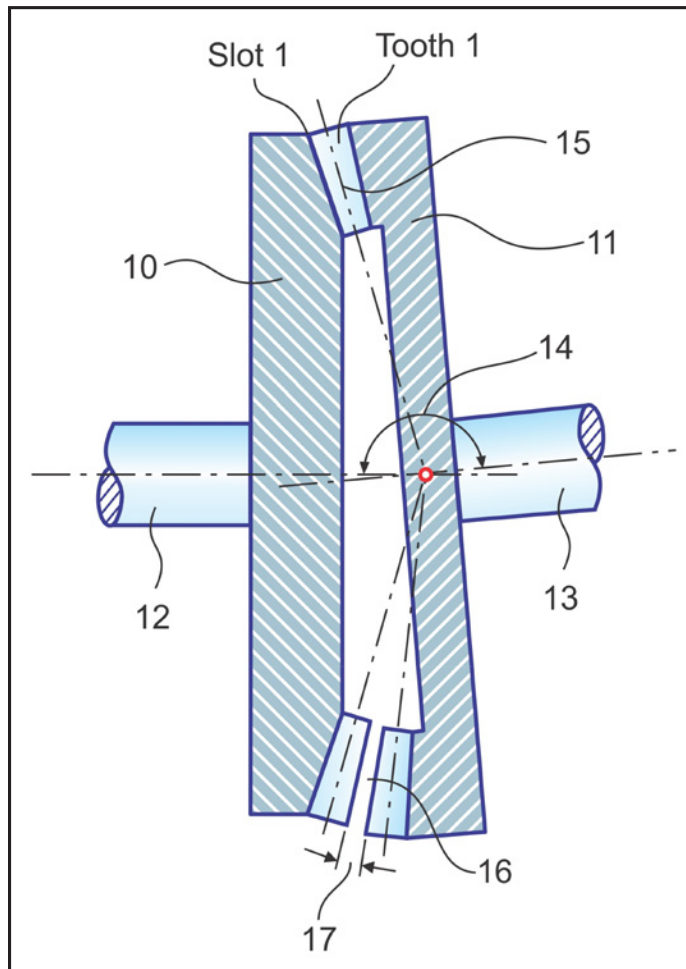
Figure 1   Two ring gears with one tooth difference.

The clearance amount 17 needs to be about 50% of the whole depth of the teeth or larger to allow meshing between the two mating gears. Meshing conditions are different from standard bevel gear ratios of one to five. Due to the nearly 180° shaft angle there is a large engagement zone 15 between the meshing teeth. The size of the engagement zone angle is normally chosen below 90°, because the difference of one or two teeth between the mating gears will result in one of the two gears to rotate faster. This means in case the first gear 10 has one tooth more than the second gear 11 and if tooth No. 1 of the second gear is engaged with slot No. 1 of the first gear, then tooth No. 1 will get disengaged at the end of the engagement zone and pass one tooth of the first gear in order to re-engage but now with slot No. 2 of the first gear while it enters at the other end of the engagement zone. The process of disengagement, passing one tooth and re-engaging with the next slot requires not only enough clearance between the tips of the mating teeth, it also requires a sufficient angle of the dis-engagement zone to make the passing of one tooth possible without interference.

If the first gear 10 and the second gear 11 are connected to separate shafts (12 and 13), having a shaft angle smaller than 180°, as shown in Figure 1, then the ratio will be the number of teeth of the second gear 11 divided by the number of teeth of the first gear 10 (z_2/z_1). In the case of $z_1 = 40$ and $z_2 = 41$, the ratio is commonly expressed as 40×41 or 0.9756.

In a pericyclic transmission the nearly 180° shaft angle bevel gear pair is utilized differently than shown in Figure 1. Figure 2 shows gear 20 meshing in zone 22 with gear 21. Gear 21 is rigidly connected (or one piece) with gear 23 and gear 23 meshes with gear 24 in zone 19. The shaft angle between gear 20 and gear 21 is 26 and the shaft angle between gear 23 and gear 24 is 27. The ratio calculation of pericyclic transmissions is significantly different from the common ratio calculations of gear transmissions. The calculation is explained with the following example:

Number of teeth gear 20: $z_{20} = 40$
Number of teeth gear 21: $z_{21} = 41$
Number of teeth gear 23: $z_{23} = 61$
Number of teeth gear 24: $z_{24} = 60$

The calculation begins at the rotationally constrained gear and its mate which in Figure 2 is gear 20 which is rigidly connected to the gearbox housing 31 and therefore constrained and gear 21 which is the first gear in mesh with the constrained gear. In a pericyclic transmission the input rotation rotates the inclined center shaft 30, which holds gears 21 and 23 via bearings (no positive torque connection). When the input rotation 28 rotates the input shaft 29 which is connected to inclined shaft section 30, then instead of a nearly same fast rotation of gears 21 and 23, only a nutating or wobble motion occurs. Each

nutation of the inclined shaft 30 will rotate gear 21 (and the connected gear 23) by one pitch backwards based on the angular pitch of gear 21 ($\Delta_{\phi1} = -360°/41 = -8.7805°$). The nutating interaction between gear 23 and 24 will rotate gear 24 forward by one pitch based on the pitch of gear 23 ($\Delta_{\phi2} = 360°/60 = 6.0°$). This means the output shaft 32 rotates $\Delta_{\phi1} + \Delta_{\phi2} = -2.8789°$ for each full revolution of the input shaft 28. The ratio of this pericyclic transmission is $i_{Pericyclic} = 360°/(-2.7806°) = -129.47368$. This ratio calculation is based on on the convention of:

$$\omega_{Output} = \omega_{Input}/i_{Pericyclic}$$

Another notation for the ratio calculation is:

$$i_{Pericyclic} = [(z_{constrained} - z_{first\ not\ constrained})/z_{first\ not\ constrained} + (z_{indirectly\ constrained} - z_{second\ not\ constrained})/z_{indirectly\ constrained}]^{-1}$$

whereas:

$i_{Pericyclic}$ Ratio of pericyclic transmission
ω_{input} Angular velocity of input shaft
ω_{output} Angular velocity of output shaft
$z_{constrained}$ Gear 20 (connected to housing)
$z_{first\ not\ constrained}$ Gear 21 (meshing with constrained gear)
$z_{indirectly\ constrained}$ Gear 23 (indirectly constrained with connection through 21 to 20)
$z_{second\ not\ constrained}$ Gear 24 (output gear is not constrained)

$$i_{Pericyclic} = [(z_{20} - z_{21})/z21 + (z_{23} - z_{24})/z24] - 1$$
$$= [(40-41)/41 + (61-60)/60] - 1$$
$$= -129.47368$$

A transmission like the one shown (Fig. 2) is fully functional, but it generates fluctuating axial forces due to the unbalance of the intermediate gears 21/23 (Refs. 1–2). Although the rotation of gears 21/23 is slow compared to the input RPM ($RPM_{21/23} = RPM_{input}/i_{Pericyclic}$), the nutating wobble motion is fast and has the same frequency (1/min) as the input RPM. The nutating wobble motion will cause fluctuating moments around axis 50 which alternates between the CW direction 26 and the CCW direction 27 which act on the gearbox housing 31. The generated vibrations due to the unbalance are not acceptable for all applications with input speeds above 100 RPM.

The state of the art elimination of the unbalance is achieved by connecting a second, mirror imaged pericyclic unit with the first pericyclic unit as shown (Fig. 3) (Ref. 3). The two units in Figure 3 are connected with the output gear 34. Gear 40 is the mirror image of gear 24. Gear pair 41/43 is the mirror image of gear pair 21/23 and gear 42 is a mirror image of gear 20. Gear 42 is rigidly connected with the gearbox housing 31, like gear 20. The shaft sections 29, 30, 33, 35 and 44 are rigidly connected like one solid piece. The nutation wobble motions of the two intermediate gear pairs 21/23 and 41/43 in Figure 3 have opposite directions, which leads to the cancelation of any system-related axial unbalances. The output gear 34 is rigidly connected to gear 24 and gear 40. The ratio between the input shaft 29 and the output gear 34 is identical to the ratio of the transmission in Figure 2.
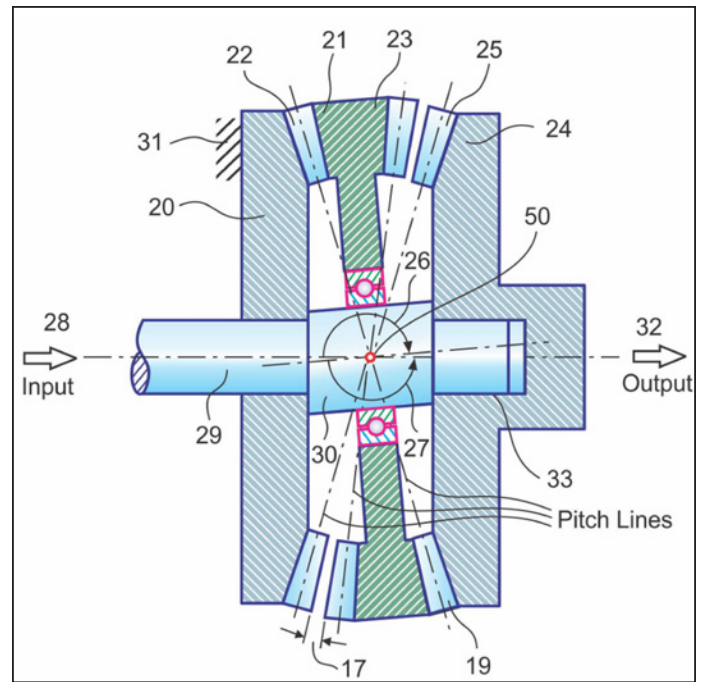
Figure 2   **Concept of pericyclic transmission (Refs. 1–2).**
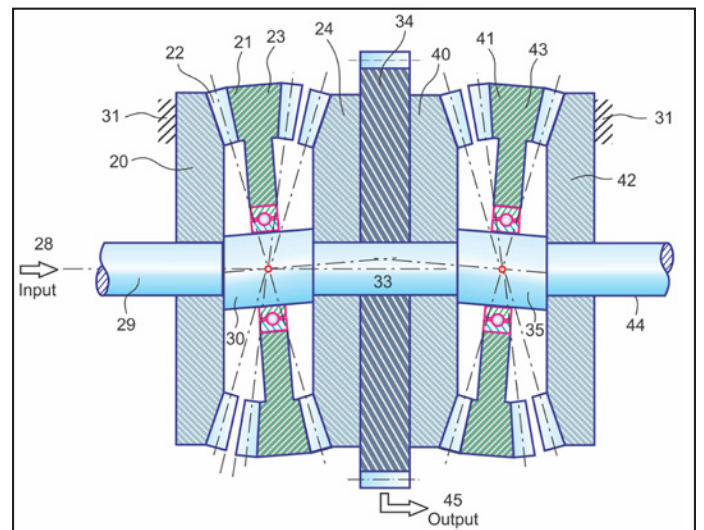
Figure 3   **Balanced pericyclic transmission.**

The three obvious disadvantages of the state of the art solution are the fact that the number of gears required for balancing the pericyclic transmission has to double. Also the size of the transmission increases to about twice the size of the transmission shown in Figure 2. The third disadvantage is the central location of the output gear 34 which requires an additional gear which meshes with 34 in order to provide a rotating output shaft.

Reversed pericyclic transmission with center output. A more cost effective high reduction transmission utilizing the pericyclic principle requires a reduced number of gears by still providing a cancellation of the unbalancing moments or forces as discussed with Figure 3.

The first version of the simplified pericyclic transmission is shown in Figure 4. The kinematic principle reverses the concept of Figure 2 and uses a centric mounted intermediate gear pair 51/53. The intermediate gear pair 51/53 has a cylindrical gear 59 on the outer circumference which is the pericyclic transmission output. The gears 52 and 54 perform the nutating motion initiated by the inclined bearing seats 55 and 56. The gears 52 and 54 are restrained from rotation by the swing pins 61 and 62 that are engaged in slots inside of the transmission housing 60. The input shaft 58 is rigidly connected with the shaft sections 55, 57, 56, and 65. If for example gears 52 and 54 have 41 teeth, gears
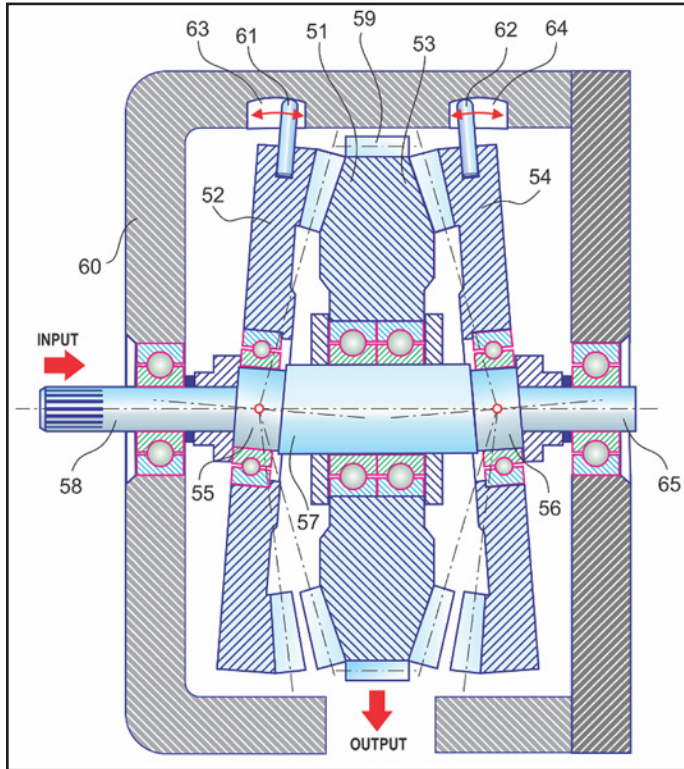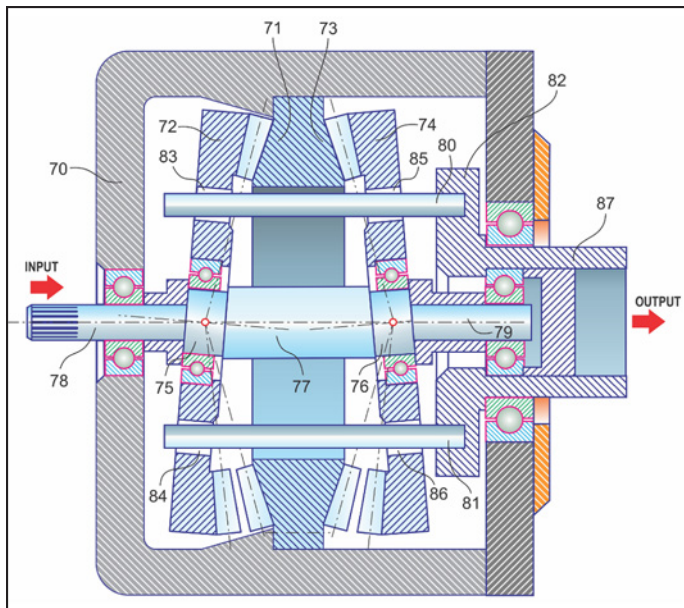
51 and 53 have 40 teeth, then each revolution of the input shaft 58 will nutate but not rotate gears 52 and 54. The interaction between gears 52 with 51 and 54 with 53 rotate the intermediate gear pair by one pitch in negative direction for each full rotation of the input shaft.

The rotation is transmitted via the cylindrical gear 59 to a second cylindrical gear at the outside of the transmission housing 60 which is mounted on a not shown output shaft. Gear 59 will make one revolution forward if the input shaft 58 turns 40 times (ratio $i_{Pericyclic} = [1/40]-1 = 40$).

$$i_{Pericyclic} = [(z_{constrained} - z_{first not constrained})/z_{first not constrained}]^{-1}$$
$$i_{Preicyclic} = [(z_{52} - z_{51})/z_{51}] - 1 = [(z_{53} - z_{54})/z_{54}] - 1 = [(41-40)/40] - 1 = 40$$

Reversed pericyclic transmission with axial output. The second version of the new pericyclic solution with an output shaft 87 that is in-line with the input shaft 78 is shown (Fig. 5). The concept in Figure 5 also reverses the concept of Figure 2 by using a centric mounted intermediate gear pair 71/73. The intermediate gear pair 71/73 is connected with the gearbox housing 70, while the gears 72 and 74 perform the nutating motion initiated by the inclined bearing seats 75 and 76. The input shaft 78 is rigidly connected with the shaft sections 75, 77, 76, and 79. If for example, gears 72 and 74 have 41 teeth, and gears 71 and 73 have 40 teeth, then each revolution of the input shaft 78 will rotate gears 72 and 74 by one pitch. The rotation is transmitted via the pins 80 and 81 to the flange 82 of the output tube 87. The output tube 87 will make one revolution backwards if the input shaft 78 turns 41 times (ratio $i_{Pericyclic} = -41$).

$$i_{Pericyclic} = [(z_{constrained} - z_{first not constrained})/z_{first not constrained}]^{-1}$$
$$i_{Pericyclic} = [(z_{71} - z_{72})/z_{72}] - 1 = [(z_{73} - z_{74})/z_{74}] - 1 = [(40-41)/41] - 1 = -41$$

A disadvantage of the solution in Figure 5 is the sliding of the transmission pins 80 and 81 in the holes 83 and 84 of gear 72 and in the holes 85 and 86 of gear 74. The sliding will reduce the efficiency of the transmission and it will cause wear. Furthermore, the cantilevering pins 80 and 81 will transmit more torque from gear 74 than from gear 72 due to the larger axial distance of those holes from the transmission flange 82.

Figure 4   Reversed pericyclic transmission with output through the side of the transmission housing.

Figure 5   Reversed pericyclic transmission with input and output shafts in-line.
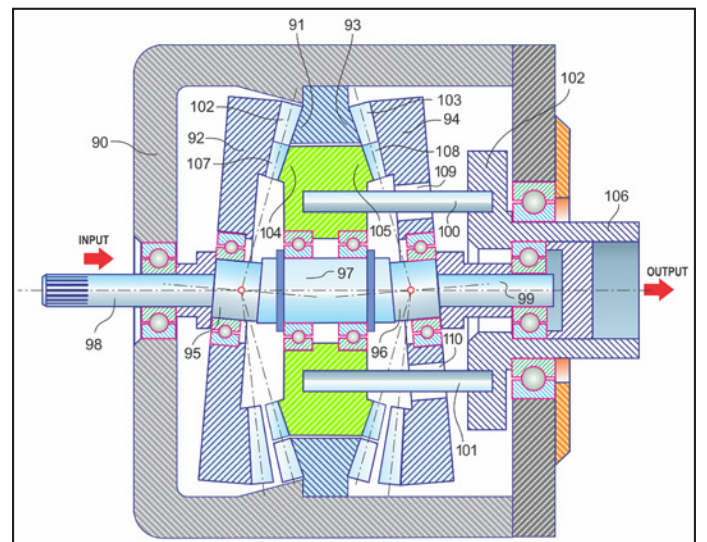
Figure 6   Advanced reversed pericyclic transmission – concept 3.

[www.geartechnology.com]

Reversed pericyclic transmission with integrated transfer gears. The third version of the new pericyclic solution shown in Figure 6 is the preferred embodiment for an electric vehicle application. The concept in Figure 6 also reverses the concept of Figure 2 by using a centric mounted intermediate gear pair 91/93. The intermediate gear pair 91/93 is connected with the gearbox housing 90, while the gears 92 and 94 perform the nutating motion initiated by the inclined bearing seats 95 and 96. Gears 92 and 94 are engaged with the outer halves of their face widths with intermediate gears 91 and 93. The input shaft 98 is rigidly connected with the shaft sections 95, 96, 97, and 99. If for example, gears 92 and 94 have 41 teeth, and gears 91 and 93 have 40 teeth, then each revolution of the input shaft 98 will rotate gears 92 and 94 by one pitch.

In case of the transmission in Figure 6 the rotation of gears 92 and 94 is transmitted to the output shaft via the centric mounted transfer gear pair 104/105 via transfer pins 100 and 101 to the flange 102 and the output shaft 106. The transfer gear pair 104/105 is positioned centric to shaft 97 and can freely rotate around shaft 97 with the teeth engaged with the inner halves 107 and 108 of the face widths of gears 92 and 94. The number of teeth between gears 92 and 104 and between gears 94 and 105 are identical which achieves the transmission of the exact rotational component of the motion of gears 92 and 94 (excluding the nutating wobble component) via transfer pins 100 and 101 to the flange 102 and then to the output shaft 106. The output shaft 106 will make one revolution backwards if the input shaft 98 turns 40 times (ratio $i_{Pericyclic} = -41$).

$$i_{Pericyclic} = [(z_{constrained} - z_{first\,not\,constrained})/z_{first\,not\,constrained}]^{-1}$$
$$i_{Pericyclic} = [(z_{91} - z_{102})/z_{102}] - 1 = [(z_{93} - z_{103})/z_{103}] - 1 = [(40-41)/41] - 1 = -41$$

The holes 109 and 110 provide a sufficient amount of clearance to the transfer pins 100 and 101 while the gear pair 104/105 rotates in mesh with gears 92 and 94. In order to maintain the clearance between pins 100 and 101 and the holes 109 and 110, the number of teeth of gears 92 and 104 as well as 94 and 105 are required to be identical.

Configuration with integrated electric motor. Electric vehicles are propelled with high-speed electric motors. Those electric motors operate at RPM's that are 3 to 5 times higher than the RPM's of internal combustion engines (SEE BOOK Chapter 1). The requirement of a speed reducing transmission between electric motor and driving wheels with very high ratios is therefore evident. Pericyclic transmissions can realize the required high ratios and also allow the high input speeds without the risk of flank surface scoring due to the fact that the relative motion between the meshing teeth is considerably lower compared to conventional high speed cylindrical gearboxes.
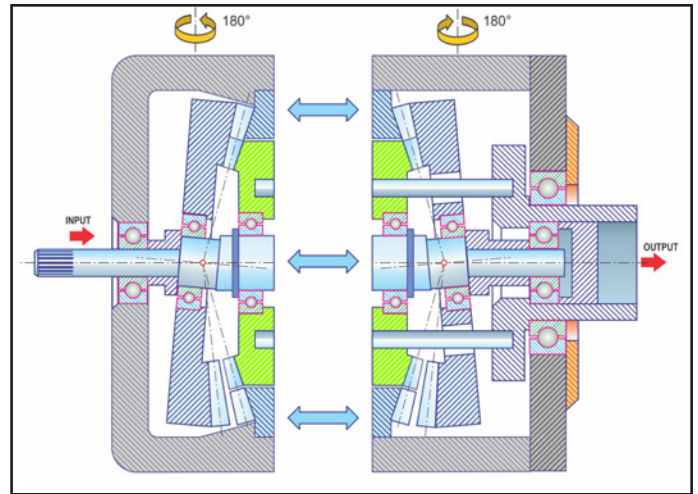
Figure 7   Separation of the two nutating members.
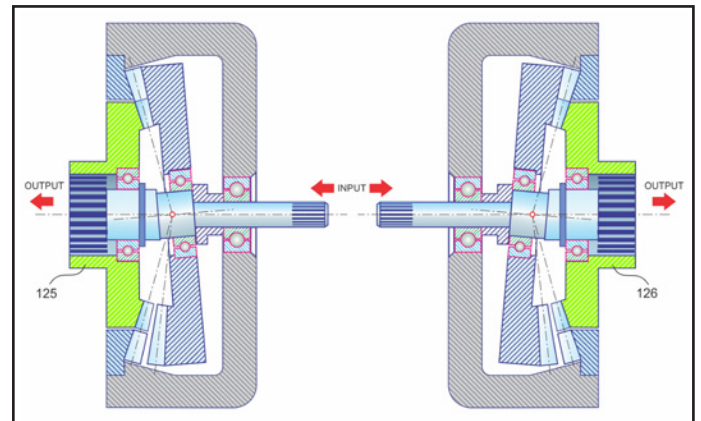
Figure 8   Nutating members after rotation and after modifying input and output shafts.

In cases where the drive unit with motor and transmission has to fit between the driving wheels, a compact solution is required. The power density and the compact layout of the inventive transmission examples in Figures 4, 5 and 6 appear to be well suited for the speed reduction task in an electric vehicle. One requirement of a final drive unit is the output shafts on both sides of the transmission. The drive shafts to the wheels have to be connected to the output shafts (or output flanges).

Figure 7 shows the transmission of Figure 6 cut in two halves. After separating the two nutating members, each half is rotated around a vertical axis by 180°. The result of this rotation is shown in Figure 8. Also the input and output shafts have been reversed such that an electric motor 140 can be placed between the two units and the drive shafts to the wheels can be connected on the outside of the two units.
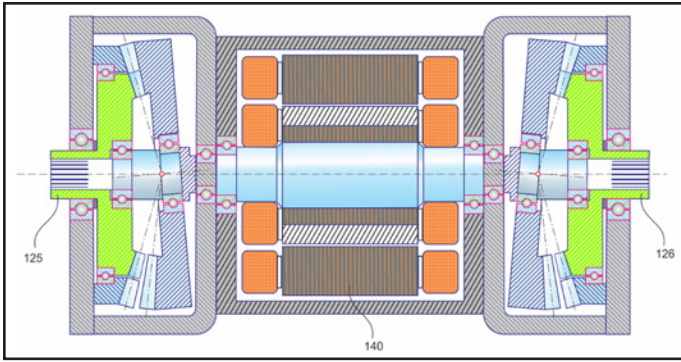
Figure 9   Transmission units connected on each side of an electric motor.
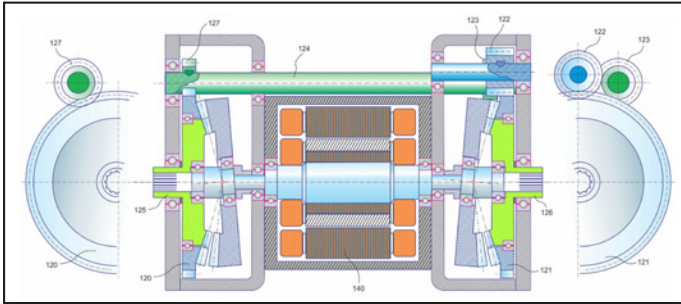
Figure 10   Transmission units connected with a differential shaft and idler.
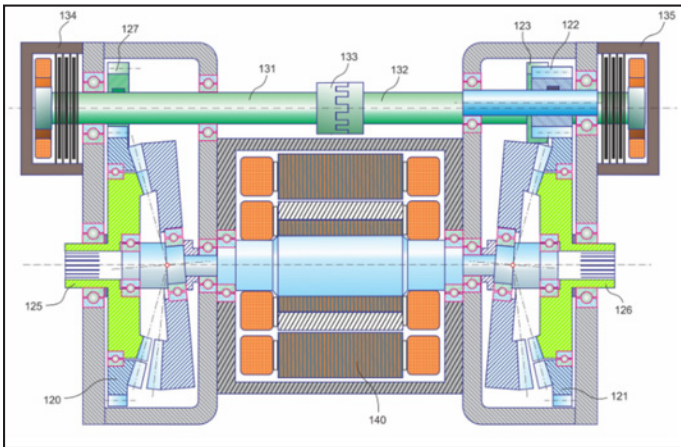
Figure 11   Additional coupling and clutches for torque vectoring and traction control.
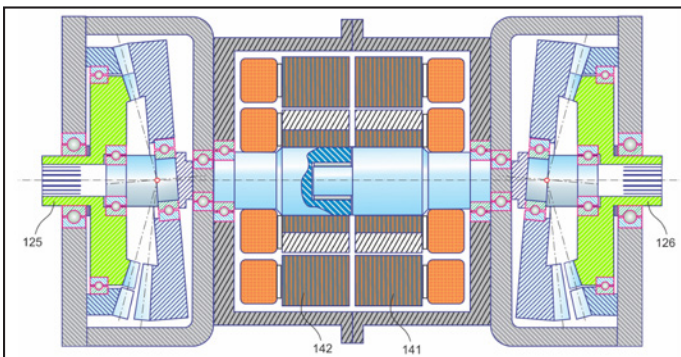
Figure 12   Double motor arrangement.

If an electric motor 140 is placed between the two transmission units of Figure 8, then the result is the arrangement shown in Figure 9. The rotor shaft of the electric motor 140 has on each side an output shaft with a connection to one of the two pericyclic transmission halves.

In a real design, the two pericyclic transmission halves and the electric motor can be integrated in one single eDrive housing. This compact inline unit can be mounted between the driving wheels of an electric vehicle. The space consumption between the wheels compares favorably to the eDrive examples presented in Chapter 1. The design shown in Figure 9 is perfectly symmetric which gives an optimal weight balance and an even heat radiation towards the wheel housings and wheels on both sides of the transmission.

Configuration with Integrated Electric Motor and Differential

The unit in Figure 9 does not have a differential functionality. This functionality is required if a vehicle drives through a curve and the outer wheel drives a longer distance (has to rotate faster) than the inner wheel.

The design shown (Fig. 10) solves the task of a differential function between the two output shafts 125 and 126. The two reaction members 91 and 93 in Figure 6 are in Figure 10 no longer connected to the transmission housing but have received teeth on their outside and are now numbered 120 and 121. Gear 121 is in mesh with idler pinion 122 which drives pinion 123 on shaft 124. Shaft 124 is rigidly connected to pinion 125 which is in mesh with gear 120. Pinions 122,123 and 125 have the same number of teeth. This arrangement acts like a differential between output shafts 125 and 126. If the vehicle, propelled with this unit drives through a curve, then the speed of the vehicle remains constant but if shaft 125 is connected to the wheel which drives on the outside of the curve, then shaft 125 will rotate a certain amount faster than the motor RPM and shaft 126 will rotate the same amount slower than the motor RPM in order to maintain the vehicle speed and accommodate the different arc lengths the two driving wheels have to travel while driving through the curve.

Torque Vectoring with Pericyclic Transmission

In Figure 11, a coupling 133 is placed between the two half shafts 131 and 132. The additional clutches 134 and 135 can connect or disconnect shaft 131 and/or 132 to the transmission housing after coupling 133 is disengaged. This arrangement allows controlling the amount of torque transmitted to the output shafts 125 and 126.

For example, if disk clutch 135 is fully actuated, gear 122 will be locked and 100% of the available torque and rotation will be applied to the output shaft 126. In the case of a disengaged disk clutch 135 no torque and no rotation is transmitted to the output shaft 126. Such functionality is called "torque vectoring" or "traction control".

The standard differential function as shown in Figure 10 can be achieved in the operating case when coupling 133 is closed and the disc clutches 134 and 135 are disengaged.

Configuration with integrated double-motor. If the motor 140 is replaced by two separately controlled motors 141 and 142, as shown in Figure 12, then also a torque vectoring via electronic control of the two motors can be realized. One side effect of this arrangement is the fact that the two nutating gears change their angular phase relationship (if the first motor rotates faster than the second motor) which will result in a certain unbalance of the unit.

The unbalance caused by the incorrect phase relationship between the two nutating gears may be difficult to compensate with balancing weights or other means. In conclusion, this very attractive appearing solution may have to be avoided. It should only be seen as a study in order to show the limits of the possibilities with the reversed pericyclic transmission.

Application Examples

Three examples of electrically actuated truck axles are shown in Figure 13. The inline solution a) requires a large space around the axle shafts. The steering axle b) and the rear axle c) with a front mounted motor and a transmission which is partially located in line and partially front mounted appear to be more compact (Ref. 5).

A proposed solution with a front mounted motor and a front mounted pericyclic transmission is shown (Fig. 14). This compact arrangement can achieve a ratio of up to 200 (Ref. 5).

Summary

The reversed pericyclic transmission principle presents a very compact solution for very high ratios. Due to the reversal of the common pericyclic transmission principle, the number of required gears can be reduced from eight bevel gears plus two cylindrical gears down to only four bevel gears. The more advanced solution requires six bevel gears and no additional cylindrical gears.

The ideal gear type for the reversed pericyclic transmission is the straight bevel gear. The nutating gear members are internal bevel gears with a pitch angle larger than 90°. Internal spiral bevel gears cannot be cut or ground on a bevel gear manufacturing machine due to cutter interference at the opposite side of the cutting action. Also a generating motion is not possible for internal bevel gears due to the same reasons why internal cylindrical gears cannot be manufactured with a hob cutter. As a solution, the internal bevel gears in pericyclic transmissions are Formate Coniflex straight bevel gears. The peripheral Coniflex cutter has no interference conditions in case of the slightly above 90° pitch angles of pericyclic transmissions (Ref. 4). Extensive development revealed, that also the external straight bevel gear in a pericyclic transmission, which is considered the pinion, can be manufactured by a Formate process. With the two meshing Formate gears, length crowning and profile crowning can still be realized as known from generated straight bevel gear sets.

The rolling conditions of the low shaft angle gears in a pericyclic transmission are ideal. In case of customary shaft angles and number of tooth combinations, the number of teeth in mesh is 20 to 30% of the number of teeth of the pinion. This amounts in practical applications to 10 or more teeth in mesh at the same
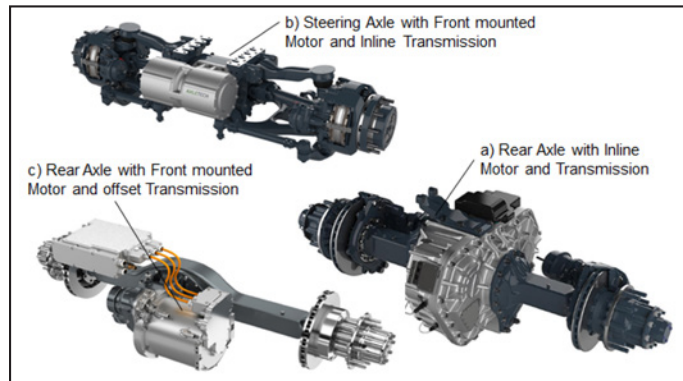
Figure 13   Examples of class 8 semi-truck axles.
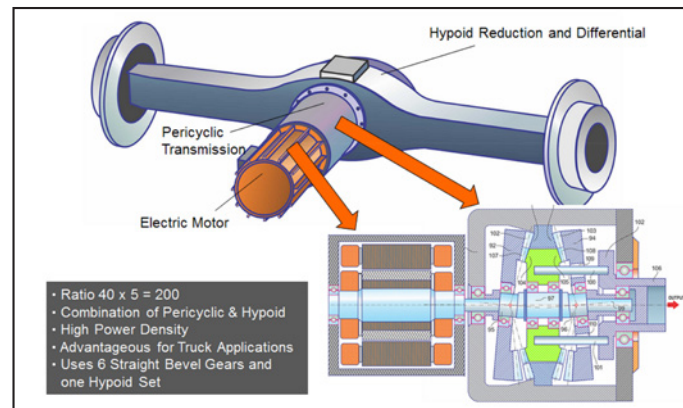
Figure 14   Application of pericyclic transmission in truck axle.

time. This in turn means that the transverse contact ratio also is 10 or higher. Such a high contact ratio results in an exceptional smoothness of the rolling action. In addition, the load carrying capacity of a nutating gear pair is a multiple of conventional straight bevel gears with a shaft angle of 90°.

In case of electric motors which run with high RPM and require high reductions, the question regarding the value of the sliding velocities is often a concern. Due to the low shaft angle, the sliding velocities between the teeth of a nutating gear pair are very low. The explanation is delivered by an analogy. If the shaft angle was 0°, then the straight bevel gear pair would have the function of a clutch without any sliding action between the teeth. In the case of 90° shaft angle, the same size gearset could have about 800m/min relative sliding. A nutating bevel gearset of the same size with a shaft angle of 15° has therefore only about 100m/min relative sliding between the tooth surfaces. The effect of the low sliding velocities presents a very compelling advantage for the application of nutating gears for high speeds.

An area of attention in nutating bevel gear applications should be the angled bearing seat of the nutating member. The bearing has to be pre-loaded without backlash and requires high stiffness against the forces which try to press the two engaged members out of mesh. During the development of pericyclic transmissions for rotorcrafts, transmission designers and bearing manufacturers found reliable and high efficiency solutions which should also be implemented in all applications of pericyclic and reversed pericyclic transmissions (Refs. 2–3). ⚙

For more information.
Questions or comments regarding this paper? Contact Hermann Stadtfeld at *hstadtfeld@gleason.com.*

References
1. Lemanski, A. "Variable Speed Power Transmission", United States Patent No.: US 7,147,583 B2, December 2006.
2. Saribay, Z. B. "Geometry and Kinematics of Conjugate Meshing Face-gear Pairs," 3rd International Basic Research Conference on Rotorcraft Technology, Nanjing, China, October 2009.
3. Mathur, T. "Pericyclic Transmission Prototype: Detailed Component Design, et al.Analysis and Fabrication", Vertical Flight Society 75th Annual
4. Forum & Technology Display, Philadelphia, Pennsylvania, May 2019.
5. Bolze, M. J. "Internal Bevel Gear", Company Publication, The Gleason
6. Stadtfeld, H. J. Works, Rochester, New York, June 2013.
7. Stadtfeld, H. J. "Effective eDrive Concepts, possible with new Bevel Gear Solutions", Innovations in Bevel Gear Technology, Seminar, WZL Technical University of Aachen, Germany, March 2020.

Dr. Hermann J. Stadtfeld is the Vice President of Bevel Gear Technology and R&D at the Gleason Corporation and Professor of the Technical University of Ilmenau, Germany. As one of the world's most respected experts in bevel gear technology, he has published more than 300 technical papers and 10 books in this field. Likewise, he has filed international patent applications for more than 60 inventions based upon new gearing systems and gear manufacturing methods, as well as cutting tools and gear manufacturing machines. Under his leadership the world of bevel gear cutting has converted to environmentally friendly, dry machining of gears with significantly increased power density due to non-linear machine motions and new processes. Those developments also lower noise emission level and reduce energy consumption.

For 35 years, Dr. Stadtfeld has had a remarkable career within the field of bevel gear technology. Having received his Ph.D. with summa cum laude in 1987 at the Technical University in Aachen, Germany, he became the Head of Development & Engineering at Oerlikon-Bührle in Switzerland. He held a professor position at the Rochester Institute of Technology in Rochester, New York From 1992 to 1994. In 2000 as Vice President R&D he received in the name of The Gleason Works two Automotive Pace Awards — one for his high-speed dry cutting development and one for the successful development and implementation of the Universal Motion Concept (UMC). The UMC brought the conventional bevel gear geometry and its physical properties to a new level. In 2015, the Rochester Intellectual property Law Association elected Dr. Stadtfeld the "Distinguished Inventor of the Year." Between 2015–2016 CNN featured him as "Tech Hero" on a Website dedicated to technical innovators for his accomplishments regarding environmentally friendly gear manufacturing and technical advancements in gear efficiency.

Stadtfeld continues, along with his senior management position at Gleason Corporation, to mentor and advise graduate level Gleason employees, and he supervises Gleason-sponsored Master Thesis programs as professor of the Technical University of Ilmenau — thus helping to shape and ensure the future of gear technology.

For Related Articles Search

electrification

at www.geartechnology.com

Our Librarian Will <u>Never</u> Shush You

at the **GT LIBRARY**

That's because the MICHAEL GOLDSTEIN GEAR TECHNOLOGY LIBRARY is all online, and you can visit it anytime. Just go to *www.geartechnology.com* and use the search box for access to 36 years of technical content focused on gears.

- **Every issue since 1984**
- **More than 2,000 technical articles**
- **More than 6,000 archived news items**
- **Addendum, Publisher's Page, Back to Basics and more**

And the best news of all? You don't even need a library card. That's because the GT LIBRARY is open to everyone. Knowledge is free. All you have to do is go and get it.

www.geartechnology.com

Case Study of ISO/TS 6336-22 Micropitting Calculation

Robin Olson, Mark Michaud, Jonathan Keller

Introduction

Micropitting is a form of Hertzian fatigue damage that occurs on gear teeth. It appears as ultrafine cracks on the surface of the flank, with the resulting loss of material looking like grey staining. Although the cause of micropitting is not fully understood, it appears to be caused by cyclic stresses and plastic deformation on the asperity scale. In addition, sliding between gear teeth causes traction forces that subject asperities to shear stress. Micropitting is influenced by a number of factors including loads, speeds, temperatures, gear tooth macro- and microgeometry, flank surface finish, heat treat, and lubricant properties.

Micropitting predominantly occurs on case-hardened gear teeth. Figure 1 illustrates the appearance of micropitting.

Multiple papers have been written about micropitting, its description, and its causes (Refs. 1–2). Micropitting can lead to significant surface damage, macropitting, and catastrophic failure. Alternatively, it may appear in patches and arrest its growth as tribological conditions improve during run-in. If one is designing gearing for critical applications, it is desirable to be able to calculate the risk of micropitting in an effort to avoid it.

The presence or absence of micropitting is not easy to determine with an analytical model because micropitting occurs on the asperity level, The engineer needs to determine what percentage of the asperities will come into contact through the lubricant film thickness, the asperity plasticity, the number of cycles the asperities experience as they travel through the contact zone, the fatigue limit of the asperities, and the pressure applied to the asperities. In 3-dimensional calculations, this is dependent on loads, local tooth geometry, roughness along the direction of tooth motion, lubricant selection, and the metallurgy of the gear. As a result,

Figure 1   Micropitting on a carburized gear (From ANSI/AGMA 1010-F14 [1]).

there is no comprehensive model to predict micropitting risk.

ISO/TS 6336-22 (*Calculation of load capacity of spur and helical gears — Part 22: Calculation of micropitting load capacity*) is the ISO technical specification containing a proposal for a calculation of risk of micropitting in gear sets (Ref. 3). This document was originally published in 2010 as ISO/TR 14179-1 and added to the ISO 6336 suite of documents in 2018. It was developed based on testing and observations of many gear sets with normal modules between 3 millimeter (mm) and 11 mm, and pitch line velocities between 8 meters-per-second (m/s) and 60 m/s. The analytical calculation in ISO/TS 6336-22 focuses on film thickness as a determinant for when micropitting will occur. This paper uses ISO/TS 6336-22 to calculate the risk of micropitting for gear sets in three different operating conditions and compares that to field experience. The simplified computation in Method B is utilized in order to simulate how the typical gear

engineer will use the method. For these examples, micropitting is not predicted to occur and this points out some limitations in the method.

Overview of the ISO/TS 6336-22 Calculation

ISO/TS 6336-22 contains a calculation of the micropitting load capacity of external gear sets that is based on testing. It assumes that micropitting occurs when the minimum specific film thickness of a gear set in application falls below a permissible value for specific film thickness. The ratio of the minimum specific lubricant film thickness to the permissible specific lubricant film thickness is the safety factor against micropitting. "Specific film thickness" is also called "lambda ratio" in some industries and is expressed as the ratio of the film thickness to the arithmetic mean roughness.

In other sections of ISO 6336, safety factors are used to calculate the risk of macropitting and bending fatigue. Advice about the acceptable minimum

value of the factor can be found in a general rating calculation, and app 6336-22 does not contain advice for a minimum safety factor; instead, it provides the following guidance:

"In other sections of ISO 6336, safety factors are used to calculate the risk of macropitting and bending fatigue. Advice about the acceptable minimum value of the factor can be found in a general rating calculation, an application rating specification, or a user specification for equipment design. ISO/TS 6336-22 does not contain advice for a minimum safety factor. Instead, it provides this guidance:"

Minimum specific film thickness. The calculations for minimum specific film thickness are performed at multiple contact points in the tooth mesh region, with the minimum selected as the lowest value in the results array. This allows for the prediction of both the risk of micropitting and the region on the tooth flank that will experience damage.

In the document, the minimum specific lubricant film thickness can be determined using two different methods. Method A allows the engineer to calculate the value with a gear computing program that models the complete contact area of the mesh. The results appear as a map of pressures and film thicknesses across the face of the pinion and gear flanks.

Method B starts with the assumption that the minimum specific film thickness will be on the tooth flank in the region of negative sliding. The lubricant film thickness is calculated with a modified Dowson/Higginson analysis along the line of action. It deviates from the norm, though, with the addition of a local sliding parameter. This parameter accounts for the influence of sliding on temperature, which affects film thickness. This changes the pressure-viscosity coefficient and dynamic viscosity, thus adjusting the film thickness in the regions of negative-specific sliding.

$$\lambda_{GF,Y} = h_Y / Ra \qquad (1)$$

$$h_Y = 1600 \cdot \rho_{n,Y} \cdot G_M^{0.6} \cdot U_Y^{0.7} \cdot W_Y^{-0.13} \cdot S_{GF,Y}^{0.22} \qquad (2)$$

Where
λ_{GF} is the local specific film thickness
h_Y is the local lubricant film thickness
Ra is the effective arithmetic mean roughness value (averaged between pinion and gear
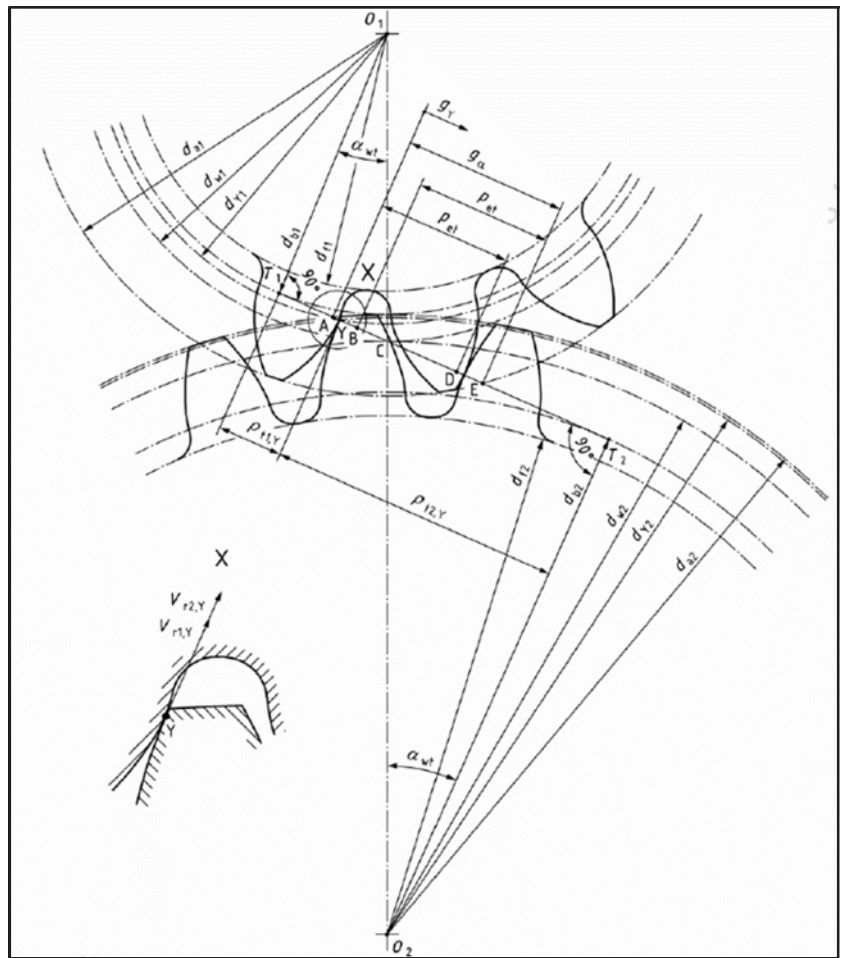
Figure 2   Points along the line of contact as illustrated in ISO/TS 6336-22.

roughnesses), µm
Y indicates the local contact point along the line of action
$\rho_{n,Y}$ is the normal radius of relative curvature at point Y along the path of contact, mm
G_M is the material parameter
U_Y is the local velocity parameter
W_Y is the local load parameter
$S_{GF,Y}$ is the local sliding parameter

The contact points along the line of action are determined with the familiar calculations for the lower point of active profile, lower point of single tooth contact, pitch point, upper point of single tooth contact, and upper point of active profile. Figure 2 shows this in a gear mesh. ISO/TS 6336-22 also considers mid- points between the lower and upper points of active profile and single tooth contacts.

Permissible specific film thickness. The permissible specific film thickness can be determined using several different procedures. All procedures require some level of experimental investigations, whether they be conducted with the actual gear set or with representative gear sets. Ideally, testing is conducted with the actual gear sets, lubrication, and inlet temperatures that match the operating conditions of the gearing. Method A recommends that this testing be conducted until micropitting begins to occur. The permissible specific film thickness is then calculated per the Method A calculation for minimum- specific film thickness using the conditions of the final load stage.

Method B uses two different options to set the permissible specific film thickness. One option is to conduct studies with gearing that is similar in geometry, quality, and material of the gearing being designed. Using controlled tests, the gearing is run until the micropitting failure limit is reached. The critical specific film thickness for the test gearing is then calculated using the data from the failure stage. This is the permissible specific film thickness.

If comparative testing cannot be performed (due to cost, timeline, test stand availability, etc.), the permissible specific

film thickness can be generally determined from a simplified set of curves based on the lubricant's performance in FVA-FZG micropitting tests (Ref. 4) and its viscosity. These curves are derived from mineral oils and are shown (Fig. 3).

ISO/TS 6336-22 also contains alternative curves that can be used to determine a value of the permissible specific film thickness based on the results of FVA-FZG micropitting testing of mineral oils at temperatures of 60°C, 90°C, and 120°C. These curves account for the additives in the lubricant by accounting for its "quality." High-quality lubricants

are specifically formulated with base stocks, additives, and thickeners to prevent micropitting. These are used when the costs of failure are high and maintenance is challenging. Mid-quality lubricants have some micropitting-preventing additives and are used in industrial gear lubrication when reliability is important and maintenance is scheduled. Low-quality lubricants have not been adjusted to prevent micropitting and are used in basic applications. In application, the choice of lubricant can be recommended by the gear manufacturer or specified by the equipment owner. It can result in

micropitting if the lubricant is not formulated to minimize the phenomenon.

Clearly, testing is a prominent theme in the determination of the permissible-specific film thickness! ISO/TS 6336-22 is careful to point out that testing should be carefully conducted and well-documented; testing variability is a risk to the precision and/or accuracy of the results. Practically speaking, three to five tests are conducted with comparable load stage results and either the average or (more conservatively) the minimum value is used for the calculation.

In summary, the uncertainty in the permissible specific film thickness value increases as one moves further from Method A. Figure 4 illustrates the options for methods in ISO/TS 6336-22.

Case Study – Using the Calculation

Case studies using ISO/TS 6336-22 or its predecessor document, ISO/TR 15144-1, have been performed in previous papers (Refs. 5–6). Many of those focus on using the Method A calculations for calculating tooth pressure and the specific film thickness.

Of particular interest is a paper by Pinnekamp and Heider (Ref. 7) that contains ISO/TR 15144-1 calculations with practical examples from industry. The FVA-FZG software *RIKOR* was used to determine the specific film thickness per Method A. Method B was used for the permissible specific film thickness. The resulting safety factors ranged between 1.0 and just over 3.0. Micropitting was observed on examples with safety factors over 2.0. The authors created a zoned diagram to predict the risk of
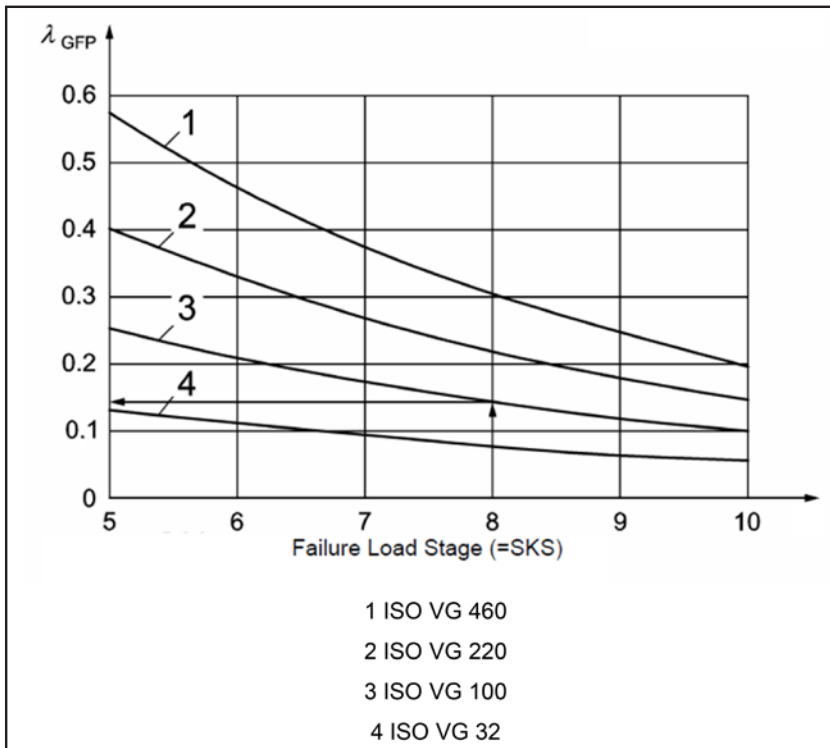
Figure 3 ISO/TS 6336-22 Figure A.1 - Minimum permissible specific film thickness for mineral oils as a function of nominal lubricant viscosity and failure load stage in FVA-FZG micropitting tests.
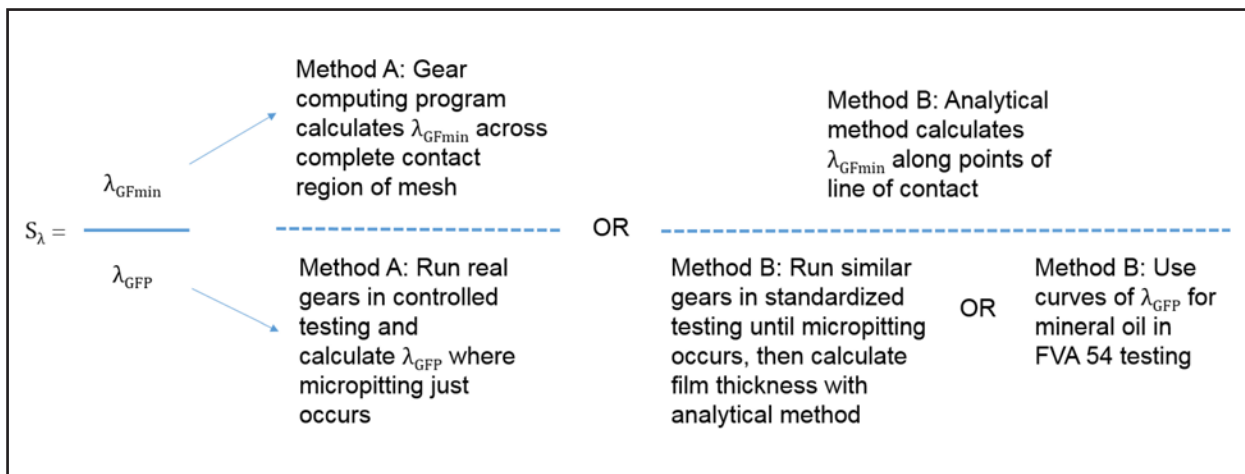
Figure 4 Options for calculation of the micropitting safety factor.

micropitting based on quality of the calculation, knowledge of operating conditions, and calculated safety factor.

This paper tests the behavior of the calculation using the analytical calculations in Method B to calculate specific film thicknesses. In two of the cases, it was not practical to calculate the permissible specific film thickness with comparative testing. The simplified curves based on viscosity and failure load stage of the lubricant were used for these. As much as possible, the paper simulates the path that the typical gear engineer would take to evaluate an existing gear set that experienced micropitting in operation or to assess a new design for the risk of micropitting.

The input data for each calculation consists of the gear geometry and arrangement, the lubrication, and the gear loads. The results are presented as the minimum specific film thickness, the permissible specific film thickness, and the safety factor that is calculated. Pictures of micropitting damage are also included.

Case 1 – high-speed gear set. The first case is a speed increasing gear set from a centrifugal compressor. Micropitting was found on the pinion on the dedendum extending through the pitch line to the addendum, favoring the drive end. Macropitting was also present. Micropitting was also found on the gear around the pitch line. The gear set had run for approximately 120,000 hours (54.6×10^9 cycles) (Figs. 5–7).

ISO/TS 6336-22 applies to gearing with pitch line velocities between 8 m/s and 60 m/s. This example has a pitch line velocity of 88 m/s, which exceeds the limits of the calculation. We will apply the analysis to see how it works in this case. The input data for this calculation is shown in Table 1.

ISO/TS 6336-22 calculates the minimum specific film thickness as 2.117, meaning that the minimum film thickness of the lubricant was much larger than the average roughness value of the tooth surfaces. This minimum occurred at the lower point of the active profile, which corresponds with the actual location of micropitting in the zone closest to the compressor (Fig. 8).

The permissible specific film thickness was calculated using the lubricant viscosity and failure load stage. The value determined from ISO/TS 6336-22, Figure A.1 was 0.157. This is consistent with the expectations of the performance of an ISO viscosity grade
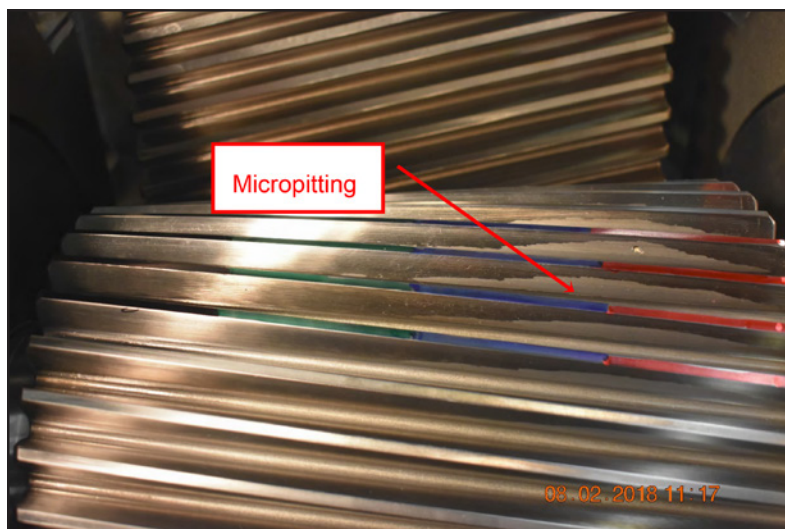
Figure 5   Micropitting on the flank of the pinion teeth. The red zone is closest to the compressor (drive end). The black zone is the motor side. (Photo courtesy of Artec Machine Systems).
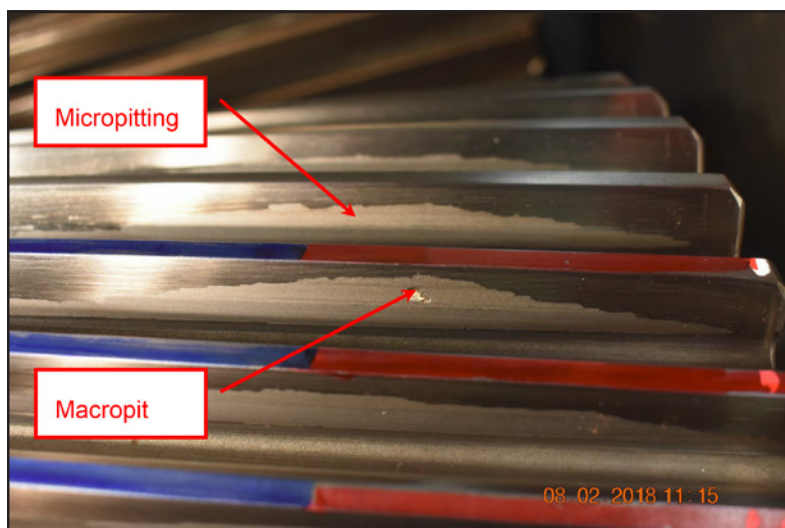
Figure 6   Close-up of micropitting, which begins 100 mm into the face and extends to 270 mm. There is a single macropit on one tooth. (Photo courtesy of Artec Machine Systems).
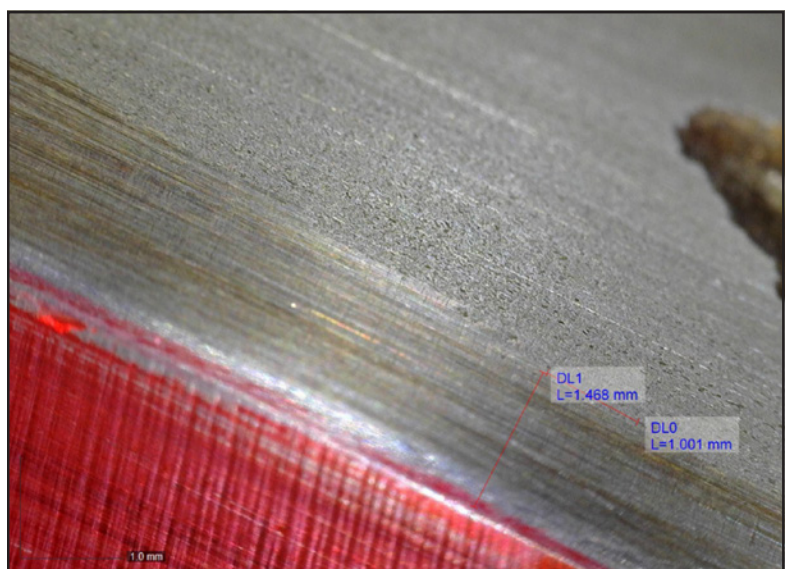
Figure 7   Close-up of the micropitting in the region just above the macropit. (Photo courtesy of Artec Machine Systems).

(vg) 32 mineral oil in an FVA-FZG micropitting test rig. By comparing the values of the minimum specific film thickness and the permissible value, a safety factor of 13.484 was calculated.

This safety factor is very high and our first concern is that the high pitch line velocity is outside the regime where the calculation model has been tested. In order to test whether the result is more reasonable within the limits of 8 m/s to 60 m/s, we assumed constant torque and brought the pinion speed down to 5,000 rpm; the pitch line velocity became 58 m/s. This resulted in a minimum specific film thickness of 1.68 and a safety factor of 10.701. We cannot claim that being outside the limits of the calculation is the only reason for the high safety factor.

Safety factors of this magnitude normally indicate that this gear set is safe

from micropitting, which is not the case in operation. The large value occurs as the specific film thickness becomes much larger than the permissible specific film thickness of the lubricant. With a specific film thickness that is over 2.0, the film thickness is much larger than the average roughness value of the surfaces. Theoretically, the tooth surfaces are not coming into contact and we are in a regime of full elastohydrodynamic lubrication (EHL) lubricant film (Ref. 8). This can be verified by observing the non-micropitted tooth flanks in Figures 5 and 6, which look almost new. Micropitting has occurred without apparent tooth flank or asperity contact! In this regime, film thickness is not an accurate indicator of micropitting risk. Micropitting may have been caused by hydraulic forces due to contact pressure, lubricant viscosity, or

shear forces.

Case 2 – wind turbine gear set. Case 2 is a gear set from a 1.5-MW wind turbine at the National Wind Technology Center on the National Renewable Energy Laboratory's (NREL's) Flatirons Campus in Colorado. The turbine began operating in May 2009. It was physically inspected in 2012 with a borescope with no signs of damage to the bearings or gear teeth. Further inspections revealed damage, though, such as:

- A 2015 borescope inspection of the gearing and bearings showed damage on the sun pinion teeth in the form of hard contact lines on several teeth, abrasive wear marks on one tooth, and evidence of micropitting on the flank of one tooth and in the region of the start of active profile (SAP) of several teeth. Normal wear was observed on the planet gears and bearings.
- A 2017 inspection noted excessive black sludge in the lubricant filter sediment collector. Tests of lubricant samples pointed out particle counts that were higher than acceptable, reduced lubricant performance, and warning levels of water in the lubricant.
- The gear drive was removed from service in December 2017. A third borescope inspection was conducted on the gear drive at the repair shop before tear down in April 2018. Micropitting was found in the start of active profile (SAP) of all of the sun pinion teeth. Micropitting and some abrasion were also found higher on the flanks of the sun pinion teeth. The gear set had been installed for 8.5 years. It had produced approximately 6-million kilowatt-hours of energy in 14,170 hours of grid operation time. This represents approximately 8% of its minimum design life. Micropitting was noted after 6.5 years of operation. Figure 9 contains pictures of the micropitting and additional details about the gear drive condition are reported in (Ref. 9).

Additional details about the gear drive condition are reported (Ref. 9).

As mentioned in Case 1, ISO/TS 6336-22 applies to gearing with pitch line velocities between 8 m/s and 60 m/s. This example has a pitch line velocity of 3.0 m/s, which is below the limits in the calculation. In order to review the results of the method with slow speed applications, though, we will apply the analysis to see how it correlates to field experience.

Table 1	Input data for Case 1			
Dimension	Units	Pinion	Gear
Number of teeth	-	37	163
Ratio	-	4.405	
Center distance	mm	600	
Normal module	mm	5.90	
Face width	mm	280	
Outside diameter	mm	236.30	987.29
Pressure angle	degrees	20.00	
Helix angle	degrees	10.00	
Addendum modification coefficient	-	0.2407	-0.0876
Surface roughness	μm	0.41	0.40
ISO accuracy grade	-	4	4
Material surface hardness	HRC	58-64	58-64
Pinion speed	rpm	7,582.0	
Pinion torque	N-m	12,209.3	
K_A K_v $K_{H\alpha}$ $K_{H\beta}$ product	-	1.4170	
Lubricant	-	Mobil Teresstic AC 32	
Inlet lubricant temperature	°C	54	
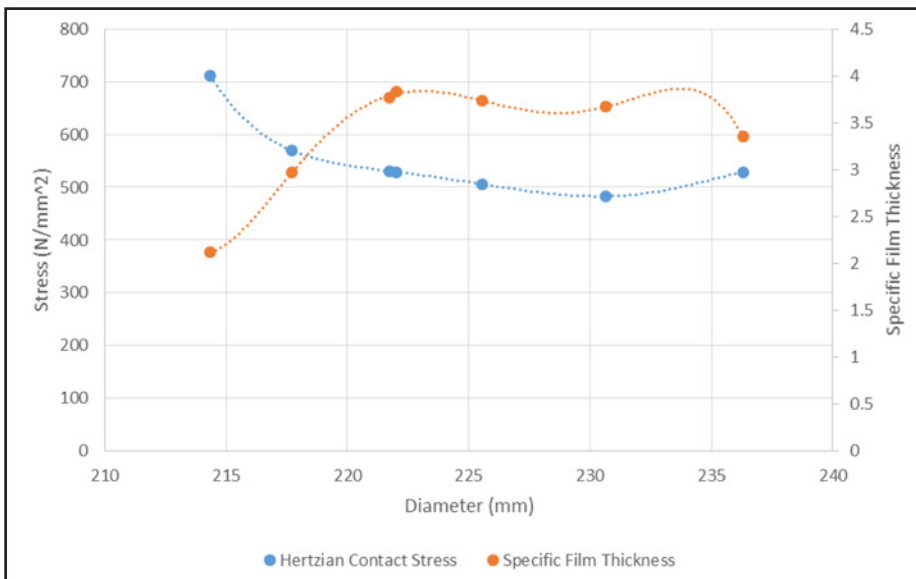
Figure 8   Graph of contact stress and specific film thickness along the line of action.
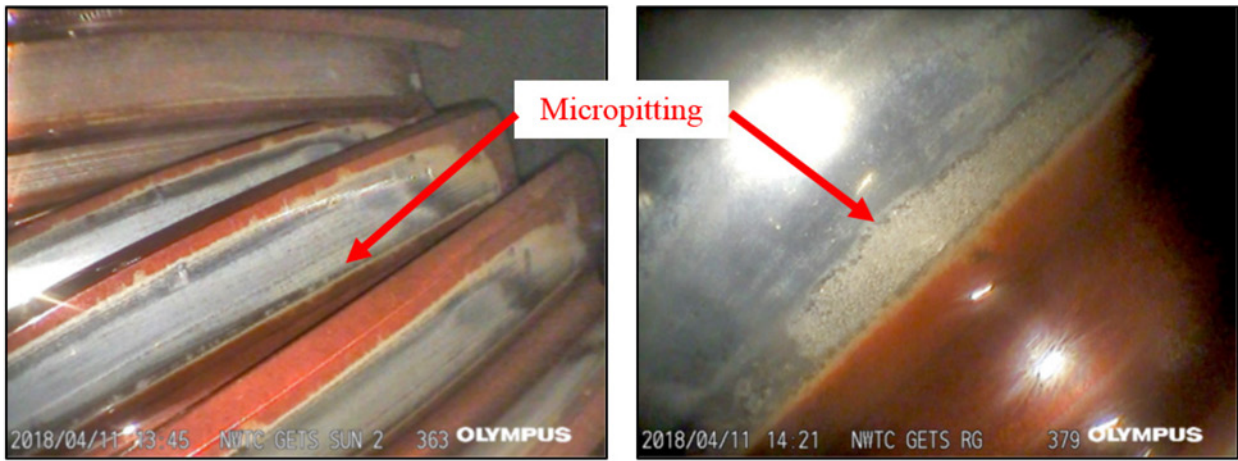
Figure 9   Micropitting on the sun pinion teeth. (Photos by Scott Eatherton, Wind Driven, NREL 61193 and 61194).

ISO/TS 6336-22 calculates the minimum specific film thickness as 1.589, indicating that the film thickness is much larger than the roughness of the teeth. The specific film thickness was determined at the lower point of the active profile of the pinion. This agrees with the location of the start of micropitting in the SAP of the flanks of the sun pinion.

The permissible specific film thickness was calculated using the simplified graphs in Method B, relying on the lubricant viscosity and failure load stage. The value determined from ISO/TS 6336-22, Figure A.1 was 0.239. This is consistent with the expectations of the performance of an ISO vg 320 synthetic lubricant in an FVA-FZG micropitting test rig. By comparing the values of the minimum specified film thickness and the permissible value, a safety factor of 6.635 was calculated.

It was noted that the gear drive sump temperature averages 50°C, but can get as high as 70°C. To test the range of sump temperatures, the calculation was run again using 70°C as the lubricant inlet temperature. The thinner film thickness caused the curve of the specific film thickness over the contact points in the line of action to flatten, decreasing the safety factor to 3.614 (Fig. 10).

This safety factor is lower than what was calculated in the first case, but still higher than what is typically seen in a mechanical rating of a gear set. Without knowing that the gear set has experienced micropitting, it would be easy to assume that a safety factor over 1.0 means that damage will not occur.

Table 2 Input data for Case 2			
Dimension	**Units**	**Pinion**	**Gear**
Number of teeth	-	28	88
Ratio	-	4.6987	
Center distance	mm	487.51	
Normal module	mm	8.0609	
Face width	mm	200.9	
Outside diameter	mm	247.955	759.079
Pressure angle	degrees	22.5	
Helix angle	degrees	17.584	
Addendum modification coefficient	-	0.0804	0.0804
Surface roughness	1.1m	0.22	0.55
ISO accuracy grade	-	6	6
Material surface hardness	HRC	59-63	58-62
Pinion speed (nominal)	rpm	254.17	
Pinion torque (nominal)	N-m	20,880	
KA Kv KHa K-03 product	-	1.478	
Lubricant	-	Castro! Optigear A320	
Inlet lubricant temperature	°C	50	
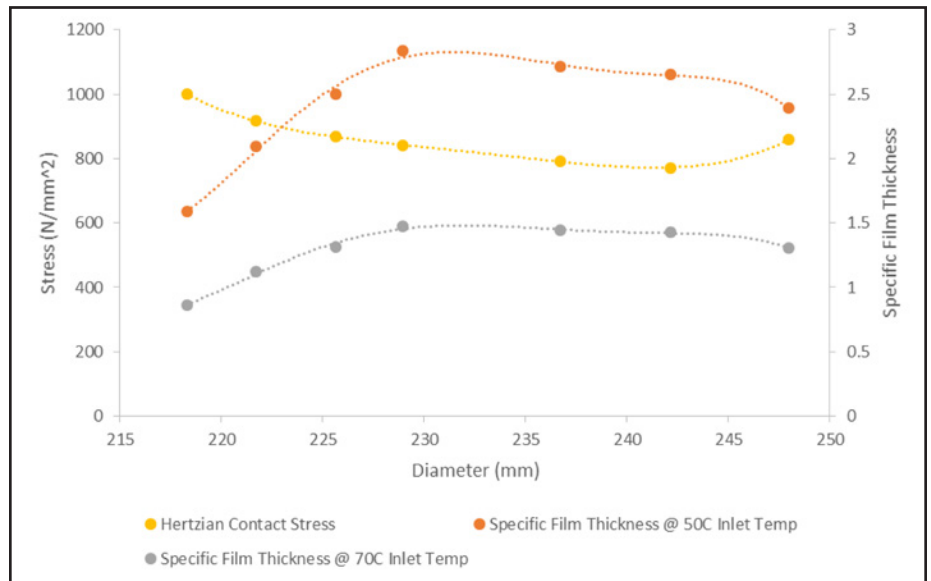
Figure 10   Specific film thickness at the points along the line of action with inlet temperatures of 50°C and 70°C.
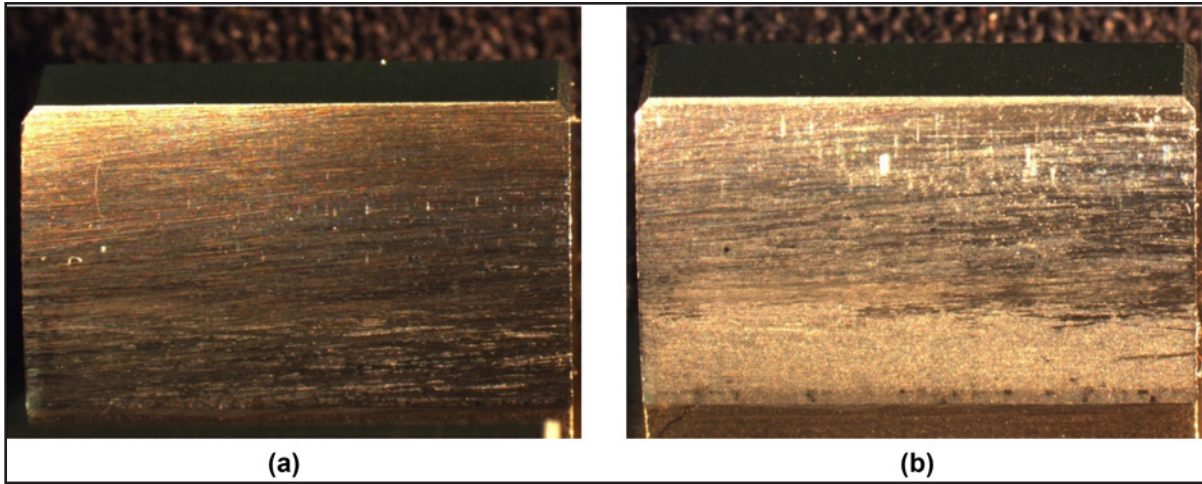
Figure 11   Micropitting images of test pinion after (a) Stage 6 and (b) Stage 10.

Table 3   Input data for Case 3

Dimension	Units	Pinion	Gear
Number of teeth	-	20	30
Ratio	-	1.50	
Center distance	mm	91.50	
Normal module	mm	3.629	
Face width	mm	13.97	
Outside diameter	mm	82.042	116.716
Pressure angle	degrees	20.00	
Helix angle	degrees	0	
Addendum modification coefficient	-	0.2533	-0.0296
Surface roughness	Idm	0.34	0.22
ISO accuracy grade	-	4	5
Material surface hardness	HRC	59-61	59-61
Pinion speed	rpm	2.250	
Pinion torque	N-m	265	
KA Kv KHot KHp product	-	1.0826	
Lubricant	-	Various	
Inlet lubricant temperature	°C	80	

Table 4   Lubricant data for Case 3

Lubricant Designation	M-460-EP	M-220-EP	M-220-RO	M-068-EP
Base Lubricant Type	Mineral	Mineral	Mineral	Mineral
Additive Type	EP	EP	R&O	EP
Kinematic Viscosity @40°C (cSt)	427.9	211.9	215.5	68.2
Kinematic Viscosity ©40°C (cSt)	30.6	18.7	19.0	8.5

Table 5   Input data for FZG "C" gear set

Dimension	Units	Pinion	Gear
Number of teeth	-	16	24
Ratio	-	1.50	
Center distance	mm	91.50	
Normal module	mm	4.5	
Face width	mm	14	
Outside diameter	mm	82.45	118.35
Pressure angle	degrees.	20.00	
Helix angle	degrees	0	
Addendum modification coefficient	-	0.1817	0.1716
Surface roughness	!dm	0.5	0.5
Pinion speed	rpm	2,250	
Pinion torque	N-m	265.1	
Ka Kv KHa KI-Ip product	-	1.05	
Inlet lubricant temperature	°C	90	

As with Case 1, this case has a high value for the specific film thickness and the tooth flanks and asperities should not be in contact. The undamaged sections of the tooth flanks are witness to this. Yet micropitting occurred on the flanks in the area of highest sliding.

As in the previous example, studies were not done with similar gearing to determine the permissible specific film thickness. Micropitting test results per Method A were not available. As a result, the calculation used the general permissible specific film thickness curves from FVA-FZG testing of mineral oils per ISO/TS 6336-22, Annex A. If the lubricant quality and operating temperature are taken into effect, the permissible specific film thickness is calculated to be 0.319 assuming a high quality lubricant.

Whether the minimum specific film thickness is calculated with an inlet lubricant temperature of 50°C or 70°C, the safety factor will still be greater than 2.50.

Wind turbines are considered to be critical applications due to the difficulty of repairing a gear drive that is high above the ground in close quarters. To seriously apply ISO/TS 6336-22 to a wind turbine gear drive, Method A should be used to determine the lubricant film thickness in the entire contact zone. A more representative way of determining the permissible specific film thickness should also be assessed.

Case 3 – AGMA tribology test gear set. The third case is the gearing used in the AGMA Tribology Test Program (Ref. 10). This program was a project of the AGMA Helical Gear Rating Committee to explore the effect of lubricants on gear

life with tests that mimic actual operation. Several AGMA member companies collaborated to design and manufacture gearing that is similar to FZG "C" gears, but more representative of industrial gears. They have finer pitch, different tooth counts, and incorporate tip relief and profile modifications to remove interference. They also have axial crowning to increase compressive stress near the center of the face width. One hundred gear sets were manufactured and run in a four-square FVA-FZG test rig with the sump temperature set to 80°C. The tests were stopped every 24 hours for inspection with a stereomicroscope set to 10x magnification. The test was terminated if one of three events happened:

- Macropitting damage that exceeded 1% of the total surface area of all pinion or gear teeth.
- Macropitting damage that exceeded 4% of the total surface area of a single tooth.
- 400 hours of running time without damage.

Note that the presence of micropitting didn't stop the test — it was noted in the results.

The gear sets were run with five different mineral lubricants from three viscosity grades (68, 220, and 640) and two additive packages (EP and R&O). The torque was set to 265 Newton-meter (N-m) and the pinion speed was 2,250 rpm. The pitch line velocity of this gear set is 8.624 m/s, which is at the lower limit of the speed range of ISO/TS 6336-22.

Unfortunately, detailed pictures of the gear teeth after testing have not been retained. The Tribology Test Program report describes micropitting on most gear teeth. Houser included some pictures of micropitted pinion teeth his 2015 AGMA Fall Technical Meeting paper (Ref. 11).

The gear sets in this example are relatively close to the FZG "C" gears. It's possible to calculate the permissible specific film thickness with the geometry of the FZG "C" gears and the failure load stage of each lubricant. ISO/TR 6336-31 (Ref. 12) illustrates this calculation in Example 1. The FZG "C" gears are known to begin micropitting at contact point A. The nominal torque for failure load stage 10 is 265.1 N-m. Method

Table 6 Results of ISO/TS 6336-22 calculations for AGMA Tribology Test gearing					
Case Number	Lubricant	Torque N-m	λ_{GFmin}	λ_{GFP}	S_λ
1	M-460-EP	265	0.331	0.185	1.79
2	M-220-EP	265	0.226	0.129	1.75
3	M-220-RO	265	0.237	0.136	1.75
4	M-068-EP	265	0.123	0.073	1.69
5	M-220-EP	300	0.201	0.129	1.56
6	M-220-EP	400	0.147	0.129	1.14

A calculations of the nominal Hertzian contact stress at point "A" come to 1,476 N/mm². This stress was entered into the analytical model to find the permissible specific film thickness. The input data for the FZG "C" gears is shown in Table 5.

The calculation results for the four different lubricants are shown in Table 6. After running all calculations at 265 N-m, additional load cases of 300 N-m and 400 N-m were calculated to see if increasing the load would push the safety factor below 1.0.

Micropitting was found in the dedendum of most gearing during the AGMA Tribology tests. The minimum specific film thickness is below 1.0 in all cases, indicating that gears are running in a boundary lubrication regime. In boundary lubrication, the properties of the lubricant and the roughness of the tooth flank surfaces can contribute to surface distress, such as micropitting. The safety factors against micropitting remain above 1.0, though.

This is not an unusual result from ISO/TS 6336-22 and it has been reported in other papers. Both Pinnekamp (Ref. 7) and Sagraloff (Ref. 13) present graphs of safety factors calculated for various examples as functions of the quality of the calculations and knowledge of the operating conditions; these graphs are similar to Figure 12. Assuming that the calculations for this case are average, the results fit into the grey space in the chart.

As the load increased, the shape of the film thickness curve along the points of the line of action remains consistent. This can be seen in Figure 13. Note that the contact stresses for each case are not shown in the figure in order to make the graph more readable. The prominent "bump" in the curves is caused by the local sliding factor in the film thickness equation, which rises sharply to a value of 1.0 at the pitch point and then drops off quickly.

Conclusion

ISO/TS 6336-22 is the only published technical document for predicting the occurrence of micropitting on gear tooth flanks. It should not be applied without a careful study of the calculations in the document and an understanding of the
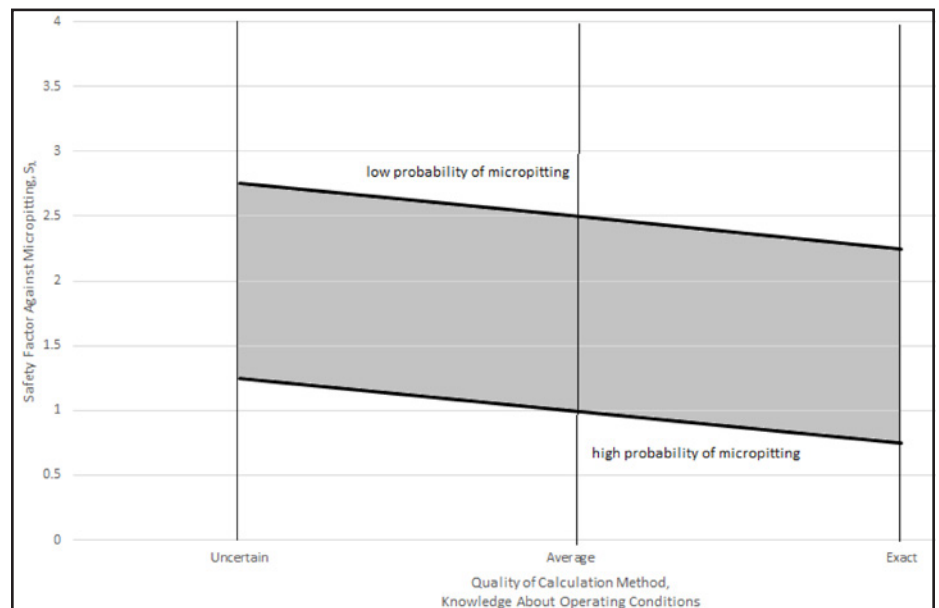
Figure 12 Probability of micropitting as a function of calculation method and application knowledge.

gear set application. This paper uses ISO/TS 6336-22 to calculate the risk of micropitting for three cases: a high-speed centrifugal compressor example, a low-speed wind turbine example, and the AGMA Tribology Test Program gearing. From the results, one can observe limitations in the method.

- When the specific film thickness is much larger than unity, micropitting cannot be predicted by film thickness and surface roughness alone. This was seen in the Cases 1 and 2. The science behind micropitting is still being researched and developed. As more is understood about the causes and predictability of micropitting, ISO/TS 6336-22 should be updated. Until then, it would be good to include in the document a discussion of the applicability of the method when the minimum specific film thickness is above 1.0.
- The permissible specific film thickness may not be representative of the lubrication used in service if testing with real gears cannot be done. ISO/TS 6336-22 contains Method B to calculate this value based on standardized testing, but this will become less certain as the geometry of the gear set differs from the geometry of the test gearing. The formulation of the lubricant used in the application also may differ from the reference curves in Annexes B and C. ISO/TS 6336-22 contains warnings about these limits and the engineer should be aware of them.
- High safety factors do not indicate low risk of micropitting. Users of ISO/TS 6336-22 should review guidance to

select the minimum safety factor based on the critical nature of the application, the accuracy of the gear measurements, the availability of test data, and the uncertainty of operating conditions. If the application is critical, Method A should be used for the calculation rather than Method B.

Future work with the cases in this paper would further explore the behavior of the ISO/TS 6336-22 specification by calculating the safety factor using Method A to arrive at the minimum- specific film thickness. Ideally, full roughness profiles would also be used for the calculations so that the impact of roughness variation in the contact zone and of different types of roughness measurements (*Ra*, *Rq*, *Rmr*, etc.) can be determined. These results would be compared to Method B and field experience.

There are limits to the accuracy of ISO/TS 6336-22, both in the specific film thickness calculation and the determination of permissible specific film thickness. It is suggested that the minimum safety factor against micropitting be selected based on experience with similar gear sets. If this is not available, the gear designer must decide if micropitting can be tolerated in the application. If not, micropitting can best be avoided by modifying tooth microgeometry to reduce overall contact stresses, reducing surface roughness (through superfinishing or by other means), and/or using high-quality lubricants.

Figure 13   Specific film thickness at the diameters along the path of contact for M-220-EP at various loads.

References

1. ANSI/AGMA. 2014, "Appearance of Gear Teeth - Terminology of Wear and Failure," 1010-F14.
2. Errichello, R.L. 2012, "Morphology of Micropitting," *Gear Technology*, November/December, pp. 74–81.
3. ISO/TC 60/SC 2/WG 6. 2018, "Calculation of Load Capacity of Spur And Helical Gears — Part 22: Calculation of Micropitting Load Capacity," ISO/TS 6336-22.
4. FVA-Information Sheet 54/7. "Test Procedure for the Investigation of the Micropitting Capacity of Gear Lubricants," 1993.
5. U. Kissling, 2011. "The Application of the First International Calculation Method for Micropitting," *AGMA Fall Technical Meeting,* Paper 11FTM12.
6. Pinnekamp, B., T. Weiss, and G. Steinberger. 2011, "Micropitting - A Serious Damage? Testing, Standards, and Practical Experience," *AGMA Fall Technical Meeting*, Paper 11FTM15.
7. Pinnekamp, B. and M. Heider. 2015, "Calculating the Risk of Micropitting Using ISO Technical Report 15144-1:2014 – Validation with Practical Applications," *AGMA Fall Technical Meeting*, Paper 15FTM26.
8. Dudley, D. 1981, "Characteristics of Regimes of Gear Lubrication," *International Symposium on Gearing 2039 and Power Transmissions*, Tokyo, Japan.
9. Keller, J., Michaud, M., and Lambert, S., 2020, "Report of the Condition of a General Electric Transportation Systems Gearbox," NREL/TP-5000-76004, National Renewable Energy Laboratory, Golden, CO.
10. Bradley, W.A. "AGMA Tribology Test Report," AGMA Foundation Report, 2008.
11. Houser, D.R. and Shon S. 2015, "An Experimental Evaluation of the Procedures of the ISO/TR 15144 Technical Report for the Prediction of Micropitting," AGMA Fall Technical Meeting, Paper, 15FTM25.
12. ISO/TC 60/SC 2/WG 6, 2018. "Calculation of Load Capacity of Spur and Helical Gears — Part 31: Calculation Examples of Micropitting Load Capacity," ISO/TR 6336-31.
13. Sagraloff, N., M. Hein, T. Tobie and K. Stahl. 2017, "Practical use of micropitting test results according to FVA 54/7 for calculation of micropitting load capacity acc. to ISO/TR 15144-1," *VDI International Conference on Gears.*

Robin Olson is the Director of Applications Engineering for the Material Handling Vertical at Rexnord here. She is a member of the AGMA Helical Gear Rating Committee, Chairperson of the AGMA 925 subcommittee, and is honored to act as US delegate to ISO Working Groups 6 (Gear calculations). Previously, Robin has also been a member of the AGMA Computer Programming, Enclosed Drives, and Marine Drive committees. Robin holds a Bachelor of Science in Physics from the University of Wisconsin—LaCrosse and a Master of Science in physics from the University of Wisconsin—Madison.

Mark Michaud recently celebrated his 40th year with REM Surface Engineering. Mark is the inventor and pioneer of REM's chemically accelerated finishing technology; currently serving as a Technical Fellow. Mark Michaud is a leading scientist, technical mentor and continues to play a crucial role in the company's future. Mark has authored numerous patents and technical papers and served a term on the AGMA Board of Directors. Mark continues to serve as vice-chair of the AGMA Aerospace Committee, as a member of the AGMA Wind Turbine Committee and as a shadow delegate on the ISO 614-4 Wind Turbine Committee. He graduated with a Bachelor's degree in Chemistry from Reed College and an MBA from the University of Hartford.

Jonathan Keller is the team leader for drivetrain technology. Jon leads projects ranging from the development and verification of new drivetrains with improved performance, power density, and efficiency and to in-depth research investigations of failure modes and improvement in reliability of existing drivetrains often conducted in the dynamometers or field turbines at the NREL Flatirons Campus. Examples of these projects are the Drivetrain Reliability Collaborative and the NREL-led Next Generation Drivetrain. Prior to joining NREL, Keller worked for the U.S. Army at Redstone Arsenal, Alabama for 10 years, where he developed condition monitoring systems for Army rotorcraft to reduce the cost and maintenance burdens while increasing availability and safety.

For Related Articles Search

micropitting

at www.geartechnology.com
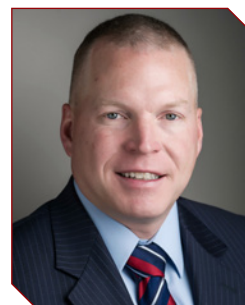
Effects of Different Shot Peening Treatments in Combination with a Superfinishing Process on the Surface Durability of Case-Hardened Gears

Dominik Kratzer, Johannes König, Thomas Tobie and Karsten Stahl

Introduction

Increasing demands on power transmission and reduction in mass of modern gearboxes lead to gear designs that are close to their load-carrying capacity limits. Therefore, the probability of different failure modes like pitting, scuffing and wear increases if there are no improvements in surface durability. Possible measures to strengthen the gear's flank load-carrying capacity include shot peening and superfinishing. During the shot peening process, compressive residual stresses are induced in the surface near area of the gear (Ref. 5). According to König et al. (Ref. 11), this can lead to a significant increase in pitting resistance. Another possibility to strengthen a gear's surface is to reduce its surface roughness, for example, with superfinishing processes. Both positive effects have been proven in multiple experimental research projects (Refs. 10, 11, 15 and 17), but the combined applicability in a predictive surface durability calculation has not been proven until now. This paper presents the results of these investigations, which were carried out as a part of the FVA (Research Association for Drive Technology) research project 521 II (Ref. 12).

State of the Art and Research Objectives

The scientific literature (Refs. 10–11; 15 and 17) contains numerous investigations describing the influence of smooth surfaces due to superfinishing processes and residual stresses on the surface durability of gears. Schwienbacher et al. (Ref. 13) and König et al. (Ref. 11) proposed an extension of the calculation approach described in ISO 6336-2 (Ref. 9) to consider these effects.

According to the international gear rating standard ISO 6336-2 (Ref. 9), the permissible contact stress for gears is calculated using Equation 1:

$$\sigma_{HP} = \frac{\sigma_{Hlim} \cdot Z_{NT}}{S_{Hmin}} Z_L \cdot Z_v \cdot Z_R \cdot Z_W \cdot Z_X \tag{1}$$

Where
σ_{HP} is Permissible contact stress
σ_{Hlim} is Allowable stress number for contact stress
S_{Hmin} is Minimum required safety factor for surface durability
Z_{NT} is Life factor
Z_L is Lubricant factor
Z_v is Velocity factor
Z_R is Roughness factor
Z_W is Work hardening factor
Z_X is Size factor

Schwienbacher et al. (Ref. 13) investigated the influence of

grinding temper on the flank load-carrying capacity of case-hardened gears. As a result, grinding temper caused reduced hardness depth profile values and reduced compressive residual stress profile values (Ref. 6). These effects were considered to be responsible for the resulting reduced surface durability.

Subsequently the calculation according to ISO 6336-2 (Ref. 9) was extended using the proposed surface factor Z_S to take these effects into consideration. Moreover, the investigations by König et al. (Ref. 11) showed that smoother flank surfaces lead to a higher pitting load-carrying capacity. In order to take this effect into consideration in the calculation model for the endurance strength in ISO 6336-2 (Ref. 9), the Z_R factor was replaced by the factor $Z_{R,GS}$. The resulting calculation approach for the permissible contact stress is shown in Equation 2.

$$\sigma_{HP} = \frac{\sigma_{HLIM} \cdot Z_{NT}}{S_{Hmin}} Z_L \cdot Z_v \cdot Z_{R,GS} \cdot Z_W \cdot Z_X \cdot Z_S \tag{2}$$

Where
$Z_{R,GS}$ is Roughness factor for superfinished gears
Z_S is Surface factor

Detailed descriptions of the calculation approaches for the factors Z_S and $Z_{R,GS}$ are presented in the following.

Calculation of Z_S

Schwienbacher et al. (Ref. 13) detected that the flank load-carrying capacity of case-hardened gears is influenced by the degree of grinding temper on the gears' flanks. The reduced compressive residual stresses and reduced hardness value in surface near material regions due to grinding temper were considered as the main reason for the reduced flank load-carrying capacity compared to gears without grinding temper. Therefore Schwienbacher et al. (Ref. 13) correlated the resulting flank load-carrying capacity of gear batches with different degrees of grinding temper with the measurement results for the residual stress depth profile and the hardness depth profile. As a result the surface factor Z_S according to Equation 3 consists of a factor regarding the influence of hardness ($Z_{S,HV}$) and a factor regarding the influence of the residual stresses ($Z_{S,ES}$) according to Equations 4–5 and as defined by Schwienbacher et al. (Ref. 13).

$$Z_S = Z_{S,HV}^{0.49} \cdot Z_{S,ES}^{0.51} \tag{3}$$

$$Z_{S,HV} = 1 + \frac{1.68 \cdot \overline{\Delta HV_{int\_xn}}}{621 \, HV1} \quad \text{with} \quad \overline{\Delta HV_{int\_xn}} = \overline{HV_{int\_xn}} - \overline{HV_{int\_xn\_Ref}} \tag{4}$$

$$Z_{S,ES} = 1 + \frac{1.91 \cdot \overline{\Delta ES_{int\_xn}}}{6575 \, N/mm^2} \quad \text{with} \quad \overline{\Delta ES_{int\_xn}} = \overline{ES_{int\_xn}} - \overline{ES_{int\_xn\_Ref}} \tag{5}$$

Where

$Z_{S,HV}$ is Surface hardness factor

$Z_{S,ES}$ is Surface residual stress factor

$\overline{\Delta HV_{int\_xn}}$ is Difference of the integral hardness value up to the depth x_n compared to a reference batch, HV1

$\overline{\Delta ES_{int\_xn}}$ is Difference of the integral residual stress value up to the depth x_n compared to a reference batch, N/mm²

$\overline{HV_{int\_xn}}$ is Integral hardness value up to the depth x_n, HV1

$\overline{HV_{int\_xn\_Ref}}$ is Integral hardness value of the reference batch up to the depth x_n, HV1

$\overline{ES_{int\_xn}}$ is Integral residual stress value up to the depth x_n, N/mm²

$\overline{ES_{int\_xn\_Ref}}$ is Integral residual stress value of the reference batch up to the depth x_n, N/mm²

Since the factor Z_S takes into account deviations in comparison to a reference, the $\overline{\Delta HV_{int\_xn}}$ and $\overline{\Delta ES_{int\_xn}}$ values are calculated by comparing the investigated gear batch ($\overline{HV_{int\_xn\_Ref}}/\overline{ES_{int\_xn\_Ref}}$) with a known reference batch ($\overline{HV_{int\_xn\_Ref}}/\overline{ES_{int\_xn\_Ref}}$). The variables $\overline{\Delta HV_{int\_xn}}$ and $\overline{\Delta ES_{int\_xn}}$ in Equations 4–5 are obtained by numerically integrating the subsurface measuring points up to the depth x_n. The depth x_n is the minimum depth from the surface at which the hardness or residual stress profile of the investigated gear batch deviates from the reference gear batch. The variables are calculated as described in Equations 6 and 7.

$$\overline{HV_{int\_xn}} = \frac{1}{x_n} \cdot \sum_{i=1}^{n-1} \frac{HV_{i+1} + HV_i}{2} \cdot (x_{i+1} - x_i) \qquad (6)$$

$$\overline{ES_{int\_xn}} = \frac{1}{x_n} \cdot \sum_{i=1}^{n-1} \frac{\sigma_{E_{i+1}} + \sigma_{E_i}}{2} \cdot (x_{i+1} - x_i) \qquad (7)$$

Where

x_i is Depth of measurement point i, mm

HV_i is Surface hardness at measurement point i, HV1

σ_{E_i} is Residual stress value at measurement point i, N/mm²

Calculation of $Z_{R,GS}$

König et al. (Ref. 11) investigated gears which were subjected to a shot peening and a superfinishing process. Shot peening leads to increased subsurface compressive residual stress values, which might affect the surface durability (Ref. 5). To take this effect into consideration when calculating the pitting load-carrying capacity, König et al. (Ref. 11) used the above mentioned approach according to Schwienbacher et al. (Ref 13). It was shown that the calculation results show a good correlation with the experimental results. Since only a limited number of gear variants were investigated, different peening conditions still had to be validated.

Since an additional superfinishing process was applied to all gear batches investigated by König et al. (Ref. 11), a significant refinement of the surface roughness values compared to the conventionally ground gear batch occurred in accordance with other research (Refs. 16–17). The influence of the surface roughness on the pitting load-carrying capacity is regarded in the rating method according to ISO 6336-2 by the surface roughness factor Z_R as defined in Equation 8 for case-hardened gears.

$$Z_R = \left(\frac{3}{Rz_{10}}\right)^{0.08} \qquad (8)$$

Where

Z_R is Roughness factor

Rz_{10} is Mean relative peak-to-valley roughness for the gear pair

The Z_R factor according to ISO 6336-2 (Ref. 9) covers values for Rz_{10} down to 1 μm. Since the Rz_{10} values for superfinished gears are below this limit, the possible extension of the given ISO formula was investigated. The experiments by König et al. (Ref. 11) showed that the ISO factor Z_R for superfinished gears might be replaced by the factor $Z_{R,GS}$. The factor can be calculated according to Table 1 or derived graphically (Fig. 1). The factor $Z_{R,GS}$ limits the theoretical curve of Z_R to the value 1.14. The factor $Z_{R,GS}$ of König et al. (Ref. 11) is calculated according to DIN 3990-2 (Ref. 2) and based on the Rz_{100} value. In the following, this factor is replaced by the Rz_{10} value according to the new convention in ISO 6336-2 (Ref. 9).

The limit of 1.14 for the $Z_{R,GS}$ factor results from the experimentally covered range of roughness values. A further extension of applicability of $Z_{R,GS}$ to lower roughness values has not yet been investigated.

In summary, the application of the surface factor Z_S for shot peened gears and the extension of the roughness factor Z_R to $Z_{R,GS}$ are possibilities for taking into consideration positive

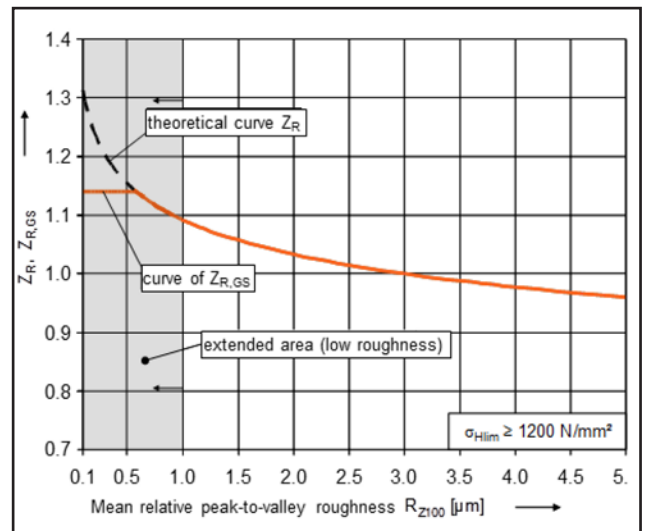| Table 1	Workflow for determining $Z_{R,GS}$ according to König et al. (Ref. 11)
Step 1: All of the following conditions must be true: 1. Gears are case-hardened 2. Gears are superfinished 3. Safety factor against micropitting of $S_\lambda > 2$	
All are true	Replace Z_R with $Z_{R,GS}$ (proceed to Step 2)
Any is false	Use Z_R according to DIN 3990-2 / ISO 6336-2
Step 2: Check if $\left(\frac{3}{Rz_{100}}\right)^{0.08} > 1.14$	
Is true	$Z_{R,GS} = 1.14$
Is false	$Z_R = \left(\frac{3}{RZ_{100}}\right)^{0.08} > 1.14$

Figure 1 Curve of the roughness factor Z_R and the extension $Z_{R,GS}$ according to König et al. (Ref. 11)

effects of gear surface refinements when calculating the pitting load-carrying capacity of gears. For the surface factor Z_S, a validation for different shot peening processes and the resulting different subsurface compressive residual stress profiles is pending, as well as the validation of the existing calculation approach for the surface roughness factor $Z_{R,GS}$ for even finer surface roughness values. These topics are addressed, evaluated and concluded in the following.

Test Program and Methods

To prove that the surface factor Z_S can be applied to consider the positive effects of increased compressive residual stresses in the flank-load carrying capacity calculation, as well as to validate the applicability of the roughness factor $Z_{R,GS}$ for smoother gear surfaces than investigated by König et al. (Ref. 11), numerous flank load-carrying capacity tests were carried out. For the tests relating to the applicability of the surface factor Z_S in the load

Table 2	Investigated variants and purpose of the corresponding shot peening treatment	
	Manufacturing	**Purpose**
R1	Unpeened reference	Reference
RGS	Shot peened and superfinished	Conventional process parameters
ET1	Shot peened and superfinished	Residual stress profile with same maximum values as RGS but closer to surface
ETT	Shot peened and superfinished	Residual stress profile with higher values into the depth of the material
EB	Shot peened and superfinished	Residual stress profile with reduced maximum value
EV	Shot blasted and superfinished	Residual stress profile after shot blasting
GSL	Shot peened and superfinished	Minimal surface roughness with conventional peening process
02	Superfinished	Minimal surface roughness without additional peening process
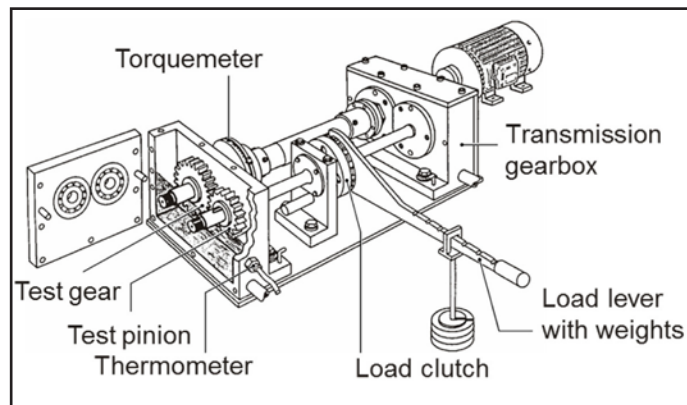
Figure 2   FZG back-to-back gear test rig (Ref. 7).

Table 3	Gear variant		
	Symbol	**Pinion**	**Wheel**
Material		16MnCr5	
Number of teeth	$z_{1,2}$	17	18
Face width	b	10 mm	
Normal module	m_n	5 mm	
Profile shift coefficient	x	0.514	0.407
Normal pressure angle	α_n	20°	
Helix angle	β	0°	

area of high cycle fatigue, five variants were tested at the same load level in order to compare the mean load cycles until failure occurs. In order to prove the applicability of the $Z_{R,GS}$ factor for values above 1.14, S-N-curves were evaluated for several variants with different flank roughness values. For the superfinished batches with very smooth surfaces, vibratory finishing with and without chemical enhancement were applied after the conventional grinding to obtain even finer surface roughness values. The shot peening process took place between the grinding and the superfinishing processes. All variants and the intended purpose are summarized in Table 2.

To validate the calculation model for the roughness factor $Z_{R,GS}$, experimental tests were carried out with a FZG back-to-back gear test rig in accordance with ISO 146351 (Ref. 7) in order to obtain the nominal endurance strength for 50 % failure probability of the variants RGS, ET1, EB, GSL and O2. Generally, the gears in the test and transmission gearboxes are loaded by rotating the two shaft parts next to the load clutch in opposite directions. By locking the load clutch, a closed mechanical power circuit results. The desired pressure on the test gears is monitored by locking the load clutch at certain angles of rotation, depending on the intended amount of load. Controlling this angle of rotation after a defined number of revolutions guarantees the stability of the applied torque. The electric motor drives the test gears at the required pinion speed of 3,000 rpm. The lubricant FVA 3 with 4 % anglamol, a sulfur and phosphorus containing additive, at 60°C by way of injection lubrication was used for the investigations, as there is an extensive data base for this type of oil.

The geometry of the test gear was used in accordance to other research projects at FZG with the aim to investigate the flank load-carrying capacity. The gears' geometry is summarized in Table 3. All gears were manufactured from 16MnCr5, case-hardened, mechanically cleaned by shot blasting and ground. Depending on the variant described in Table 2, the mentioned shot blasting respectively shot peening took place before the final superfinishing process. Details of the corresponding process parameters are described in (Ref. 12). Figure 3 shows sample gear flanks after conventional grinding in the left picture and superfinishing in the right picture.

Gear Documentation

The gear geometry, surface roughness, material characteristics and micro-structure, the hardness profile and residual stress profile were documented before each test.

The gear quality was measured according to DIN 3962 (Ref. 1)

Figure 3   Surface appearance.

Table 4	Roughness measurements	
Gear variant	Ra in µm	Rz in µm
R1	0.34	2.11
RGS	0.12	0.77
ET1	0.15	0.96
ETT	0.06	0.48
EB	0.15	0.99
EV	0.18	1.13
GSL	0.07	0.46
02	0.07	0.39

Figure 4   Sample roughness profile of a superfinished gear.

Figure 5   Etched metallographic microsection of a representative test gear.
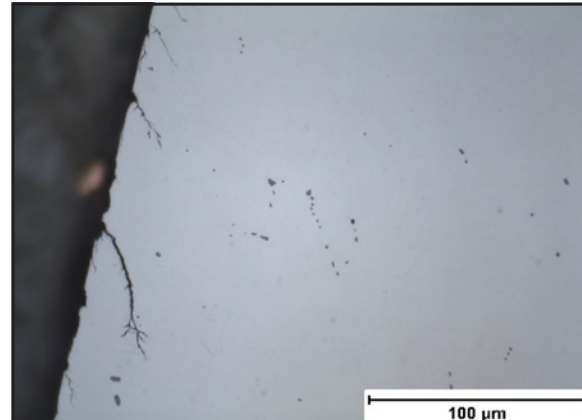
Figure 6   Unetched metallographic microsection of the variant ETT (before any testing).

using a gear measurement center Klingelnberg P40. Three teeth of every gear were measured. All relevant gear quality values were better than quality class 5, which is required for flank load-carrying tests.

The roughness was measured using the Hommel T8000 profilometer with applied high-pass filter according to DIN EN ISO 11562 (Ref. 3). Every gear was measured on three flanks evenly distributed over the circumference. A sample measurement report for a superfinished gear is documented in Figure 4. The average values of the characteristic roughness parameters for the investigated variants are shown in Table 4. Further details as well as determined roughness parameters are documented (Ref. 12).

To evaluate the microstructure of the gear variants, metallographic micro-sections were prepared for each variant. Since all gears were manufactured from the same steel bar and in the same heat treatment batch, all the gears should have the same microstructure. The typical microstructure in Figure 5 shows martensitic structure near the surface with a limited amount of retained austenite, typical for case-hardened gears. As a result, all variants fulfilled the requirements for the MQ material quality class as specified in ISO 6336-5 (Ref. 8). Thus, the microstructure is unlikely to have a negative impact on the pitting load-carrying capacity. Some undesired effects were only detected for the ETT variant. Obviously, the very intensive shot peening process resulted in small cracks on the surface before any testing was done, which can be seen in Figure 6. These small cracks are unusual for case-hardened and ground gears and therefore might influence the surface durability of this test series, as discussed later in this paper.

The hardness profile was measured for every investigated variant. Since the heat treatment was performed in one batch
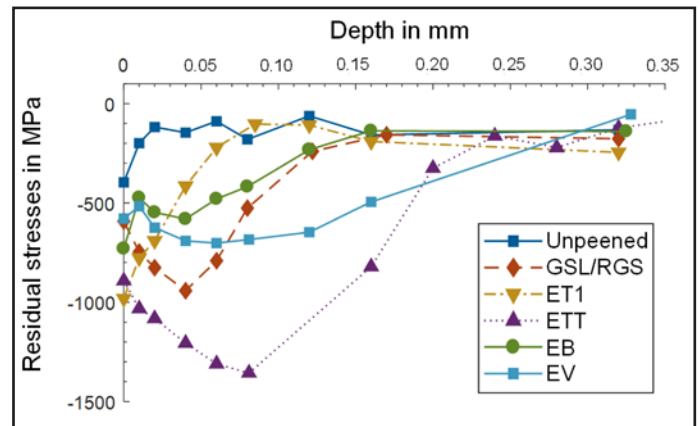
Figure 7   Residual stress profiles, measured by x-ray diffraction at the gear flank of the different test series in new condition.

for all investigated gears, the hardness depth profiles were close to identical for all variants. Surface hardness, core hardness and CHD-values corresponded to the specifications of ISO 6336-5 (Ref. 8). Therefore, the influence of the hardness on the Z_S factor mentioned previously in Section 2 can be neglected for the test series investigated here.

The residual stresses were measured using a Seifert XRD 3003 PTS x-ray diffractometer by repeatedly measuring and removing the surface layer with acid to obtain information about the depth of the material. The measurement parameters are documented in detail in (Ref. 12). The measurement results are presented (Fig. 7). As intended, the variants show different residual stress depth profiles depending on the applied shot peening treatment. It can be noted that the measurement results correspond with the intended purpose described in Table 2.

Calculation Results

To investigate if the experimental results are adequately represented by the previous calculation approaches in Section 2 the factors Z_S an $Z_{R,GS}$ have to be calculated for every gear variant. Therefore the measurement results in section 4 are utilized.

The surface factor Z_S can be calculated according to Equation 3 with the results of the hardness and residual stress measurements. As already mentioned, the hardness depth profiles do not differ significantly for any variant, and therefore the $Z_{S,HV}$ factor can be set equal to one for all test series investigated here. As a

Table 5 Calculated surface and roughness factors according to Section 2 for the investigated test series

Gear variant	Z_s	$Z_{R,GS}$	$Z_s \cdot Z_{R,GS}$
RGS	1.07	1.10	1.18
ET1	1.06	1.10	1.16
ETT	1.12	1.16	1.30
EB	1.05	1.09	1.14
EV	1.07	1.08	1.16
GSL	1.07	1.16	1.24
02	1.0	1.17	1.17

Table 6 Experimental results for the pitting load-carrying capacity (^{1}) – not investigated)

Variant	Mean load cycles at $\sigma_{H0} = 1750$ N/mm^2	$\sigma_{H0\infty,50\%}$ in N/mm^2
RGS	62 million	1701
ET1	21 million	1716
ETT	48 million	[1]
EB	21 million	1542
EV	24 million	[1]
GSL	[1]	1877
02	[1]	1746

Figure 8   S-N-curve of the variant EB.

result, the surface factor Z_S is solely influenced by the residual stress depth profile. The calculation according to the previous section results in the values shown in Table 5.

Table 5 also shows the results of the roughness factor $Z_{R,GS}$ calculation based on the measured roughness values taken from Table 4. The applicability of the calculation results for $Z_{R,GS}$ with values up to 1.14 has been scientifically proven by König et al. (Ref. 11), based on the calculation approach in ISO 6336 (Ref. 9). Values for $Z_{R,GS}$ above 1.14 for even smoother gear flanks have not been investigated until now.

Since the remaining boundary conditions influencing the factors besides Z_S and $Z_{R,GS}$ in Equation 2 are kept the same by the manufacturing and test process, the product $Z_S \cdot Z_{R,GS}$ (Table 5) represents the theoretical expectation for the resulting pitting durability. The applicability of the calculation model will be verified by experimental investigations in the following.

Experimental Results

To obtain the pitting load-carrying capacity of the investigated gear variants, tests using the FZG back-to-back test rig were carried out at different load stages. To determine the S-N-curve, load stages in the regime of high cycle fatigue and fatigue limit were investigated. Figure 8 shows by way of example the test results for the variant EB in the double logarithmic diagram as triangular markers. Test runs that reached the limit of 100 million load cycles without pitting are shown with solid markers. The tests were performed according to the FVA directive 563 I (Ref. 14). For the following evaluations, the sustained mean load cycles at a nominal contact pressure of $\sigma_{H0} = 1750$ N/mm^2 as well as the nominal endurance strength for failure probability of 50 % ($\sigma_{H0\infty,50\%}$) are summarized (Table 6).

To investigate whether the reported reduction in micropitting appearance with finer surface roughness of the gear flank can be reproduced in the current scope of experiments, sampling tests were carried out with a reference variant R1 that was manufactured using a conventional grinding process. The mean roughness value Ra was equal to 0.34 μm for this variant. During test runs with such gears, micropitting occurred over major parts of the gear flank starting in the area of negative sliding below the pitch circle, as can be seen in Figure 9. Figure 10 shows a typical superfinished gear flank with scratch marks due to the initial tooth contact after a test run. While most of the superfinished gears only show micropittings as consequential damage around

$\sigma_{H0} = 1650$ N/mm^2 | N$_1$ = 32 · 10^6

Figure 9   R1 flank surface after test.

$\sigma_{H0} = 1750$ N/mm^2 | N$_1$ = 74 · 10^6

Figure 10   RGS flank surface after test.

$\sigma_{H0} = 1650$ N/mm^2 | N$_1$ = 97 · 10^6

Figure 11   EB flank surface after test.

Figure 12   Mean load cycles until failure base on the test results at $\sigma_{H0} = 1750$ N/mm^2.

Figure 13   Calculated factors Z_S, $Z_{R,GS}$ and the resulting product.

damaged flank regions due to the locally increased stress, the variant EB shows micropittings extending from the sides of the flanks. This could be due to manufacturing deviations, which lead to local bulges on the flank sides.

In summary the results confirm the effects described in literature (Refs. 16–17) concerning the significant reduction of micropitting occurrence if smooth surfaces without local geometric deviations are guaranteed.

Evaluation of Results

Variation in residual stress profile. To determine whether the $Z_{R,GS}$ and Z_S factors can be used to qualitatively compare the mean load cycles until failure in the load region of high cycle fatigue, FZG back-to-back test rig tests were evaluated at the nominal contact stress of 1750 N/mm^2 for the variants RGS, ET1, ETT, EB and EV. For each variant, the resulting mean load cycles at that stress level and the calculated factors Z_S, $Z_{R,GS}$ as well as the product $Z_S \cdot Z_{R,GS}$ are summarized in Table 5 and Table 6. Figure 12 shows the resulting mean load cycles in a logarithmically scaled bar graph, while Figure 13 shows bar graphs of the calculated factors.

It is noticeable that the calculated factors for the ETT variant obtain high values due to the distinct compressive residual stress profile and the very fine surface roughness. In contrast to the resulting theoretical expectation, the ETT variant achieved less load cycles in the test runs than the RGS variant. This might be due to the small surface cracks shown (Fig. 6), which were caused during the manufacturing process. Therefore, the application of the surface and roughness factor in the pitting lifetime prediction is limited to manufacturing processes, which do not cause surface cracks.

The remaining variants RGS, ET1, EB and EV demonstrate a good correspondence between the test results in Figure 12 and the expectations based on t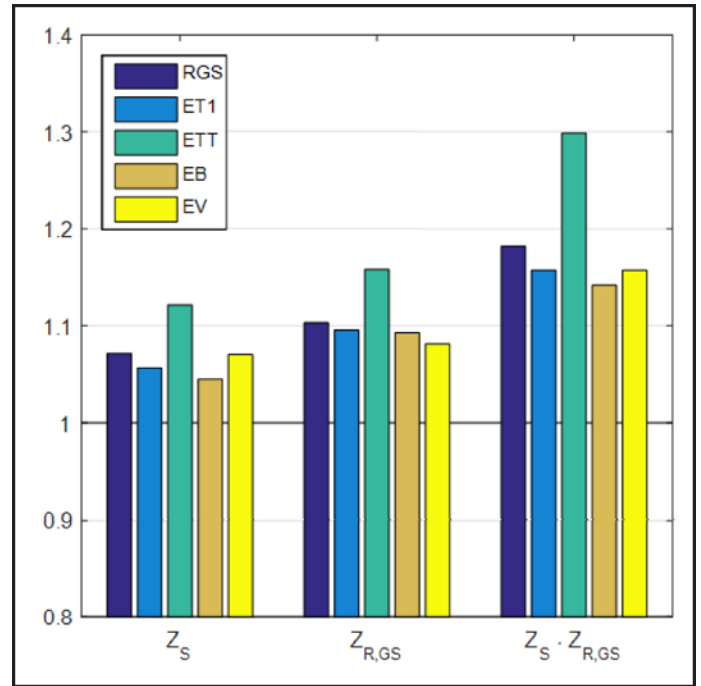he calculated factors (Fig. 13). The higher number of mean load cycles of the RGS variant is well represented by the higher value of the product $Z_S \cdot Z_{R,GS}$. The remaining variants ET1, EB and EV have similar mean load cycles, while the product of the factors has a slightly lower value for the EB variant. Since the Z_S factor was originally created to calculate the nominal endurance strength, such deviations were expected for a comparison of the mean load cycles in the load region of high cycle fatigue. Nevertheless, it was proven that the product of Z_S and $Z_{R,GS}$ can be applied to qualitatively compare the expecTable mean load cycles if the shot peening process does not result in a damaged gear surface.

Allowable stress number. Since all the investigated gears were manufactured from one material and in one heat-treatment batch, the allowable pitting stress number σ_{Hlim} should be similar. By applying the calculation approach based on ISO 6336-2 (Ref. 9), however, the results $\sigma_{Hlim,ISO6336}$ show distinct deviations (Table 7). This is due to the insufficient consideration of the compressive residual stress state and surface roughness for shot peened and superfinished gears in the current ISO standard. Therefore, the aforementioned factors $Z_{R,GS}$ and Z_S were applied. By considering these factors in the calculation of σ_{Hlim}, a significant reduction in the scattering of the results can be observed for the investigated variants. For these allowable stress numbers, labeled with $\sigma_{Hlim,experiment}$ (Table 7), only the EB variant shows a larger deviation. Some gear flanks of the EB variant showed micropittings extending from the sides of the flank as shown (Fig. 11). According to Felbermaier et al. (Ref. 4), micropittings,

Table 7	Experimental results		
Variant	$\sigma_{H0\infty,50\%}$	$\sigma_{Hlim,ISO6336}$	$\sigma_{Hlim,experiment}$
RGS	1701 N/mm^2	1701 N/mm^2	1583 N/mm^2
ET1	1716 N/mm^2	1723 N/mm^2	1631 N/mm^2
EB	1542 N/mm^2	1552 N/mm^2	1484 N/mm^2
GSL	1877 N/mm^2	1877 N/mm^2	1656 N/mm^2
02	1746 N/mm^2	1746 N/mm^2	1631 N/mm^2

which arise during the tests, might reduce the pitting load-carrying capacity by about 7%. Taking this into account, the calculated allowable stress number for the EB variant aligns with the other test results. Since the results for the variants RGS, ET1, GSL and O2 also match well, it is assumed that the effects of the peening and superfinishing processes are adequately represented by the extended calculation factors.

Extension of $Z_{R,GS}$ factor. For the extension of the upper limit for $Z_{R,GS}$, S-N-curves were determined for the variants GSL and O2. The gears of the GSL variant were shot-peened in accordance with the state of the art and then superfinished. The average surface roughness after superfinishing was $Rz = 0.46\,\mu m$, which results in a roughness factor of 1.16 according to the theoretical Z_R curve. A roughness factor of 1.17 was calculated for the variant O2. The classification of the test results with the allowable stress number according to the ISO standard, carried out in section 7.2, shows that the application of the increased roughness factor correctly reflects the obtained test results, independent of any previously applied shot peening. For the increased roughness factor, a new limit value of $Z_{R,GS,max} = 1.17$ can therefore be applied on the basis of the documented test results. $Z_{R,GS}$ is on the slightly conservative side, especially for variants with the finest surface roughness values. The scatter range already existing in the ISO standard can also be applied therefore to the newly set limit value. However, this range should not be used without further experimental verification. Following the approach of König et al. (Ref. 11) the upper limit for $Z_{R,GS}$ in Table 1 can be set to 1.17 and the graph for the roughness factor can be extended as shown in Figure 14.
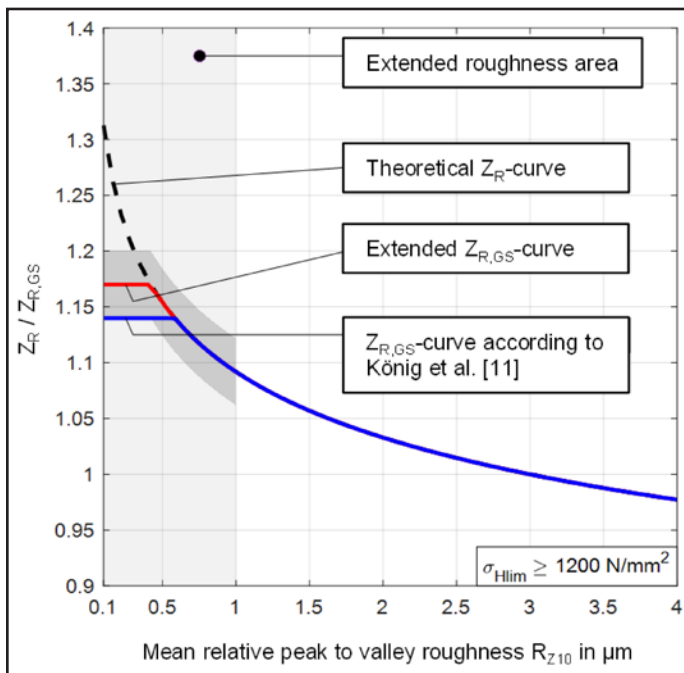

Figure 14 Curves of the roughness factor Z_R and the extension $Z_{R,GS}$.

Conclusion

An extensive experimental study with differently shot peened and superfinished gears was carried out in order to investigate the applicability of the proposed surface factor Z_S for different residual stress profiles and to extend the scope of application for the roughness factor $Z_{R,GS}$.

Superfinished variants showed significantly less micropitting appearance after testing compared to the conventionally ground variant. As root cause for this effect it is presumed that the superfinished flank surfaces are smooth and without bulges. If bulges are present, they may lead to a locally increased stress, which results in a higher probability of micropitting.

In order to investigate the resulting mean load cycles until failure, numerous variants, which underwent different shot peening processes and therefore showed different subsurface compressive residual stress profiles, were tested at the same load level in the region of high cycle fatigue. It was possible to show, that the factors Z_S and $Z_{R,GS}$ can be applied to qualitatively compare the different variants, provided that no surface damage was caused by the shot peening treatment.

So far the calculation approach according to ISO 6336 (Ref. 9) is based on investigations with conventionally manufactured, ground gears. Gears with increased compressive residual stresses due to shot peening processes and smooth surfaces due to superfinishing processes are not considered yet. By extending the ISO 6336 (Ref. 9) calculation approach by the Z_S factor as well as the $Z_{R,GS}$ factor according to König et al. (Ref. 11) a good correlation results for the calculated allowable stress numbers. Therefore, it is assumed that the factor Z_S and $Z_{R,GS}$ are suiTable to take the positive effects of different shot peening processes as well as superfinishing processes into account for gearbox design and rating processes. Furthermore the roughness factor for superfinished gears $Z_{R,GS}$ can be applied to higher values than suggested by König et al. (Ref. 11). The new maximum value for $Z_{R,GS}$ resulting from the surface roughness of the investigated gears is 1.17.

In summary, shot peening and superfinishing processes can increase the surface durability of case hardened gears significantly. To obtain the optimal effect, the superfinished gear surface must be smooth without bulged flanks and without prior damage originating from the shot peening process.

For more information.
Questions or comments regarding this paper? Contact Dominik Kratzer at *kratzer@fzg.mw.tum.de.*

References

1. Deutsches Institut für Normung e.V., 1978, "Tolerances for Cylindrical Gears, Part 1 to 3 (in German)", Norm DIN 3962. Beuth Verlag, Berlin.

2. Deutsches Institut für Normung e.V., 1987, "Calculation of load capacity of cylindrical gears - Part 2: calculation of pitting resistance (in German)", Norm DIN 3990-2. Beuth Verlag, Berlin.

3. Deutsches Institut für Normung e.V., 1998, "Surface texture: Profile method - Metrological characteristics of phase correct filters (in German)", Norm DIN EN ISO 11562. Beuth Verlag, Berlin.

4. Felbermaier, M., Tobie, T., and Stahl, K., 2014, „Micropitting - Pitting II". Influence of micropitting on the pitting durability of case-hardened gears in the regime of high cycle fatigue and fatigue limit (in German)" ,Project Nr. 459 II (IGF-Nr. 16088 N), Final report, FVA magazine Nr. 1087, Frankfurt am Main.

5. Güntner, C., T. Tobie and K. Stahl, K. 2017, "Influence of the Residual Stress condition on the Load Carrying Capacity of Case Hardened Gears," American Gear Manufacturers Association, AGMA Technical Paper, 17FTM20.

6. Höhn, B.-R., Stahl, K., Oster, P., Tobie, T., Schwienbacher, S., and Koller, P., 2012, "Grinding Burn on Gears - Correlation between Flank-Load Carrying Capacity and Material Characteristics", The 4th International Conference on Power Transmission, pp.113–123

7. International Organization for Standardization, 2000, "Gears - FZG test procedures - Part 1: FZG test method A/8,3/90 for relative scuffing load-carrying capacity of oils", Norm ISO 14635-1

8. International Organization for Standardization, 2003, "Calculation of load capacity of spur and helical gears – Part 5: Strength and quality of materials", Norm ISO 6336-5:2003(E). Beuth Verlag, Berlin

9. International Organization for Standardization, 2006, "Calculation of load capacity of spur and helical gears – Part 2: Calculation of surface durability (pitting)", Norm ISO 6336-2:2006(E). Beuth Verlag, Berlin

10. Kobayashi, M. and K. Hasegawa. 1990, "Effect of Shot Peening on the Pitting Fatigue *Strength of Carburized Gears,*" *Proceedings of the IV International Conference on Shot* Peening,, pp.465–476

11. König, J., P. Koller, T. Tobie and K. Stahl. 2015, "Correlation of Relevant Case Properties and the Flank Load Carrying Capacity of Case-Hardened Gears", Proceedings of the ASME Design Engineering Technical Conference, 10.

12. König, J., T. Tobie and K. Stahl. 2017, "Optimized flank load carrying capacity II," Load capacity of shot peened and superfinished gear flanks under considerations of the case properties and the lubrication condition (in German)," Project Nr. 521 II (AiF-Nr. 17145), Final report, FVA-magazine Nr. 1245, Frankfurt am Main.

13. Schwienbacher, S., B. Wolter, T. Tobie, K. Stahl, B.-R Höhn, B.-R. and M. Kröning. 2007, „Case properties - gear flank." Investigation and characterization of case parameters and properties and their influence on the flank load carrying capacity of case-hardened, grinded gears (in German)," Porject Nr. 453, Final report, FVA-magazine Nr. 830, Frankfurt am Main.

14. Tobie, T. and P. Matt. 2012, "Recommendations for the Standardization of Load Capacity Tests on Hardened and Tempered Cylindrical Gears," FVA 563/I. Forschungsvereinigung Antriebstechnik e.V. (FVA), Frankfurt am Main.

15. Townsend, D. P. and E.V. Zaretsky. 1982, "Effect of Shot Peening on Surface Fatigue Life of Carburized and Hardened AIS1 9310 Spur Gears," NASA Technical Paper, 2047.

16. Winkelmann, L., O. El-Saeed and M. Bell. 2009, "The Effect of Superfinishing on Gear Micropitting," *Gear Technology*, pp.60–65.

17. [17] Zhang, J. and B.A. Shaw. 2011, "The Effect of Superfinishing on the Contact Fatigue of Case Carburized Gears," *Applied Mechanics and Materials*, 86, pp.348–351

For Related Articles Search

shot peening

at www.geartechnology.com

Dominik Kratzer is since 2017 a Research Associate at the FZG Gear Research Centre of the Technical University of Munich. He graduated from the Technical University of Munich with a master's degree in mechanical engineering. His research focuses on the impact of surface finishing processes and material treatments on the load-carrying capacity of gears.

Dr.-Ing. Johannes Koenig studied (2006–2012) Mechanical Engineering at the Technical University of Munich (TUM). From 2012 to 2019 he worked as Research Associate, Team Leader "Materials and Processing" Department "Load Carrying Capacity of Gears" at the Gear Research Centre (FZG), Techncal University of Munich (TUM). He received his PhD in 2020. He currently is an Engineer in the Gear Development Department (Corporate R&D), focusing on Plastic Gear Design & Strength Calculation for ZF Friedrichshafen AG, Friedrichshafen, Germany.

Dr.-Ing. Thomas Tobie studied mechanical engineering at the Technical University of Munich (TUM), Germany. Today he is head of the Load Carrying Capacity of Cylindrical Gears department at the Gear Research Centre (FZG), where he specializes in gear materials, heat treatment, gear lubricants and gear load carrying capacity research. Concurrently, Tobie brings to that work a particular focus on all relevant gear failure modes such as tooth root breakage, pitting, micropitting and wear, as well as sub-surface-initiated fatigue failures.

Prof. Dr.-Ing. Karsten Stahl has since 2011 been Full Professor, Institute for Machine Elements, Technical University of Munich, and the Director Gear Research Centre (FZG). He studied at the Technical University of Munich (TUM) beginning in 1989, with a focus on design and development, receiving his Final Mechanical Engineering Degree (Dr.-Ing) there in 1994. In 2001, he received his Doctorate TUM with the topic: Pitting Resistance of Carburized Spur and Helical Gears. Among his responsibilities during his Professorship: 2009–2010 — Head of Advanced Engineering and Innovation Management, Powertrain and Driving Dynamic Systems, BMW Group, Munich; 2007–2009 — Head of Validation Driving Dynamics and Powertrain, BMW Group, Oxford, UK; 2006–2007 — Head of Quality and QMT MINI Transmission, MINI Plant, BMW Group, Oxford, UK; 2003–2006 — Head of Prototyping, Gear Technology and Methods, BMW Group, Dingolfing; 2001–2003 — Development Engineer in Gear Production, BMW Group, Dingolfing; and 1994–2000 — Scientific Research Assistant (Ph.D. candidate) at Gear Research Centre (FZG), TUM. Prominent among his Professional Activities: Since 2020 DFG: Member of Review Board 402-01; 2016–2018 AiF: Member of Review Board 4. His many honors and awards include (2019) VDMA Faculty Teaching Concept Award, "Bestes Maschinenhaus"; (2019) VDMA Faculty Teaching Concept Award; and (2019) Student Award "Goldene Lehre," Best course of lectures in MW-Bachelor; and (2005) VDI Ring of Honors Award; he has chaired and participated in numerous international conferences, particularly for VDI Gearing Conferences. Stahl's Editorial and many other activities (too numerous to list all here) include: Springer-Nature: Forschung im Ingenieurwesen, journal, Editor in Chief ASME: Journal of Vibration and Acoustics (JVA), Associate Editor Inderscience: International Journal of Powertrains (IJPT), Member of the Editorial Board EDP Sciences: International Journal of Mechanics & Industry, and Editor Tecniche Nuove: Organi di Trasmissione.

AGMA
923 REVISIONS EXPECTED IN Q3

According to Dr. Carl Ribaudo, Chairman of the AGMA Metallurgy and Materials Committee, the next edition of the widely used and referenced AGMA 923 Information Sheet is expected for publication by the third quarter of 2021. The revision is the first major update since the first edition was published in 2000. The Committee is currently working through its second draft of review and comments. The title of the Information Sheet has been expanded to "Metallurgical Specifications for Steel and Cast-Iron Gearing" to reflect first-time guidance on gray iron, ductile iron, and austempered ductile iron materials.

The definitions section has been thoroughly reviewed to provide greater clarity and accessibility. For example, all terms related to hardness, such as core hardness, continue to be listed individually, but the definitions now appear under a single heading.

In the procedures section, both methods and references have been updated. The reduction ratio calculation methodology has been expanded with new figures that illustrate several common metal conversion sequences including closed die forging and ring rolling.

- Significant changes were made to the tables of metallurgical characteristics in the document:
- Requirements now appear in the order of processing
- Chemistry and cleanliness requirements have been revised to reflect current processing capabilities and field experiences.
- The footnotes have been reworded and renumbered for uniformity.

It should be noted here that this revision project would not have been possible without the active participation, collaboration and contributions of U.S. as well as international gear manufacturers, steel suppliers, forge shops, heat treaters, testing and certification firms and many others.

And finally, when published, the new edition will be more closely aligned with the current edition of ISO 6336-5. AGMA Metallurgy & Materials committee members actively participated in the development of the ISO standard's development, adds Dr. Ribaudo, who is also the U.S. delegate representing the metallurgical and materials interests of the U.S. gearing industry on the ISO TC 60/ WG 14.

www.agma.org

EMAG Group
ACQUIRES SAMPUTENSILI MACHINE TOOLS AND SAMPUTENSILI CLC

The acquisition of Samputensili Machine Tools and Samputensili CLC by the EMAG Group - including the 87 employees across two sites near Bologna and Reggio Emilia, Italy - took place on February 3, 2021. The two companies will be legally integrated into the newly founded EMAG technology company, EMAG SU Srl. Over time, the plan is for the two plants of Samputensili Machine Tools and Samputensili CLC to physically merge, with a shared location near Bologna, Italy. The new company is aiming to reach 35 million euros in sales by 2025.

EMAG has decades of experience in an extremely diverse range of technologies and applications. The machine builder from southern Germany controls the entire process chain from soft to hard machining — a key factor in its ability to successfully manufacture individual production solutions and complete production systems. With the acquisition of Samputensili Machine Tools and Samputensili CLC, EMAG is systematically expanding its scope of technology by adding a range of gear production processes: shaving, gear shaping, tooth flank grinding as well as profile grinding and generating grinding. These methods perfectly supplement EMAG's existing portfolio, which already includes hobbing, chamfering and deburring. The benefits of this addition are bigger than just the individual technologies, it shapes EMAG's entire mechanical engineering process by making new, holistic production solutions possible. These include everything from the first turning and gear cutting operations on a blank, to the grinding of diverse shoulders, and even the final tooth flank grinding step — the latter with Samputensili technology.

By acquiring Samputensili Machine Tools and Samputensili CLC, EMAG is not only expanding its technologies, but also its customer base. This is because the technology of the Italian machine manufacturers is also used in the production of pumps and compressors, as well as components for wind turbines, aerospace applications, shipbuilding, industrial transmissions and agricultural machinery.

"The powertrain electrification in automotive engineering increases the quality requirements for gears in terms of mechanical load, accuracy and noise emission. The hard fine machining of gears plays a decisive role here," explains Achim Feinauer, CTO of the EMAG Group. "We are also striving to highlight our extensive process expertise in the non-automotive industries. The networking opportunities for our sales department within Samputensili's customer industries provides us with a really great opportunity to do that."

Win-Win for Both Companies

Samputensili Machine Tools technology is in high demand all over the world, in industries ranging from aerospace, automotive, shipbuilding and more. These industries profit from the expertise and experience that the Italian machine manufacturer has in gear machining. Within these industries, high-precision grinding, shaping, and shaving machines are used, and few companies can match the wide variety offered by Samputensili. With this background, and wide-ranging level of experience, Samputensili has an excellence chance of continuing its success within the market. This is even more true because each of these industries is undergoing technological transformations, while still striving to stay competitive on a global level. These changes require very specialized mechanical engineering, with many users requiring increasingly powerful production solutions that reduce costs per unit, while also meeting growing demands on component quality, within the micrometer range. In this area, Samputensili will profit from the global reach of the EMAG Group. The South German machine manufacturer handles the global distribution of machines, laying the foundation for a successful future, by supplementing and expanding existing sales and service structures within Samputensili.

When it comes to application areas for certain EMAG technologies, customer consulting is vital. "Most markets and industries are very tight-knit and having a presence close by to provide advice and support for individual questions or concerns is critical. With EMAG's global sales and service organization, we are guaranteeing that. We have set a goal for ourselves to open up new application areas for EMAG SU, and are focused on continued growth," says Markus Heßbrüggen, CEO of EMAG GmbH & Co. KG. Additionally, the companies are combining their production network: In the future, various subassemblies, and parts for Samputensili machines will be manufactured at EMAG's production site in Zerbst — one of the most sophisticated tool factories in Europe. The final assembly of machines will remain in northern Italy. With this system, many Samputensili solutions will be completed faster, and more efficiently.

www.emag.com
www.samputensili.com

Star Cutter
ANNOUNCES NEW SERVICE MANAGER

Star Cutter Company has promoted **Bradley Cooper** to service manager at its Elk Rapids, Mich., location, responsible for the Star brand CNC tool and cutter grinders. Cooper will be responsible for managing and developing service group offerings, enhancing customer communication, order processing procedures and project management, and supervising the service team.

Cooper was previously the production supervisor at the Elk Rapids facility, providing him with a strong background knowledge of the company's CNC equipment and customer base. Prior to joining Star Cutter Company, he was plant manager for Inphastos and an electronics production supervisor for Microline Technology Corporation, both located in Traverse City.

Before entering the private sector, Cooper served as a United States Marine where he was an electro-optical ordinance technician for TOW/SABER missile guiding systems, night vision and thermal sights for the US Military where he received the Navy and Marine Corps Achievement Medal.

He has a bachelor of science degree in business and organizational leadership from Arizona State University. In addition to this education, he is a certified ABB US420 Programmer, and CIT (Association Connecting Electronics Industries) trainer.

www.starcutter.com

MHI
ANNOUNCES NAKAMURA TO REPLACE KAWAGUCHI

After nearly six years, Atsuhiro Kawaguchi, general manager of Mitsubishi Heavy Industries America, Inc.'s Machine Tool Division, will rotate back to Japan. Filling the newly created role of president is Katsunori Nakamura.

Nakamura has served numerous roles for Mitsubishi, most recently leading the cutting tool division in Ritto, Japan. Nakamura stated, "We will work together to ensure a smooth transition and maintain the USA Machine Tool Division to be in a strong position for the sustainable growth, smooth operations and profitability, all with keeping our concept of 'Legendary Reliability' for the future."

In other personnel actions, Neil Sawyer has been promoted to senior vice president—service and administration. Sawyer, with over 20 years with Mitsubishi, will take on more duties including development of suitable organization structure and strategic planning for the future needs of MTD.

The Machine Tool Division in Wixom, MI, provides service, support and sales for Mitsubishi Heavy Industries machine tools. These include gear hobbers, shapers, shavers, gear grinders, as well as large machines such as the MVR-Ex double column milling machine.

www.mitsubishigearcenter.com

Marposs
ANNOUNCES INTERACTIVE VIRTUAL SHOWROOM FOR E-MOBILITY SOLUTIONS

Marposs has launched a new virtual and interactive showroom that highlights its solutions for the gauging, inspection and testing of components manufactured for the electric vehicle market. Upon visiting the URL at *www.marposs.com/vs/ev/index.htm*, visitors press an arrow to enter the virtual

showroom where they can use the 360° navigation tool to view content, which is divided into two areas — Electric Drive Units and Battery+Fuel Cells. From there, information is available on:

- Functional testing of stators (electrical discharge)
- Dynamic dimensional gauging of rotors (contact electronic)
- Dimensional gauging of hairpins
- Dimensional gauging of gears
- Inline gauging stations for magnet wire (laser technology)
- Inline gauging of film thickness (confocal technology)
- Thickness measurement of pouch welding (interferometric technology)
- Flexible dimensional gauging of rotors (optical and contact technology)
- Leak testing stations for the cooling jacket, battery pack, battery cell and PEM bi-polar plate (helium and air); and
- Automated assembly solutions for quality assurance

The navigation tool enables users to click on they solution they are interested in and see a video and other supporting documentation on that particular technology. General information on the Marposs Corporation is also available.

Said Matteo Zoin, Marposs market development manager, "Many of the solutions we are known for within powertrain quality assurance can be applied to electric vehicles. Plus, we have made strategic acquisitions within this area, positioning Marposs as a comprehensive solution provider within the emobility sector."

www.marposs.com/vs/ev/index.htm

FANUC and Rockwell Automation
FORM COALITION TO ADDRESS MANUFACTURING SKILLS GAP

FANUC America and Rockwell Automation officially formed a coalition to kick off accelerated work and learn apprenticeship programs designed to upskill current and future workers for jobs in advanced manufacturing, robotics and automation.

The coalition includes APT, a FANUC and Rockwell Automation systems integrator, and NOCTI Business Solutions, which provides independent assessments of occupational standards and validation using recognized International Organization for Standardization (ISO) process validation methods. Franklin Apprenticeships is also a key partner of the coalition, ensuring apprenticeship support structure and success enablers for employers and apprentices.

The coalition has developed new apprenticeship programs offering people opportunities to gain credentials that include fundamental robotics (Robot Operator) and automation (PLC Operator). The program offers a second level of credentials for Robot and PLC Technicians. A third credentialing level called Integration Specialist builds on the fundamental and technical skills that teaches people to operate and troubleshoot integrated FANUC-Rockwell Automation technologies. All of the new apprenticeship offerings will provide more people with fulfilling careers and help companies to bridge the demand for skilled workers.

"Our number one goal is to help create a worker pipeline that will not only help people increase their skills and future earning potential, but to help manufacturers achieve their production goals and maintain a thriving economy," said Paul Aiello, director of education, FANUC America. "In most cases, current and future workers can complete the apprenticeship skills training

and achieve their industry-recognized certifications in less than one year. It's also important to note that these programs support all types of apprenticeship and certification models, including pre-apprenticeships."

"As industry adopts new technologies, it is vital to be able to quickly adapt with a well-trained workforce," said Michael Cook, director global academic organization, Rockwell Automation. "Having the most current standards will drive manufacturing competitiveness and simultaneously grow new talent to these new occupations, upskill current employees, and allow companies to be more agile in their workforce planning."

The apprenticeship programs aim to help companies rapidly upskill employees at every level from Operator to Technician to Integration System Specialist. In addition to improving the skills of current production workers, these programs will be extremely valuable for engineers who are working to implement new automation systems and processes that require new employees trained in the latest automation technologies.

"As technology advances at a fast pace, it is important that companies play a bigger role in education to ensure a safe, productive and sustainable work environment," said Aiello. "FANUC and our coalition look forward to helping as many people as possible take advantage of these accelerated work and apprenticeship programs."

Over 40 leading companies, including Dana, Magna, Tyson Foods and Flex-N-Gate, have agreed to support and participate in apprenticeships for automation technologies, ensuring that their employees receive adequate training and are qualified to succeed.

Industry leaders FANUC and Rockwell Automation have worked together over the past decade developing training, certifications and an education and training delivery network. FANUC's network of educational partners includes more than 1,200 high school and post-secondary FANUC-certified training organizations, and over 150 university and career technical training partners associated with this industry team. FANUC's network of schools coupled with Rockwell Automation's education partners represent nearly 1,600 schools, the largest nationwide collaboration of industry and education working to narrow the skills gap.

Verisurf Software
APPOINTS BAER REGIONAL SALES MANAGER

Verisurf Software has appointed **Milton 'Milt' Baer** to the position of regional sales manager, North East. In his new role, Baer will assist current customers and help develop new opportunities by identifying and solving measurement, inspection, reverse engineering, and tool-building challenges across all manufacturing segments.

"We are happy to have Milt as part of our team leading the North East Region. His customer focused approach and experience in selling engineering solutions will prove valuable to our customers and partners alike," said Pat Bass, director of sales for Verisurf.

Baer has been directly involved in sales management, marketing, manufacturing, training, and customer service for more than 27-years. He has spent the last 10-years applying his experience to consult, sell, and support engineering software solutions to customers throughout the North East region.

Baer completed his undergraduate studies at Penn State University and earned his bachelor of arts degree in business administration from the University of Pittsburgh.

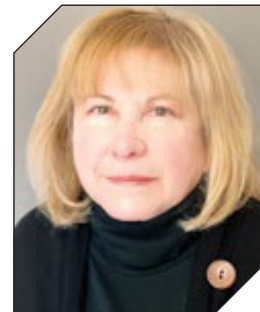# APMI International
NAMES 2021 FELLOW

APMI International's most prestigious award recognizes APMI members for their significant contributions to the goals, purpose, and mission of the organization as well as for a high level of expertise in the technology, practice, or business of the industry. The 2021 Fellow Award recipient will receive elevation to Fellow status at

PowderMet2021, during the Opening General Session on Monday, June 21, in Orlando. The 2021 recipient is **Cynthia Freeby**, regional sales manager, Ametek Specialty Metal Products.

During her 40 plus year PM industry career, Cindy has been dedicated to the advancement of the PM industry. She co-chaired the annual MPIF PM/87 technical conference and served on many boards and committees. She is the only person to have chaired three APMI chapters, Philadelphia, Dayton, and Michigan, after holding numerous officer positions within each Chapter. She received the MPIF Distinguished Service to PM Award in 2005, as well as the ASTM Distinguished Service Award in 2019 for her work in developing PM standards.

Established in 1998, the Fellow Award recognizes APMI members for their significant contributions to the society and high level of expertise in the technology of powder metallurgy, practice, or business of the PM industry. Fellows are elected through their professional, technical, and scientific achievements; continuing professional growth and development; mentoring/outreach; and contributions to APMI International committees.

gear
TECHNOLOGY

FREE SUBSCRIPTION

18GTPAGE

RESPONSE REQUIRED

☐ **YES** I want to receive/continue to receive *Gear Technology*

☐ **NO** Thanks anyway, but I don't need the world's best publication on gear engineering and manufacturing.

Name _____ Job Title _____
(please print)

Signature _____ Date _____
(required)

How would you like to receive *Gear Technology*?

☐ PRINT version (Verify mailing info below)
☐ DIGITAL Version (E-mail required)
☐ BOTH Print AND Digital (E-mail required)

E-mail _____ *

How are you involved with GEARS?

☐ My company MAKES GEARS (20)
☐ My company BUYS GEARS (22)
☐ I DESIGN gears (23)
☐ I am a SUPPLIER to the GEAR INDUSTRY (24)
☐ OTHER (Please describe) _____

What is your company's principal product or service? _____

_____

*Your PRIVACY is important to us. You get to CHOOSE how we use your personal information. The next e-mail we send you will have clear instructions.

MAILING INFORMATION

NAME:

JOB TITLE:

COMPANY:

ADDRESS:

☐ Check if this is a home address

CITY:

STATE/Province:

ZIP/Postal Code:

PHONE:

FAX:

Put your business card here to make it easier!

Mail to:
1840 Jarvis Ave., Elk Grove Village, IL 60007 USA

or

FAX to 1-847-437-6618
SCAN to: subscribe@geartechnology.com

America's Arsenal of Democracy

Matthew Jaster, Senior Editor

While we recently celebrated women in manufacturing and engineering on International Women's Day on March 8, 2021 there is rarely a day that goes by that I don't think back to the stories my own grandmother, Laurel McKinley (Hartner), shared about her experience working at the Willow Run manufacturing complex during World War II.

Growing up in Michigan, my family was *very familiar* with the Rosie the Riveter stories about the women that worked on the B-24 bombers at Willow Run. Of course, we had no idea my grandmother was part of the program until she nonchalantly mentioned working on the bombers many years later.

I still remember the expression on my mother's face when we realized my grandmother was talking about the famous plant between Ypsilanti Township and Belleville, Michigan.

"You and Aunt Janet worked at Willow Run during WWII?"

"It wasn't a big deal at that time," she told my mother. "We were expected to do our part here at home during the war."

According to the Detroit Historical Society, the Ford Motor Company initially struggled to transfer automotive assembly practices into aircraft production during the war. The use of steel cast dyes hindered design changes to the bomber. And it was difficult to attract workers away from Detroit auto factories due to the distance and lack of local housing. Many women were hired to replace men drafted into the war, leading to the creation of the "Rosie the Riveter" character.

Despite these issues, Willow Run was able to achieve remarkable production rates. At its peak in 1944, it produced a B-24 bomber every hour. By 1945, it was able to produce 70 percent of its B-24s in two nine-hour shifts, with pilots and crew members sleeping on 1,300 cots as they waited for the B-24s to roll off the assembly line. The Ford Motor Company eventually produced half of their 18,000 total B-24s at Willow Run — just an hour away from my grandmother's hometown of Holly, Michigan.

Rosie the Riveter culturally represented a shift in American economics that saw the number of working women in the United States increase from 12 million to 20 million by 1944. Many of these women — including my grandmother — broke social norms at the time by working in manufacturing.

As the story goes, Laurel McKinley (Hartner) and her sister Janet Wolverton (Hartner) spent time during the war at

The Willow Run Bomber Plant built half of the 18,000 B-24 Liberators used during WWII.

Willow Run. Aunt Janet worked in the offices while my grandmother worked directly on the aircrafts in the production line. She told my mother that her relatively small stature was perfect for moving around inside the aircraft where taller individuals had a difficult time. My mother wanted all the details, but my grandmother gave her very little to go on. She said it was hard work, challenging work, but rewarding at the same time. It was also problematic because some of the men that remained at the plant during the war didn't exactly make the women feel very comfortable. They persevered, however, doing what they could do in Michigan while so many Americans were fighting in Europe and the Pacific — including her future husband, a U.S. Marine fighting in Guadalcanal in the Solomon Islands.

She never mentioned a word of her time at Willow Run until much later in life, throwing the family a curveball as grandmothers tend to do! I cannot help but get a little smile on my face when I think about that girl in her early twenties, climbing through airplanes, getting her hands dirty and playing a small yet pivotal role in our country's rich, vibrant manufacturing history.

It wasn't a big deal to her at the time, it's certainly a big deal to me. Share your family manufacturing stories and we'll include some in a follow-up article in a future issue. Contact Matthew Jaster at *jaster@agma.org*.

For more information on the Willow Run Bomber Plant, visit: *www.thehenryford.org/collections-and-research/digital-collections/expert-sets/101765*

Janet Wolverton (Hartner) (left) and Laurel McKinley (Hartner) grew up in Holly, Michigan and worked at the Willow Run Bomber Plant during WWII.

IS PRODUCTION QUALITY AND RELIABILITY YOUR TOP PRIORITY?

RETROFIT & REFURBISHMENT SOLUTIONS BY KLINGELNBERG

KLINGELNBERG

Full refurbishment incl. ball screws, bearings, rails, belts and couplings – restoration of the original production quality

Performance package incl. faster gap finding and improved contact detection – higher efficiency and lower tooling costs

BEFORE AND …

AFTER RETROFIT & REFURBISHMENT

New control cabinet incl. cables, motors, measuring systems and sensors – high production reliability and reduced failure probability

Modern machine control – intuitive touch display and the latest operating software

Subject to changes

Custom retrofit & refurbishment solutions by Klingelnberg ensure top quality and a long service life for your machine. Through selective modernization of software and hardware components, your machinery can be updated with state-of-the-art technology at your request, thereby significantly increasing quality, productivity, and energy efficiency on the shop floor. Our service experts will be happy to assist you in selecting the appropriate measures, with a focus on your individual requirements and specifications.

Contact us at: retrofit@klingelnberg.com

Refurbishment the Video

BEVEL GEAR TECHNOLOGY | CYLINDRICAL GEAR TECHNOLOGY | PRECISION MEASURING CENTERS | DRIVE TECHNOLOGY

WWW.KLINGELNBERG.COM